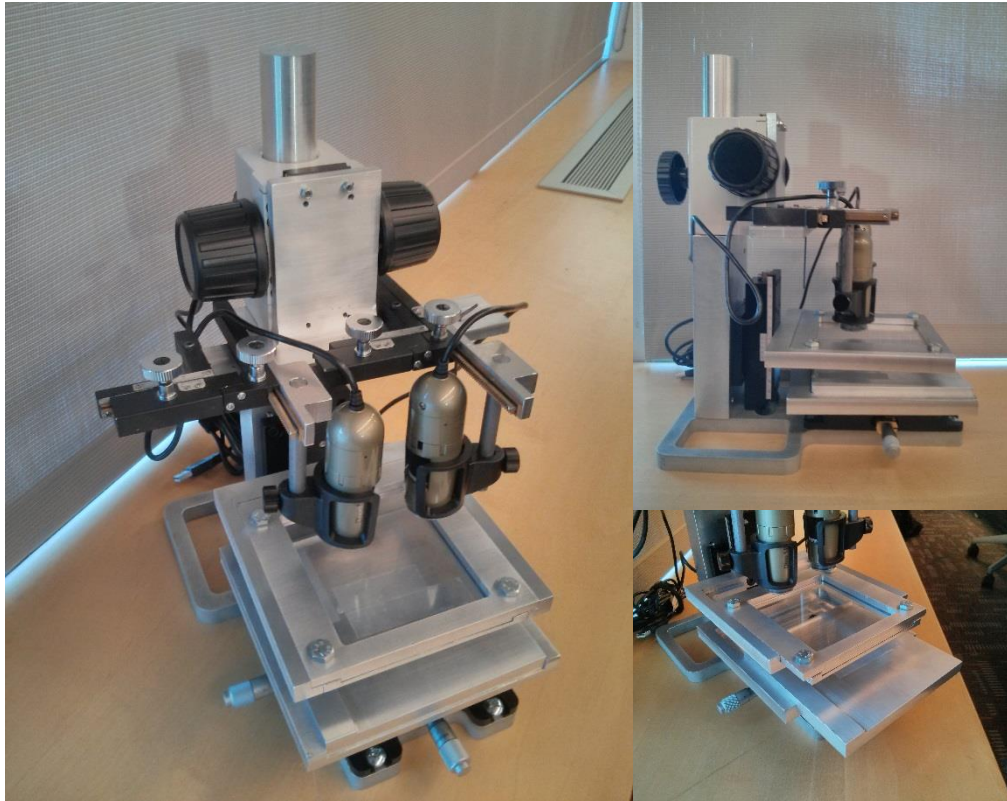


**ME 450 Fall 2013**

# Alignment Platform for Multilayer Soft Lithography



**Project 5 Team:**

Nitesh Alve  
Andy Dun  
Akshay Kini  
Karan Patel  
Roberto Shu

**Sponsor:** Dr. Jianping Fu  
**Section Instructor:** Dr. Nikolaos Chronis

December 12<sup>th</sup>, 2013

## EXECUTIVE SUMMARY

Our project is to design a high accuracy alignment platform for Multilayer Soft Lithography that is easy to use. The following page discusses the contents of our report including the design problem, customer requirements, engineering specifications, project plan, concepts generated, concept selection methodology, the final chosen concept, the prototype design, manufacturing plan, and validation results.

Multilayer Soft Lithography (MSL) is a microfabrication technique that constructs 3D structures by bonding layers of elastomers such as polydimethylsiloxane (PDMS). Each layer is first individually cast on a micromachined mold or engraved pattern before being aligned and, subsequently, bonded. Our sponsor, Professor Fu of the Integrated Biosystems and Biomechanics Laboratory (IBBL), has tasked us to develop a PDMS to PDMS alignment system that was more accurate and less tedious than their current platform.

We first collected user feedback to form our design requirements. These user requirements were substantiated with findings from our literature review, patent search, and benchmarks from relevant commercially available products. The requirements were then converted into quantifiable engineering specifications and ranked in importance, shown in Table 1.

Next, we resolved the primary function of our device, which is to align two PDMS layers, into its constituent parts that are represented via a Functional Decomposition chart. We then targeted each sub-function individually and developed several modules to address them. We employed a Go/No Go strategy and a Pugh chart to filter down the ideas and select the one that best met our specifications. We conducted a thorough analysis of our design concept to finalize our parameters and dimensions.

Every component of our final prototype has higher accuracy and tolerances than the current crude platform. By keeping the basic inputs the same and removing all the redundant ones, we've ensured that even a novice user will be able to align two layers quickly and accurately. Our device consists of two digital microscopes, three high resolution stages, and two focus racks that were purchased. All other parts, including the baseplate, top and bottom frame and holder were manufactured out of aluminum.

Overall, we met all but one of the specifications laid out by our sponsor. The only criteria we were unable to meet was the budget, which was a soft constrain. Our design performs better than the current benchmark device and all the stakeholders were satisfied with the result. Our sponsor has encouraged us to address additional features and improvements, such as improved rotational control of the platform, which we will continue working on outside the scope of the class.

**Table 1:** Engineering specifications and validation results

Requirements	Engineering Specifications	Validation Results
Accuracy	20-50 microns	$33.6 \pm 20.5$ microns
Pre-activation alignment time	< 10 minutes	$4.1 \pm 1.0$ minutes
Post-activation alignment time	< 5 minutes	$4.0 \pm 1.9$ minutes
# of inputs	<14	12
Height adjustability	> 7 cm	8 cm
Alignment stage size	> 2" x 3"	4.5" x 5.1"
Repeatability of top stage	< 500 microns	$12.7 \pm 5.4$ microns
Repeatability of bottom stage	< 500 microns	$9.0 \pm 3.4$ microns
Stability better than benchmark	$< 41.9 \pm 61.6$	$24.9 \pm 24.4$
Portability – Weight	< 40 lbs	20 lbs
Portability – Size	< 14" x 14"	8" x 10"
Cost	<\$2000	\$2019.18

## Table of Contents

<b>EXECUTIVE SUMMARY</b>	<b>2</b>
<b>ABSTRACT</b>	<b>5</b>
<b>REPORT OVERVIEW</b>	<b>5</b>
<b>PROJECT BACKGROUND</b>	<b>6</b>
<b>PROJECT MOTIVATION</b>	<b>6</b>
<b>INFORMATION SOURCES</b>	<b>7</b>
<i>Sponsor and Graduate Student Interviews</i>	7
<i>Commercial Mask Aligners</i>	8
<i>Custom-made PDMS Aligner – Dankook University</i>	9
<b>CUSTOMER REQUIREMENTS AND ENGINEERING SPECIFICATIONS</b>	<b>10</b>
<i>Converting Requirements to Specifications</i>	10
<i>Summary of Requirements and Specifications</i>	11
<i>Quality Function Deployment Chart Development</i>	13
<b>FUNCTIONAL DECOMPOSITION</b>	<b>14</b>
<b>CONCEPT GENERATION AND SELECTION</b>	<b>15</b>
<i>Preliminary Concept Selection</i>	15
<i>Full Concept Generation</i>	15
<i>Final Concept Selection</i>	22
<b>FINAL CONCEPT DESCRIPTION</b>	<b>23</b>
<i>General Overview</i>	23
<i>Detailed Explanation of Concepts Selected</i>	23
<b>PARAMETER ANALYSIS</b>	<b>25</b>
<i>Accuracy Analysis</i>	26
<i>Material Selection</i>	29
<i>Thermal Analysis</i>	29
<i>Structural Deflections</i>	30
<i>Full Structure Analysis</i>	32
<b>FINAL DESIGN DESCRIPTION</b>	<b>33</b>
<i>Top Stage</i>	34
<i>Bottom Stage</i>	35
<i>XYR Translation Stage</i>	35
<i>Z-Translation Rack and Pinion</i>	36
<i>Digital Microscope System</i>	36
<i>Digital Microscope XYZ Stage</i>	37
<i>Dinolite Transparency Function</i>	38

<i>Base and Pillars</i>	38
<b>MANUFACTURING PLAN</b>	<b>39</b>
<b>VALIDATION AND VERIFICATION</b>	<b>40</b>
<i>Accuracy and Less Tedious</i>	40
<i>Adjustability</i>	42
<i>Project Cost</i>	42
<i>Repeatability</i>	42
<i>Stability</i>	42
<b>DESIGN CRITIQUE AND RECOMMENDATIONS</b>	<b>43</b>
<i>Rotation Control of Bottom Stage</i>	43
<i>Digital Microscope Aligner System and Mounts</i>	44
<i>Weight Reduction</i>	45
<i>Automated Alignment</i>	45
<i>LCD Screen</i>	45
<i>Optical Table</i>	45
<b>PROJECT DRIVERS AND CHALLENGES</b>	<b>46</b>
<i>Design Drivers</i>	46
<i>Specific Challenges</i>	46
<i>Project Problem Challenges</i>	47
<i>Special Equipment, Technical Assistance, and Logistics</i>	47
<b>CONCLUSION</b>	<b>48</b>
<b>ACKNOWLEDGEMENTS</b>	<b>48</b>
<b>TEAM PROFILE</b>	<b>49</b>
<b>REFERENCES</b>	<b>51</b>
<b>APPENDIX A - BILL OF MATERIALS AND MANUFACTURING PLAN</b>	<b>53</b>
<b>APPENDIX B - DESIGN CHANGES</b>	<b>57</b>
<b>APPENDIX C - MATERIAL SELECTION AND ENVIRONMENTAL IMPACT ASSIGNMENTS</b>	<b>59</b>
<i>Material Selection</i>	59
<i>Environmental Impact</i>	62
<b>APPENDIX D - CONCEPT DESIGNS</b>	<b>65</b>
<b>APPENDIX E - ENGINEERING ANALYSIS CALCULATION</b>	<b>79</b>
<i>Structural Deflection Calculation</i>	79
<b>APPENDIX F - ASSEMBLY PLAN</b>	<b>81</b>
<b>APPENDIX G - ALIGNMENT PROCESS</b>	<b>84</b>
<b>APPENDIX H - ENGINEERING DRAWINGS</b>	<b>87</b>

## **ABSTRACT**

Multilayer Soft Lithography (MSL) has the ability to generate complex 3D structures, and is extensively used in the fabrication of microfluidic valves, pumps, and filters. Even though this technique is widely used in microfluidic research, there is a lack of quick, convenient, and highly accurate methods to align the structures on different layers before they are bonded – the critical step in MSL. The goal of this project is to design and build an alignment platform for MSL that will allow users to align two layers quickly and with an accuracy of between 20 to 50 microns.

## **REPORT OVERVIEW**

This report outlines our understanding of the design problem and the user's requirements. It summarizes our findings from relevant literature, patents, and commercially available products and how we used these to convert user requirements into specifications. It further discusses how our primary function was resolved into its various constituent parts and how concepts were generated to carry out each of those sub-functions. It briefly describes our diverse ideas and our five main concepts that rose from them, in great depth. This report also explains the logical, systematic procedures used to score our ideas. The sections following present our final selected concept with justification for why it is the most efficient and feasible for our purpose.

In the later sections, this report outlines our approach to the engineering analysis and assessment of the quality of our chosen design, followed by a complete description of our final design. A thorough fabrication plan has been included as well. This report discusses the results of the validation tests that were conducted to ensure that the user requirements had been met. The report concludes with a description of possible modifications and improvements on our design.

## PROJECT BACKGROUND

Multilayer Soft Lithography (MSL) is a rapid prototyping technique which uses elastomers like polydimethylsiloxane (PDMS) and creates microstructures within them. Each microstructure is etched onto a mold of PDMS and multiple layers of such molds can be bonded together to create a three dimensional structure. Two surfaces can be bonded together by contact. Thus we can use bonding to increase the range of use of our substrates for microfluidic purposes.

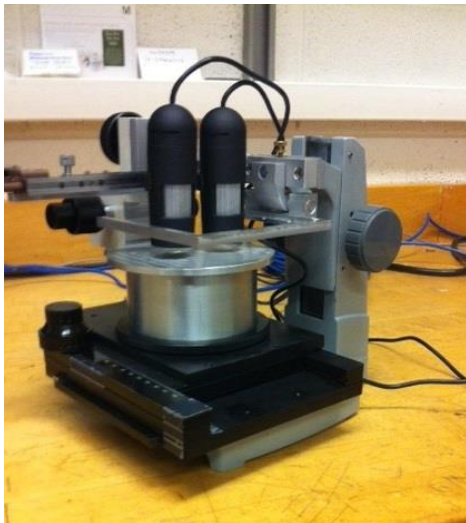
Microfluidics deals with the manipulation of fluids in channels which have cross-sectional dimensions in the order of a few tens of microns. At this scale, the fluids exhibit characteristics that differ from “macrofluids” with regards to surface tension, fluidic resistance, etc. This unique behavior allows them to serve several useful applications in biomedical devices, inkjet printheads, and miniature analytical systems [2, 3]. At the University of Michigan, the Integrated Biosystems and Biomechanics Laboratory (IBBL) investigates the use of microfluidic systems in the field of immunology for the purpose of transformative diagnostics; a project that stands to revolutionize the way patients with immune dysfunctions are treated and can drastically improve their survival rates [4].

## PROJECT MOTIVATION

At IBBL, the microfluidics devices are fabricated using Multilayer Soft Lithography. The microstructures in the PDMS layers are in the range of .25 to 50 microns [5] and each of them needs to be accurately matched up to allow fluid material to pass through the channels. Therefore, precise positioning of the PDMS layers before bonding is both the most crucial and the most tedious part of the operation. However, there is currently no proper device that allows a user to bond two PDMS layers in a way that is both accurate and easy.

Many students do this by hand, taking upwards of 30 minutes and often making accuracy errors. Dr. Zeta Yu, a postdoc fellow at IBBL, created a device to help with the alignment (see Fig. 1). It consists of two moveable stages. Each stage can be manipulated to achieve the required position. The bottom stage has three degrees of freedom (X, Y, and rotates about the Z axis) while the top stage is free to rotate about the X and Y axes and can be moved in the Z direction to bring the two PDMS layers into contact. Along with these movable stages there are two cameras which can individually be moved to visualize two alignment markers and determine when the correct alignment is achieved.

**Fig. 1:** Crude alignment platform currently used at IBBL that has an average accuracy of 100 microns



There are, however, several major drawbacks in the current system. First, there is insufficient alignment accuracy. The current device has an accuracy of alignment within 100 microns of the target. There are 14 different adjustable knobs on the device with individual functions, making it difficult to operate. The current operators of the platform agreed that the mechanism is not intuitive and does not allow proper control over required degrees of freedom. The components such as the moving platforms and the microscopes, lacked the resolution to align the PDMS layers accurately, and the overall design of the platform was too complex to carry about the alignment quickly with ease.

As a part of ME 450, we, a team of 5 mechanical engineering students, had been tasked with the challenge of developing an alignment platform under the sponsorship of Professor Jianping Fu. This device will help the user in the final stages of MSL and will address the drawbacks of the current platform. A highly accurate platform that allows even a novice user to carry out an alignment quickly will be greatly beneficial to the research projects at the IBBL. It will not only save valuable time and resources but will also generate high quality microfluidic devices that will boost their efforts to make great strides in the field of affordable public health care.

## INFORMATION SOURCES

We conducted a broad literature review to understand our current problem and benchmarked some of the specifications we are looking to add to our device against current solutions which exist. Our information sources broadly fell into three categories. First, we interviewed our sponsor and his graduate student researchers who will be users of our product. Next, we looked a little deeper into how PDMS bonding occurs and the science behind the process of soft lithography [5, 16, 17, 21] and alignment of these PDMS layers for bonding and the different parts of this process. Lastly, we looked into commercial mask aligners and relevant designs available in the market. Later in the project, we were able to find a research group that developed a custom-made aligner that was relevant to our project. In this section of our report we have summarized our major findings from our interviews and literature review. Please refer to the end of the report for a complete list of our references.

### Sponsor and Graduate Student Interviews

Our primary source of information came from our meetings with Professor Jianping Fu, and the members of the Integrated Biosystems and Biomechanics Laboratory (IBBL). Prof. Fu, our sponsor and the principle investigator of the IBBL, informed us of the history of the lab and their work with Multilayer Soft Lithography (MSL) in the fabrication of microfluidic devices. From our conversation we were able to gain insight into the processes used for the alignment and bonding of polydimethylsiloxane (PDMS) layers. He explicitly specified the need for an alignment platform with an accuracy of 20 microns or less and, hence, it is our most heavily weighted design specification. He mentioned, however, that there lacks an established manner of checking accuracy. Finally, he set a soft constraint for the project budget at \$2000.

Dr. Zeta Yu had previously designed and manufactured a crude alignment platform. However, it was described to be tedious, time consuming, and only accurate to 100 microns. According to Dr. Yu, the process takes 30 minutes on average during pre-alignment and 7 minutes after the layers have been activated. Through a complete demonstration of the PDMS to PDMS alignment process, Dr. Yu conveyed a lot of important information. Firstly, the entire procedure is conducted under a laminar hood in order to maintain a clean environment. An air duster is used to ensure no contaminants reside on the instrument. In his example, he used a thin layer of PDMS on a silicon wafer as the fixed layer being aligned to. Currently, the wafer is not strictly constrained on the lower stage. Instead its major flat is used to position the wafer relative to the stage's adjustment arm. The upper PDMS slab is held in position by manually pressing it against the bottom of a rectangular glass slide. Both surfaces are first rinsed with ethanol to ensure proper sealing. Dr. Yu, in his expert opinion, believed such a constraint was appropriate and would

suffice. However, the glass slide does not fit precisely into its frame and Dr. Yu agreed that the tolerance of the slot can be improved

We learnt that in order to form a good, strong bond between two PDMS layers their surfaces must first be cleaned or activated in a plasma oxidizer. The quality of the bond decreases with time taken for bonding after activation [11]. For this reason the alignment process has been broken up into two parts, namely pre-activation alignment and post-activation alignment, with the hopes that the initial rough alignment will reduce the amount of alignment needed after activation.

Dr. Yu designed the current system to have two stages and an arm that carries the two cameras. The lower stage moves in the X and Y direction. The user mentioned that giving it a third degree of freedom by means of rotation about the X axis might be beneficial in ensuring that the PDMS slabs are parallel during alignment. The aluminum cylindrical base also rotates about the Z axis. The middle stage, which contains the frame for the glass slide, moves in the Z axis and rotates about the X and Y axes. The upper arm runs along the X axis and contains two microscopes that are free to rotate about their respective Y axes. With two cameras, the user is able to align the PDMS using two separate markings simultaneously. The arm itself moves in X, Y, and Z directions. Both cameras used contain a ring light to improve video quality. Dr. Yu is not satisfied with the cameras and would like them to be replaced by ones that have a better depth of focus. It was also noticed that a third camera to view the distance between the two layers might be beneficial, but not necessary. He opted out of using a microscope because he believed the optics would be too complicated and the parts would be too expensive. A single button serves both the zoom and focus button on the cameras.

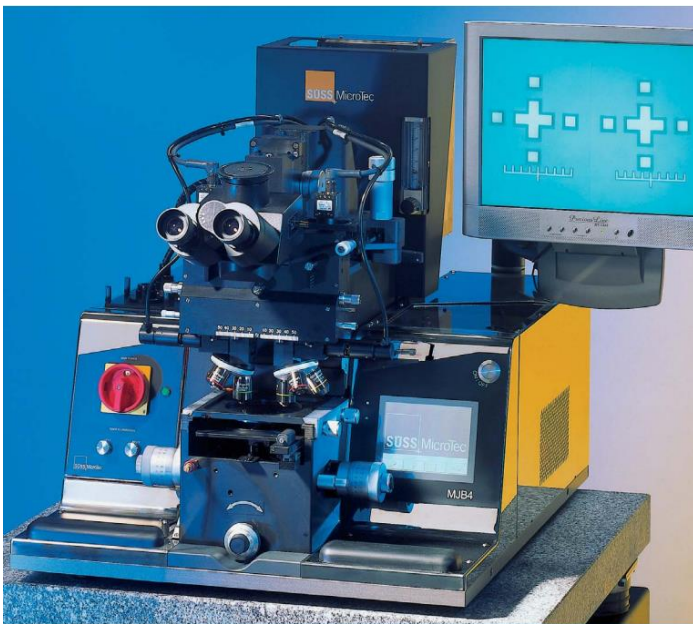
Another characteristic that adds to the complexity of the current instrument is the presence of 14 adjustment knobs and dials (excluding two that serve no purpose) each of which controls a different function that has a consequence on the overall alignment. Dr. Yu agreed that reducing this number by combining functions and removing redundancies would greatly improve the ease of operation of the device. Also, this would consequently cut down on the time taken for pre-alignment of the PDMS slabs. Dr. Yu reiterated the importance of being able to align the PDMS layers quickly and accurately after the layers have been activated as the quality of the bond decreases with time.

### **Commercial Mask Aligners**

From our benchmarking we found a similar device used in industry [8]. This device (see Fig. 2, p. 9) takes samples which are less than 4 in by 4 in. The device is free to move in the X and Y directions and also to rotate about the Z-axis. It has a resolution of 2 microns and has a range of 5 mm in X and Y and is capable of rotating up to 5 degrees. This device has a large cost of about \$25,000. This far exceeds our budget but was a good place to start from and look at reducing tolerances.

Alternative sources of alignment include infrared alignment devices [9] although these seem well outside our budget, they will give us some insight when we begin to come up with concept designs. Another typical mask aligner takes sample sizes less than 8 inches in diameter and has multiple magnification options of its optical viewer. Like the previous device it accommodates for motion in the XY plane and allows rotation around the Z axis. This device is built with dual HD monitors and illuminates the object using LEDs. It weighs 217 kg.

**Fig. 2:** Commercially available mask aligners [8]



By looking at the various commercial mask aligners we know roughly the kind of device we want to build. Although mask aligners and our alignment platform will accomplish similar goals there are some key differences. Mask aligners don't work well outside a clean room environment. Our device will most likely be operated on a desk in the IBBL and at most will be used under a fume hood. Also, mask aligners are not equipped to handle PDMS layers and have no structure with which to hold them in place.

#### **Custom-made PDMS Aligner – Dankook University**

We conducted a thorough search for custom aligners made for PDMS applications. We found just one publication in the Journal of Sensors and Actuators published by a team of researchers at Dankook University in South Korea [40]. They undertook a project to design a device to align and bond PDMS for the fabrication of 3D microfluidic channels. Their system included three moving parts: a manual device to place one layer on the other, a XYZ stage to align the two layers, and a stage for rotational alignment of the patterns. To create an image of the alignment they had a high precision stereoscope capable of 100x and 400x magnification. The stereoscope output its view to a CRT TV.

The main difference between the product this team describes in their paper and our alignment device is our budget constraint. We were given a budget of \$2000 which would not begin to cover automated motor controls and microscopes to the precision used in this device. We had to be more judicious in our selection of components so that we minimized alignment errors while spending the least amount of money.

Another difference between our alignment platform and the device from the paper is the physical space it occupies. The high precision microscope and manual device to place one layer on top of each occupy a lot of space and the total device needs its own table and so it is not portable. Portability was an important design specification because not only does our device need to be used by users in different rooms, but our sponsor aims to share this device with other labs making it easier for them to align microfluidic samples.

## CUSTOMER REQUIREMENTS AND ENGINEERING SPECIFICATIONS

We determined our project requirements based on conversations with our sponsor and the users of the current device, the primary stakeholders in this project. We carried out an extensive literature search to be able to better translate these requirements into actual engineering targets. Some of the requirements were clearly laid out by the sponsor, the rest were determined through our research.

Our sponsor also gave us a clear understanding of the degree of importance of the different specifications. This information helped us rank them and develop a Quality Function Deployment (QFD) chart (Fig. 3, p. 13). The OFD was developed by ranking the different requirements extracted from the various information sources. The sub-section on QFD lists the importance of this chart.

### Converting Requirements to Specifications

This section lists the major user requirements we deduced and describes how each one was converted into quantifiable engineering specifications.

**Accuracy:** as mentioned in our section our summary of information sources, the most important requirement is that the alignment accuracy of the device. A specification of within 20-50 microns was given to us by our sponsor. This accuracy is justified because the scale of the microfluidic channels being aligned is on the order of 100 microns [15, 18]. Also the current device has an alignment accuracy of 100 microns and it is our competitive benchmark. We determined that this specification in turn translates directly to two operational requirements:

1. **Resolution of alignment device:** this is the mechanical stage that actually aligns the two layers. It must have a resolution of less than 20 microns to be able to bring the two layers within the specified range of each other. This requirement was determined by the team.
2. **Resolution of imaging device:** this is important to visualize the actual alignment process and to verify that the two layers are indeed within the specified range of each other. As specified by the user, a magnification of 20x is more than sufficient to visualize the process. We determined that we would need a resolution of at least 10 microns at this magnification to be able to properly view the alignment markers [7].

**Less tedious:** the second most important requirement as specified by our user is to make the device less tedious to use to reduce the time and skill it takes to align two layers. The current device has 14 user-controlled inputs and takes over 30 minutes to complete the entire alignment and bonding process. Removing redundant degrees of freedom and reducing the number of inputs will make the process quicker and easier; hence, we set a specification of fewer than 14 inputs.

From our conversations with experienced operators of the device, we determined that 15 minutes would be the appropriate specification for total time of alignment. Once the two layers have been activated in the plasma oxidizer, the user has only 10 minutes to bond them to form a good bond [11]. Using this information we decided to set a target of 10 minutes for pre-activation alignment and 5 minutes for post-activation alignment.

**Adjustability:** this requirement was also specified by the user. The device should be able to accommodate layers of different sizes and thickness, and should also be able to align multiple layers one after the other. In general, the layers used in the lab are bonded to glass slides 2" x 3" in size and are approximately 1cm in thickness [19]. However, layers may also be bonded to thin layers on wafers of silicon whose thickness is on the order of tens of microns. To account for a stack of up to six layers (as specified by the user), the range of height adjustment was determined to be 7cm. While the current device is capable of accommodating layers of the given size, it only has a height adjustment range of 3cm.

**Cost:** this requirement was specified by the sponsor. The total project budget was set at \$2000. However, the sponsor indicated that this was a soft constraint and that additional funds will be provided if deemed necessary to ensure the quality of the device.

**Repeatability:** in addition to reducing the number of inputs that the user needs to make, the team also determined that making the alignment process more repeatable will also reduce the time taken for alignment. On the current device, there is slop between the glass slide and its stage. When the slide is taken out for the activation process and then put back in, the layer to be aligned shifts position by 500 microns [1, 20] to make sure that images from the center of the screen would not escape the field of view (1300 microns at 250x magnification) after activation. The team determined that by increasing the tolerances on the removable parts, it would take less time to re-align the layers after activation. In other words, the specification of 5 minutes for post-activation alignment applies to this requirement as well.

**Stability:** in order to achieve the alignment accuracy and stay under the required alignment time, it is crucial to ensure the stability of the alignment device. When adjusting the location, zoom level, or the focus of the imaging device, the force required should not cause any significant misalignment or oscillation of the alignment stage and cameras. This means that either the motion between the imaging device and the alignment stage is completely isolated, or the force applied on the device for any imaging adjustments has to be zero. Thus the reduction of physical user inputs on the device could indirectly improve the stability of the alignment platform as well. The current device is not very stable, and making any adjustment to the imaging device generally causes misalignment of the stage and the cameras. Our target for our device is to overcome this drawback and prove to be more stable than the current aligner.

**Portability:** the final user requirement was that the device be portable. It is being shared by multiple labs and is used in different spaces by different people. Users generally use the device under a standard sized laminar fume hood to prevent small dust particles from settling between the layers being aligned. The device may be stored on a desk or on a shelf. Based on these inputs, we determined that the device should weigh less than 40lbs to be easily carried by one person [14] and its dimensions should be within a 14 inches by 14 inches footprint to fit in the fume hood [1].

### **Summary of Requirements and Specifications**

The project requirements and the engineering specifications have been summarized in Table 2, on the following page. Target values and units have been provided for each specification alongside the source through which they were determined (please refer previous section for detailed explanations). We classified the requirements into functional requirements, which define how well the system must perform to meet its objectives, and operational requirements, which determine how users interact with the system to meet their specific needs. Classifying the requirements into the two categories simplified the process and allowed us to keep the big picture in mind when coming up with the engineering specification for each individual requirement. The operational requirements inherently depend on the functional requirements.

**Table 2:** Complete list of the user requirements alongside quantifiable engineering specification

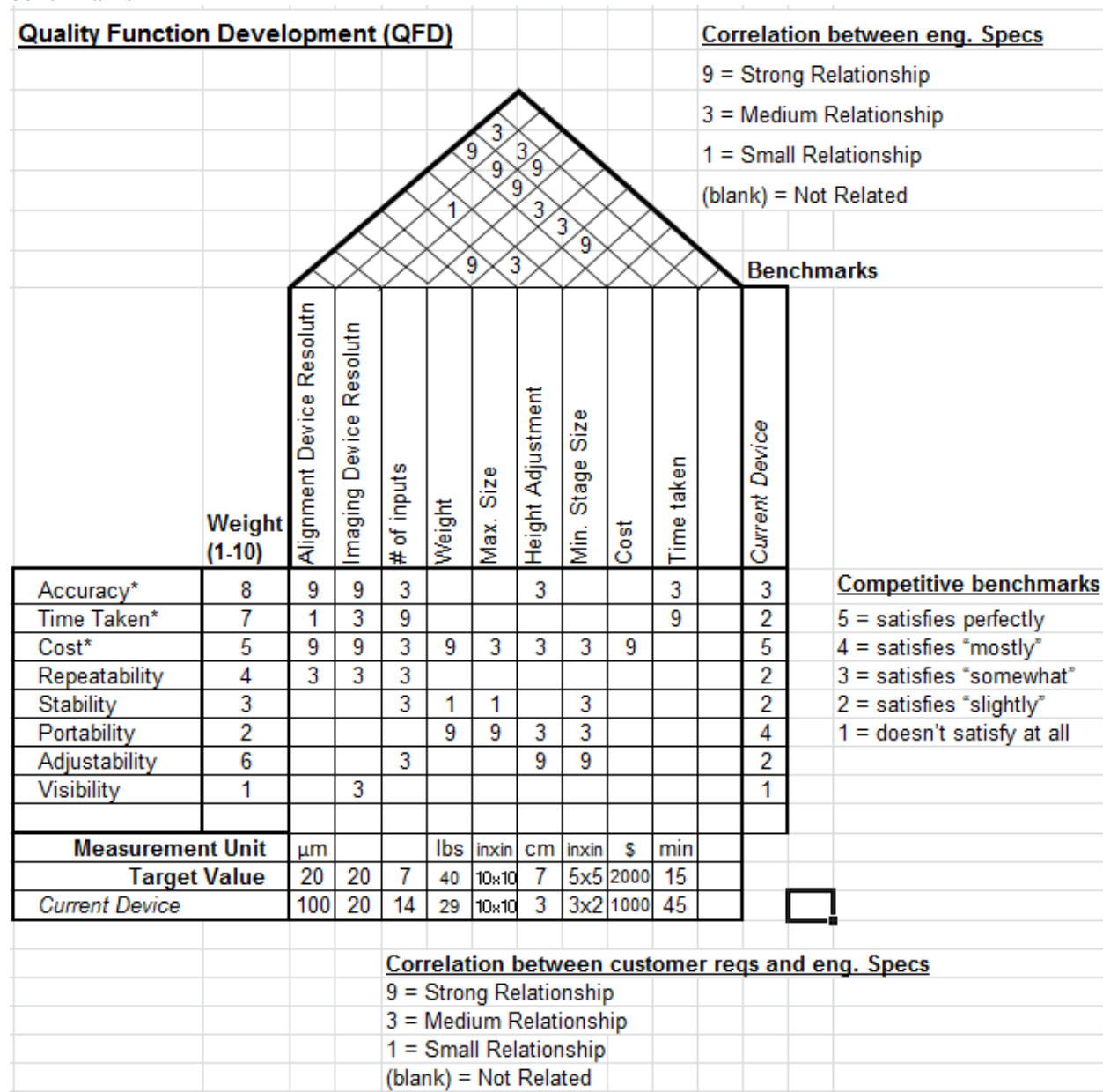
Functional Requirements	Operational Requirements	Engineering Specification	Source
Accuracy		20-50 microns	Sponsor
	Alignment Device Spec	Resolution < 20 microns	Team
	Imaging Device Spec	20x magnification	Sponsor
		Resolution < 10 microns	[6,10]
Less tedious		< 15 minutes total time	Sponsor
	Pre-activation time	< 10 minutes	Team
	Post-activation time	< 5 minutes	[11]
	# of inputs	< 14 inputs	Team
Adjustability		Fit 6 PDMS layers	Sponsor
		Fit layers on 2" x 3" slide	Sponsor
	Height Adjustment	7 cm	Team, [12]
	Alignment Stage Size	> 2" x 3"	Sponsor
Cost		< \$2000	Sponsor
Repeatability	For Top Stage	< 500 microns	Team
	For Bottom Stage	<500 microns	Team
Stability	Post alignment error vector	< benchmark	Team
Portability	Weight	< 40 lbs	[13]
	Size	Within 14" x 14" footprint	Sponsor

These requirements are listed in decreasing order of importance. We determined this order using feedback we received directly from the sponsor and users to weight each requirement against the others.

## Quality Function Deployment Chart Development

The order of importance of requirements is also reflected in our Quality Function Deployment (QFD) chart. In addition to this, we used the QFD to relate each customer requirement to the different engineering specifications, and also to relate the engineering specifications with each other. We also benchmarked the current device against the user requirements so we can compare our specifications. In this way the QFD helps us to better understand the problem and what the solution is affected by. The QFD is also important during concept generation to weigh conflicting design parameters against what the customer's requirements to ensure that what we design is truly what the customer desires.

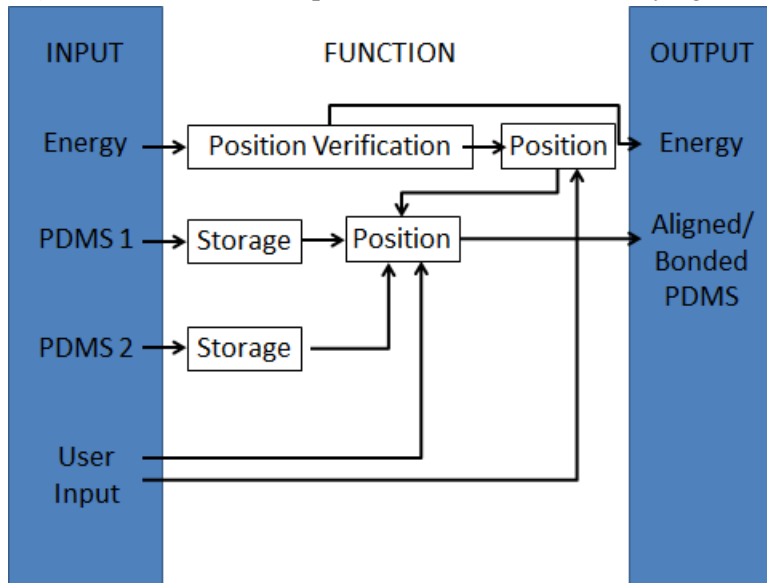
**Fig. 3:** Quality Function Deployment listing the various requirements, specifications, and corresponding benchmarks



## FUNCTIONAL DECOMPOSITION

Now that we have translated all the user requirements into engineering specifications and ranked them based on their importance, we have established the framework on which to build our design. The primary function of the device is to align two layers of PDMS quickly with a high accuracy. In order to come up with an optimized and comprehensive design the first step will be to break up this primary function into its various sub-functions. By targeting each module individually we are ensuring that we are thorough in our task of analyzing the different ways of carrying out the same function and, hence, we can be sure that the modules that make up the final device will be the most efficient and suitable for our objective.

**Fig. 4:** Functional Decomposition of our device identifying the various inputs, functions, and outputs



The Function Decomposition above resolves our primary function of aligning two PDMS layers into its constituent parts and clearly demonstrates how they interact with each other. From our conversation with the stakeholders and review of relevant literature and commercially available products, we were able to deduce the identity of the essential functions to be the following:

- 1. Position Verification:** it is crucial that the microfluidic channels and alignment markers in the PDMS slabs are easily identifiable by a user, a digital image processing input, or any tool that will be used to align the two layers. Our alignment platform will not be able to align the two PDMS layers if it does not consist of a module that helps relate the location of the microfluidic channels in the two slabs; a sensor that gives feedback of the position of the slabs. Hence, this function has been included with energy (electrical or otherwise) as its input to power it and energy (as a by-product) as its output.
- 2. Storage:** this function encompasses how the PDMS layers will interact with the device. Everything from insertion/removal of the slab to constraining it with tight tolerances is included in this block. This function allows for a lot variation in its implementation but has a significant impact on our specifications, especially repeatability. Once in place, the next step would be to move the slabs relative to each other and this is carried out in the position function block.
- 3. Position:** both the visualization tools and the PDMS slabs have to be moved with high resolution in order for the two slabs to be aligned with high accuracy. The visualization tools will most likely be oriented first depending on the location of the markers engraved into the PDMS. This process will be followed by the positioning of the layers with respect to each other, all the while keeping them in focus of the optical components. While designing this component it is critical that we keep in mind the different degrees of freedom and how they shall be addressed so as to not make our device too

tedious to operate. The positioning will require an input and based on our specifications, such as project budget, this input will most likely come in the form of a user and not an automated control system.

Now while the device will always perform the exact function, a user will go through the entire process represented in the functional decomposition twice every bonding cycle; once during the pre-alignment stage and once after the two slabs have been oxidized in the plasma etcher. The only difference between the former and the latter is that in the latter the device will perform the additional task of bringing the two slabs in contact with one another to form a permanent bond.

## **CONCEPT GENERATION AND SELECTION**

The Functional Decomposition offered a very clear representation of all the modules that is required in our device and how they must interact with each other in order to achieve our objective of aligning two PDMS layers with an accuracy of 20-50 microns. In other words, it helped us classify our required concepts into the following categories: position verification component, storage component, and the positioning component. The previous section details the method used for categorization and the tasks that each one of those categories encompasses. Our next step was to brainstorm ideas that achieved each sub-function.

### **Preliminary Concept Selection**

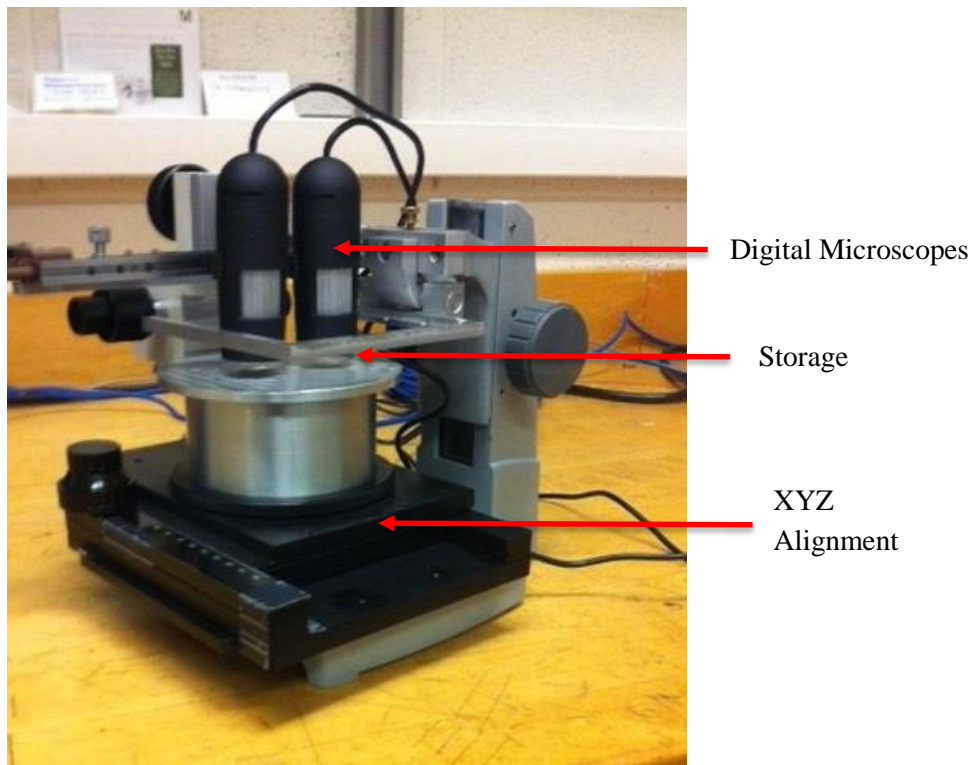
As a team we came up with close to 30 different ideas (see Appendix D for the complete list). We narrowed down those results using the Go/No Go strategy. In this method, we examined each of these modules and used our best judgment and research to determine if each generated design concept will or will not meet our engineering specifications. Our classification of the concepts in this way also inspired a slew of new ideas and suggestions to improve the current ones. At the end of this process we were left with 2 or 3 unique designs for each sub-function.

### **Full Concept Generation**

Each team member was then tasked with developing a complete, fully functional device using the remaining concepts. We each picked one idea from each sub-function and combined them to create what we believed to be the most efficient and optimized solution to our project challenge. Five complete designs of the system were then brought together for critiquing by all the members of the group for a final round of evaluation and benchmark against the current aligner. Included in this section are those final five designs along with their unique features. We have also evaluated how each might prove to be an asset or a liability to the final alignment platform.

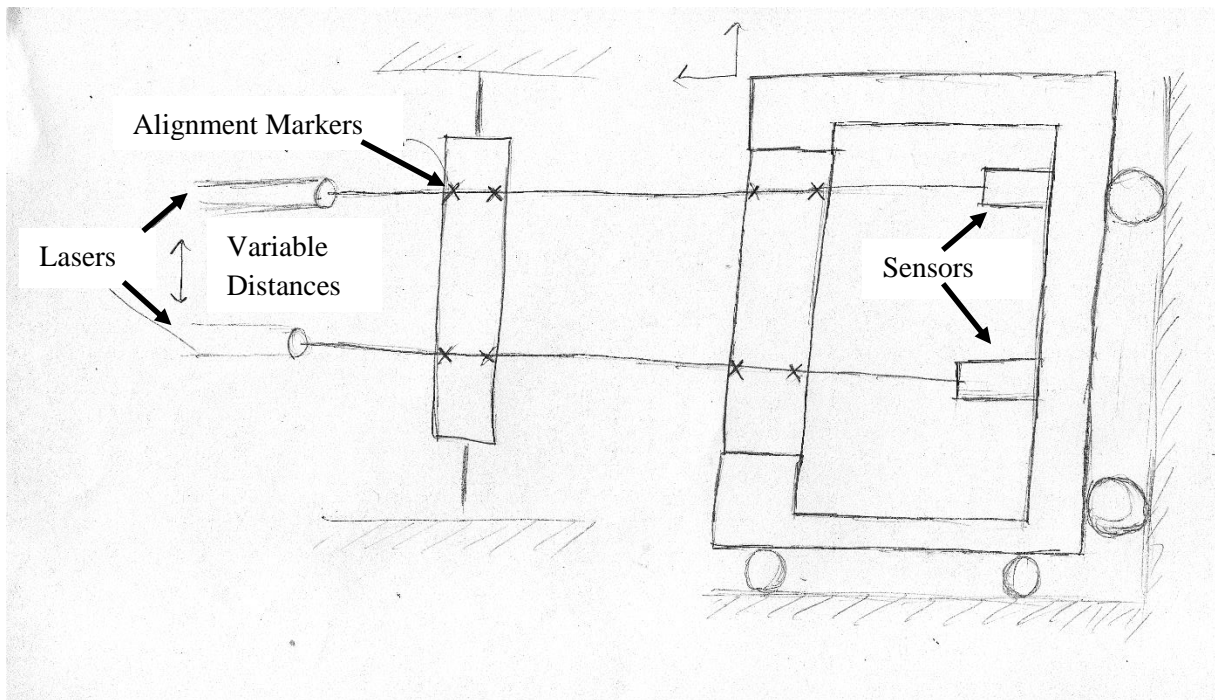
**Benchmark:** The benchmark that our designs were compared against is, naturally, the current aligner that the lab uses (Fig. 5). For position verification, it uses two digital microscopes that output the image on to a laptop using USB connections. The positioning of the digital microscopes is movable in the X and Y direction independently, and in the Z direction collectively, while each of the digital microscopes also rotates on its Y-axis with no particular purpose. The current aligner chose a dual digital microscope set up because two alignment markers need to be aligned at the same time in order to constrain the position of the PDMS layers. This also eliminates the use of optical microscopes since it is difficult for one person to view two different images through the lens at the same time, as opposed to digital microscopes that display two images onto a screen. The storage system uses a manufactured aluminum frame and a glass slide to hold the upper PDMS layer by the natural adhesion between PDMS and glass; and a purchased alignment stage with a height extension to hold the bottom PDMS layer. Neither the top nor bottom stage fully constrains the position of the PDMS layers. The bottom stage only has a flat edge to align the bottom layer against in the Y direction, while the glass slide on the top is approximately 2mm smaller than the aluminum holder. The positioning of the current aligner can also be tedious due to extra degrees of freedom. In addition to moving in the Z direction, the top stage also rotates in X and Y axis as well. The bottom stage moves in X, Y, and rotates in the Z axis using knobs in the alignment stage.

**Fig. 5:** The currently used alignment platform will be used the competitive benchmark



**Design 1:** it is a laser aided, horizontally bonded aligner (Fig. 6). This design challenges the idea that the PDMS layers have to be bonded vertically. In this design, the PDMS layers are each placed on a vertically oriented glass slide by the natural adhesion between glass and PDMS. The slide on the left is stationary while the slide on the right moves in X, Y, Z, and rotates about the X-axis. The position verification module for this concept is implemented with two lasers and laser sensors. During the manufacturing of the PDMS layers, precise holes were punched on each of the slides. The laser shoots through both of the precise holes to align the PDMS layers. The accuracy for lasers is very high, [27] but we are uncertain of the lab's ability to punch precise holes on a compliant material such as PDMS. The horizontal nature of the devices inherently introduces complexities, which also negatively affected the manufacturability and the intuitiveness of the device.

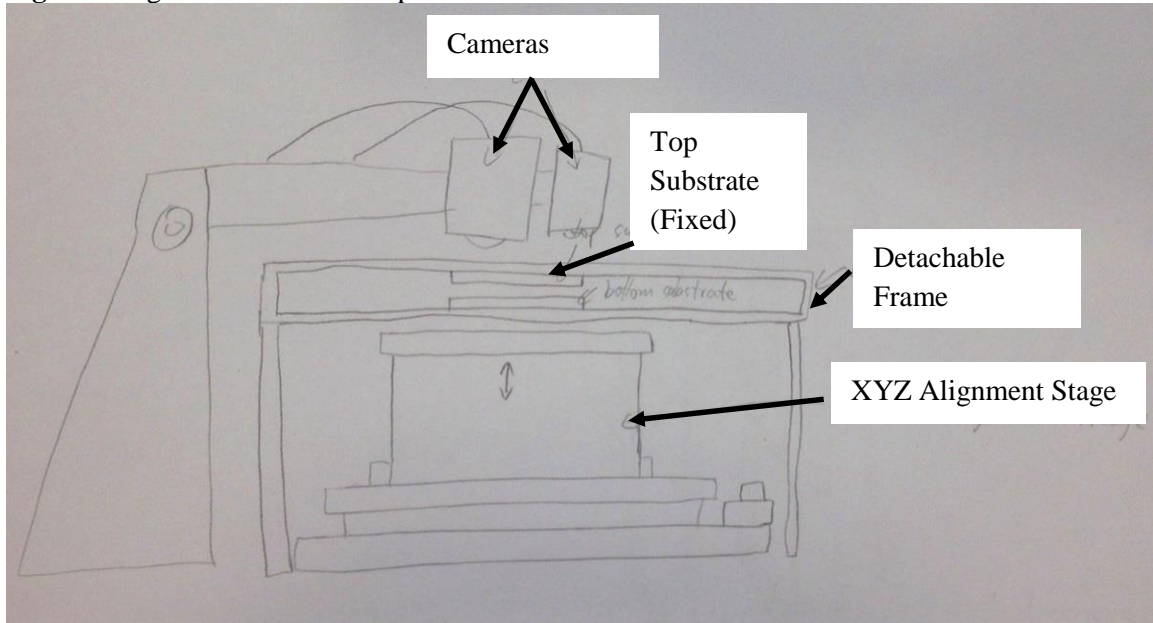
**Fig. 6:** Design 1, a horizontally bonding aligner



**Design 2:** it has kept the positioning mechanism the same as the benchmark, while improving the position verification and storage function. The position verification function in this design incorporates the same hardware as the benchmark, but aims to increase the alignment accuracy by means of image processing. A challenge of the current aligner that the digital microscope does not have a high enough depth of view to focus on both PDMS layers at the same time. This design addresses this issue by focusing the digital microscope on the top stage, which does not move in the X, Y direction, capturing an image, and then overlaying a live video of the digital microscope focusing on the bottom stage, which translates and rotates to align with the top stage. This allows both PDMS layers to be focused and displayed on a screen at the same time with a transparent blending. This design achieves the best visualization accuracy out of the five designs, but the programming required may prove to be challenging [28].

The storage module for this design is a detachable frame that holds two PDMS layers and their glass slides (Fig. 7). Instead of separating the glass slides during the plasma oxidation, the idea is to align the two PDMS layers precisely, and then activating the surfaces together with the detachable frame. After plasma oxidation, the two layers can be bonded without post alignment, significantly reducing the post-alignment period, increasing the quality of the bonded surface. The problem with this design is that the detachable frame only accommodates the bonding of similar PDMS thicknesses. New frames need to be made for aligning more than two layers of PDMS or other surfaces. Also, in order to activate a PDMS surface, it has to be facing upward in the plasma oxidizer, making this design infeasible for actual practice.

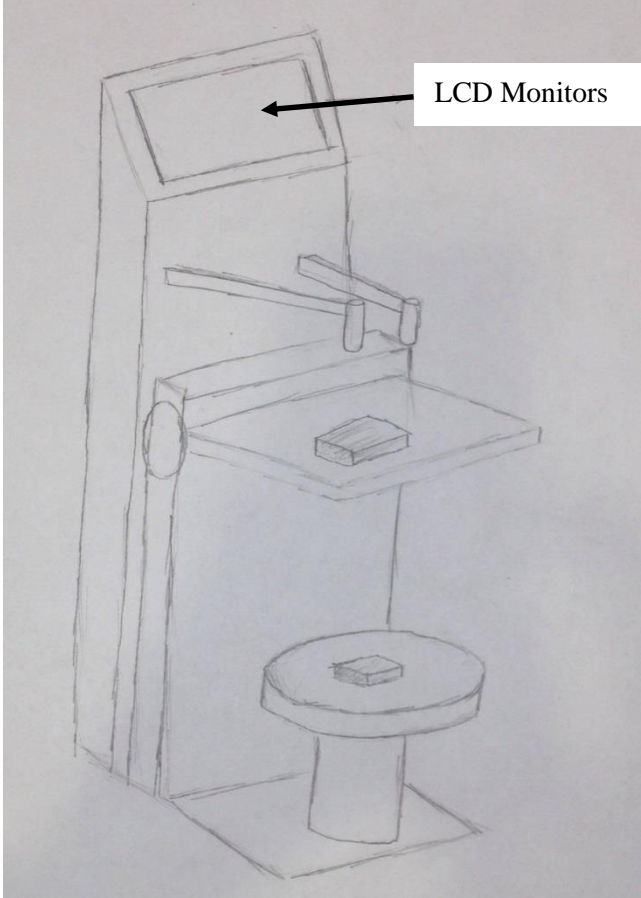
**Fig. 7:** Design 2 with detachable platform



**Design 3:** this design mainly aims to improve the portability and the user interface of the system, while keeping the storage function the same as the benchmark (Fig.8). For the position verification function, a LCD monitor is integrated into the device. This allows the system to be more portable, which is important because the device will potentially be shared among different lab groups. This concept also utilizes a composite video signal instead of a laptop computer with USB, which reduces the lag time between the video recording device and the visual output, making the alignment process less tedious.

The positioning function is addressed here using a motorized alignment stage instead of a manual one. This allows the user to align the layers using a joystick instead of using the manual alignment knobs. This is more direct and intuitive for the user but it is more expensive to implement, since we would have to purchase the alignment stage and potentially create control programs for it. Having extra motors may also introduce more vibration into the system and decrease the alignment accuracy.

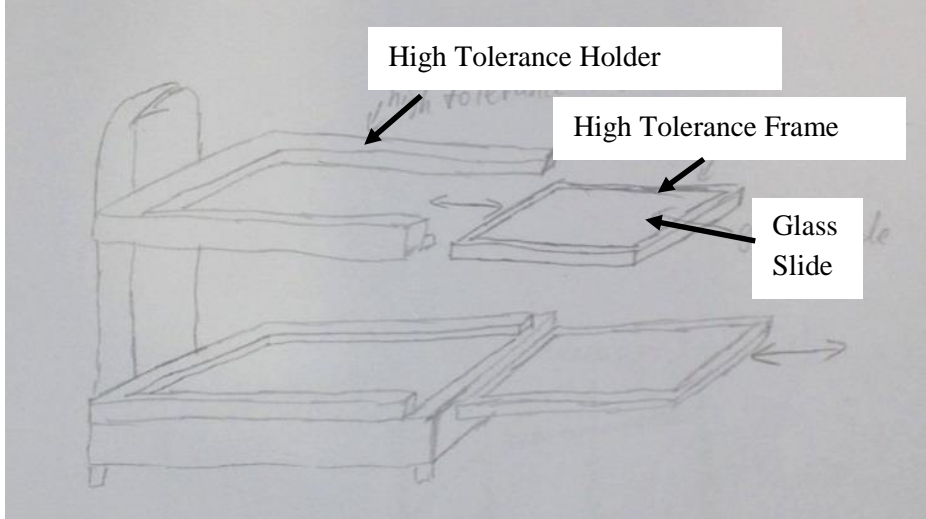
**Fig. 8:** Design 3 with integrated LCD and motorized stages



**Design 4:** this design focused on reducing the degrees of motion and post-alignment time, while keeping the position verification system the same as the benchmark. In order to reduce the degrees of freedom that the user has to adjust, the top layer holder is fixed from all degrees of rotation to be always parallel with the bottom stage. The digital microscopes are fixed from all degrees of rotation as well to be always perpendicular with the alignment stages. This significantly reduces the unwanted degrees of freedom in the system and saves time for the user. However, the decreased degrees of freedom may reduce the flexibility of the system for peculiar cases, for instance if the PDMS layers were not parallel.

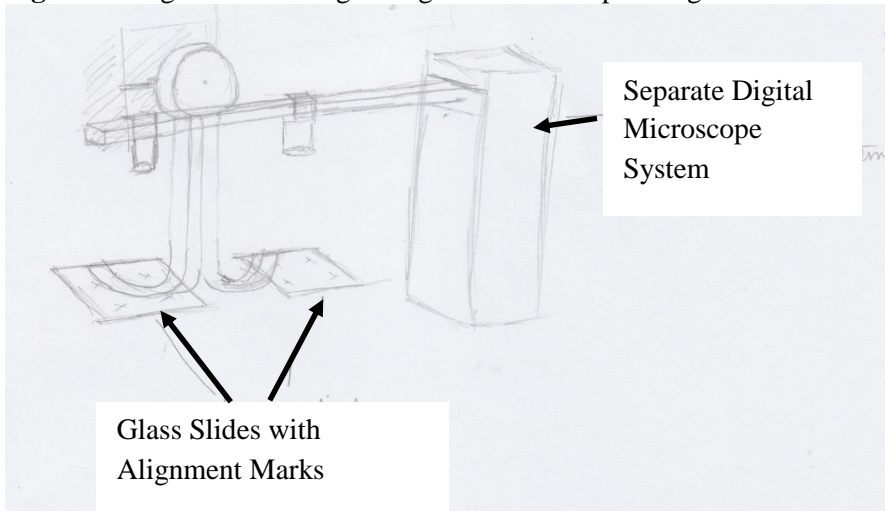
In order to reduce the post-alignment time, this design improves the tolerance between the frame of the glass slide and the holder. In the benchmark alignment device, the glass slide is approximately 2mm smaller than the holder, creating a range of error before and after plasma oxidation. This design puts a precisely manufactured aluminum frame around the glass slide, improving the tolerance in the sizes. The holder for the frame is also manufactured with high precision to ensure a tight fit between them. This allows the slides to be re-inserted into the alignment device after pre-alignment and plasma oxidation with high accuracy, reducing the post-alignment effort.

**Fig. 9:** Design 4 with high tolerance frame and holders to improve repeatability



**Design 5:** the last design concept aims to eliminate the post alignment process to shorten the alignment time and improve the bonding quality. The PDMS layers are aligned to pre-determined alignment marks on the glass slides. The glass slides are both facing up and are connected using a hinge design. This allows the PDMS layers to be aligned before activation, and then bonded immediately after oxidation by rotating the hinge and bringing the PDMS layers against each other. The open face design also allows this device to fit under an optical microscope, which provides better clarity but lacks the flexibility of aligning two markers at the same time like the other concepts do with digital microscopes. The fact that the PDMS layers are not aligned directly against each other provides difficulties in ensuring the alignment accuracy and repeatability, since errors on the glass slide markers or in the tolerance of the hinge cannot be corrected through visual alignment. This idea is also later rejected by the sponsor due to its complexity and the lack of similar designs on the market. Our sponsor emphasized that accuracy is still by far the most important requirement and that this design could compromise accuracy for ease-of-use.

**Fig. 10:** Design 5 with a hinge design to eliminate post alignment



### Final Concept Selection

For the final round of concept selection, a weighted scale in the form of a Pugh Chart was used to determine the alpha design. The user requirements were weighted according to the preferences of our sponsors and stakeholders. The performance of each of the designs was rated according to its performance against the current aligner on a scale between 1 and 5. The currently aligner used in the lab was considered as the benchmark, and it was scored a 3 across the board. The members of the team rated each of the designs and the average was taken for the final Pugh Chart. The rating of each of the categories was multiplied with the weight and summed up for the total score of the design. Design 4 totaled the highest overall score. We compared Design 4 closely with Design 2 that achieved the second highest score. After a thorough assessment we decided that Design 4 was, in fact, superior but our alpha design ended up being a combination of the five ideas.

**Table 3:** Design 4 was determined as the alpha design using the following Pugh Chart

Requirements	Weight	Benchmark	Design 1	Design 2	Design 3	Design 4	Design 5
Accuracy	7	3	4.2	4.4	3	3.6	2.4
Less Tedious	6	3	3.6	3.2	4.2	3.6	4
Adjustability	5	3	2.8	1.6	3.4	3	2.8
Manufacturability	4	3	1.8	3	3.2	3.4	0.8
Cost	4	3	2.8	3.6	2.6	3.2	2
Repeatability	3	3	3.8	4.4	3	4.6	3.6
Stability	2	3	3	3.4	3	3.4	2.4
Portability	1	3	3.2	3.2	4	3.2	2.4
Total		<b>96</b>	<b>104</b>	<b>107.6</b>	<b>105.4</b>	<b>112</b>	<b>84</b>

Our alpha design utilizes the storage function from Design 4, which has tight tolerance aluminum frame to reduce the post-alignment effort needed by the user. The advantage of this design is that it has no downside or trade-off in performance compared with the benchmark, and simply improves the alignment process. The positioning function is also derived from Design 4. This design kept the overall concept the same as the benchmark while reducing the degrees of motion on the top stage, reducing the amount of input needed from the user and speeding up the alignment process. This limits the aligner to only function for parallel PDMS substrates and requires tighter manufacturing tolerances, but we decided that this is a small trade-off for a much less tedious alignment system. The position verification function draws the concept from Design 2, which uses two digital microscopes on X, Y, Z stages much like the benchmark, but uses software to overlay two layers of focused image onto the screen to drastically increase the alignment accuracy. The choice of dual digital microscopes allows two alignment markers to be viewed at the same time, while allowing the video signal to be processed through a computer. Overall our alpha design seeks to improve on top of the current benchmark aligner without making compromises in any performance category.

## FINAL CONCEPT DESCRIPTION

Our chosen design (see Fig. 11) is a combination of a couple different ideas. A general overview of the design is given below followed by a detailed explanation of each sub-function.

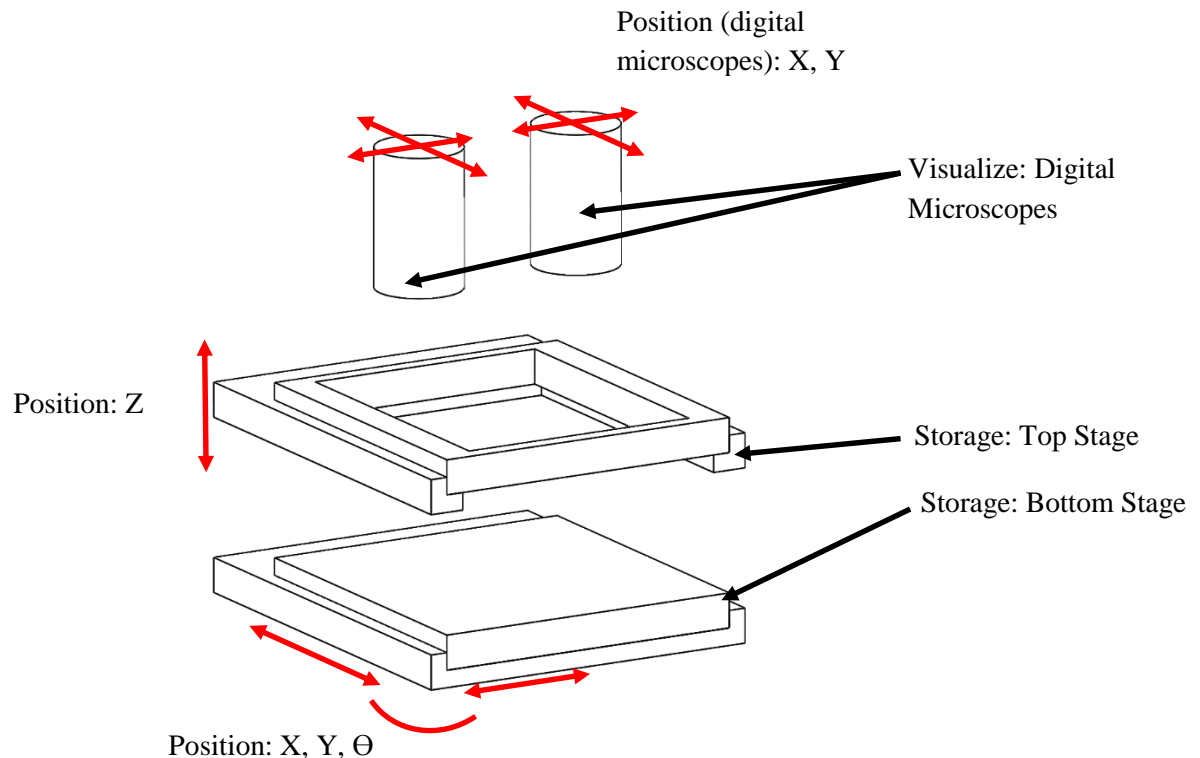
### General Overview

The design consists of a top stage and a bottom stage, each consists of a holder and frame. The holders are fixed to the device and the frames can slide into the holders. The latter has a piece of inset glass that the PDMS can stick to for the positioning process to be carried out. We stick the bottom PDMS layer to the top of the bottom stage, and the top PDMS layer to the bottom of the top stage. This allows the two layers to face each other so that when the final bonding needs to be carried out they just need to be brought in contact.

The top holder moves in Z and the bottom holder moves in X, Y and rotates around Z. To carry out the positioning process, the bottom slab can be moved with respect to the top slab to align them together. Once the layers have been positioned, the frames can easily be removed to be put in the plasma etcher to activate the PDMS surfaces. Once the activation process is complete, the frames can slide back into the holders for the user to complete the alignment and bonding process.

To visualize the alignment process, two cameras are integrated into the design. We use two cameras to allow the user to view two different alignment markers or channels. These cameras are connected to a supporting pillar using translational stages that enable the cameras to move in X and Y, allowing the user to position them exactly over the features that need to be viewed.

**Fig. 11:** Annotated 3D Schematic of the Alpha Design



### Detailed Explanation of Concepts Selected

Each aspect of the design was specifically chosen to best meet our user requirements. From the functional decomposition chart we identified four major sub-functions of the device: visualize, position (for

visualization device), storage (of both layers being aligned) and position (of the two layers with respect to each other).

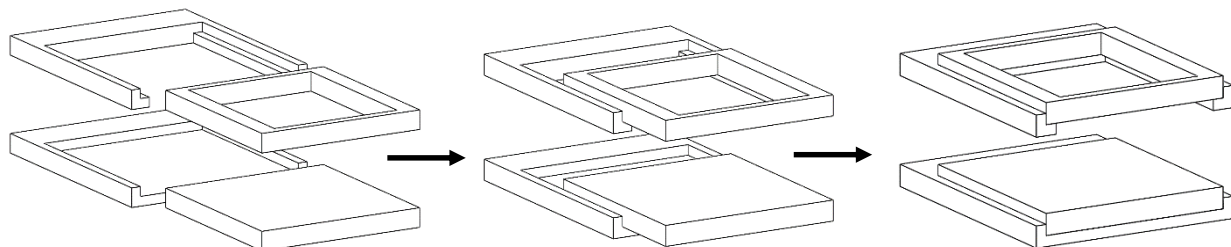
**Visualize:** two visualization devices were chosen to be used, like in the current aligner, so that the user can align two features (markers or channels) of the same devices at the same time. This makes the alignment process more accurate as it better accounts for rotational misalignment. The visualization devices used are cameras or digital microscopes. This allows the user to view both alignment features side by side on a screen, as opposed to viewing them one at a time through an eyepiece of a traditional microscope. This makes the process less tedious for the user. In addition to maintaining the necessary resolution to accurately view the alignment process, it is more cost effective.

**Position (digital microscopes):** the design incorporates a positioning mechanism for the digital microscopes (Fig. 11, p.23). This allows the user to exactly focus over the alignment features with ease and, consequently, improves the accuracy of the alignment process. The proposed design uses small XY translation stages to move the cameras in the X and Y directions independent of each other and the stages. Z-translation ability may be added if the range of vision provided by the chosen cameras is not sufficient to view the desired height of PDMS being aligned. These translational stages are mounted to a pillar that is separate from the rest of the device. This isolation ensures that while the user is making adjustment to the camera position, the positioning of the PDMS being aligned doesn't change and keeps the entire system stable when inputs are being made.

**Storage:** this is the component of the device that directly interacts with the PDMS. The storage device chosen for the top layer is a stage consisting of an aluminum frame with a piece of inset glass that can slide in and out of a holder fixed to the rest of the device. We chose glass because PDMS can attach to it temporarily and can be easily removed from it without damaging it. For the bottom layer, we used a flat piece of aluminum with a notch machined into the surface; the corner of a glass slide or plate can be aligned to this notch. One PDMS layer can be stuck to the bottom of the top frame and the other can be placed on a glass slide or plate which will, in turn, be placed on the lower stage. The user can remove the glass slide or plate to carry out surface activation in the plasma etcher without having to remove the aluminum plate. After oxidation, it can put back in its original position by realigning it with the notch on the aluminum plate.

For the top stage, we decided on an aluminum frame because the machined frame and machined holder allow for much higher tolerances than otherwise possible with just glass. This ensures that on sliding the frame back into the holder after oxidizing the surfaces, the two PDMS layers will be very close to their pre-activation alignment position. Hence the user only has to make a few inputs before the two layers are finally aligned and can be bonded together. This repeatability makes the process much less tedious for the user.

**Fig. 12:** Removable storage mechanism with holder and frame.



Initially, we designed both the top and bottom stages to be identical. Having glass inset into the bottom stage is only an advantage if you are carrying out PDMS to PDMS bonding. If in the future, the user wishes to bond PDMS to glass or PDMS to silicon, this glass storage device will be unsuitable because of its low friction. Hence, we redesigned the bottom stage with purely aluminum with a notch at the end to enhance the flexibility of our device – can be used for PDMS, glass and silicon applications. Silicon wafers have flats on one or two of their edges that can be aligned to the notch on one side of an aluminum plate.

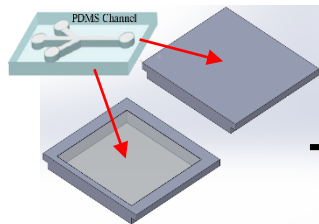
**Position (layers):** this feature of the design allows the two PDMS layers to be moved with respect to each other to carry out the alignment process. The chosen concept allows the bottom stage to move in X and Y and rotate about Z, and the top stage to only move in Z (Fig. 12, p. 24). It reduces the number of degrees of freedom to only those that are necessary for the alignment process, thereby keeping the accuracy while reducing the number of user inputs and making the process less tedious.

The resolution of these two stages allows the alignment process to be carried out accurately and easily. While positioning the two layers with respect to each other, only the bottom stage is moved to get the exact alignment desired. Once the two surfaces have been activated and re-aligned in the device, the top stage can be moved down in Z to bring the two surfaces in contact.

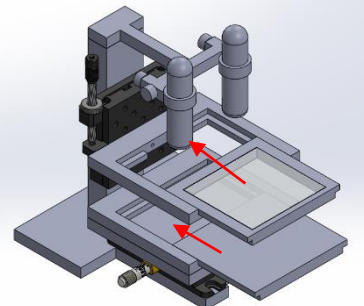
### Operational Diagram

We combined the various modules to form a complete device. Included below is a description of how we propose it will function.

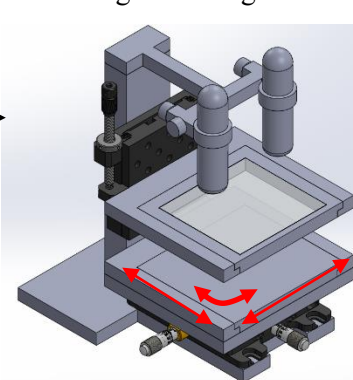
- (1) Place PDMS slabs into top and bottom frames



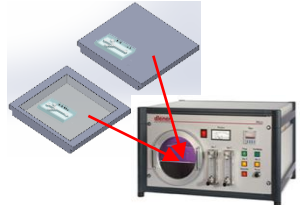
- (2) Insert Frames into their respective holders



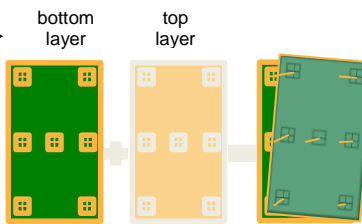
- (3) Use microscopes to view alignment markers and align them using XYΘ stage



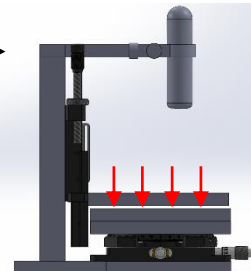
- (4) Remove frames and place them in plasma oxidizer to activate PDMS surfaces



- (5) Place frames back in its respective holders and correct for small misalignments



- (6) Bring the frames to contact and apply pressure to bond PMS slabs



## PARAMETER ANALYSIS

This section describes our approach to determining the specific parameters of our design. By analyzing the dimensions, materials, and other important properties of the different components we were able to refine our alpha design. The results of our calculations have been reflected briefly in the appropriate subsections below. Please refer to Appendix E for the complete calculation.

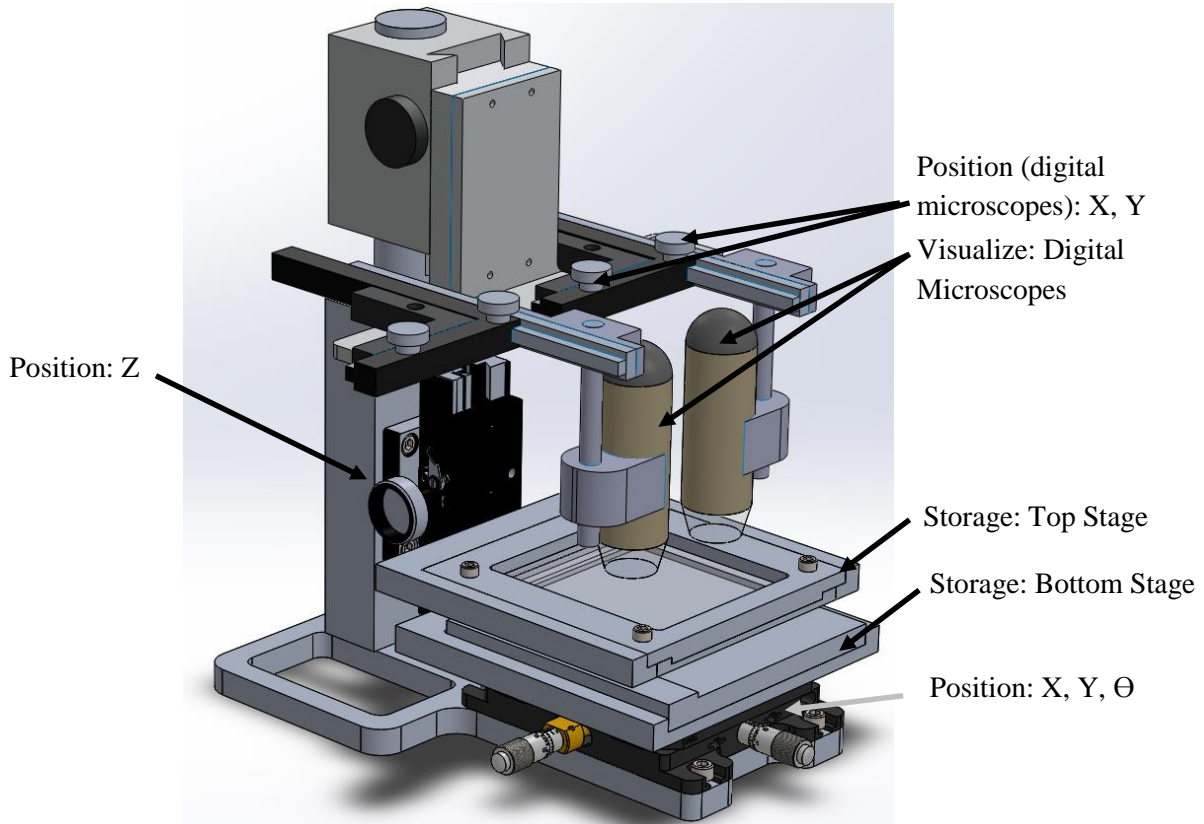
### Accuracy Analysis

The most important specification of our design is accuracy of alignment. Each component of our design influences this accuracy. Two basic functions affect accuracy: visualize and position; we determined the required parameters so that our system collectively achieves an alignment accuracy of 20-50 microns.

Since the alignment errors will be evaluated by measuring the magnitudes of the distances between known evaluation marks on the PDMS we accounted for the inaccuracies caused by all of the systems by summing the offsets. The visualization device resolution ( $A_v$ ) is 10 microns radially, the allowable  $0.1^\circ$  angle of the camera deflection offset ( $A_c$ ) is 1 micron, and the alignment stages deflection allowed of  $0.1^\circ$  causes an offset ( $A_s$ ) of 1.5 microns. The resolution of the XY stage ( $A_{xy}$ ) for the bottom layer must be 10 microns or greater. After compiling the errors for all the components, the aggregated accuracy came out to be 22.5 microns, which meets the 20-50 micron accuracy requirement.

$$\text{Total Accuracy} = A_v + A_c + A_s + A_{xy} = 22.5 \text{ microns} \quad (\text{Eqn. 1})$$

**Fig. 13:** CAD model of the design concept with all functions labelled



**Visualize:** our final visualization system consists of two digital microscopes to observe the alignment.

*Visualization accuracy:* the purpose of the visualization device is to see the offset between the alignment marks on the two PDMS layers. The relative position, instead of absolute position, is used for alignment. Therefore, we have neglected any potential inaccuracies caused by the lens and the image sensors and any other sources of error that would affect both of the alignment marks equally. However, the resolution of the visualization system is one of the largest sources of inaccuracies in the system. In order to meet the 20 micron accuracy, we decided that the resolution for the microscopes have to be 10 microns or better to leave room for error in the other sub-functions. The resolution of a digital microscope can be calculated using several methods:

The first method assumes the field of view (*FoV*) and image sensor pixel count (*n*) is known to us [29].

$$\text{Resolution} = \frac{\text{FoV}}{n} \quad (\text{Eqn. 2})$$

The second method requires the values of magnification (*M*), image sensor pixel count (*n*), and image sensor size (*S*) [29].

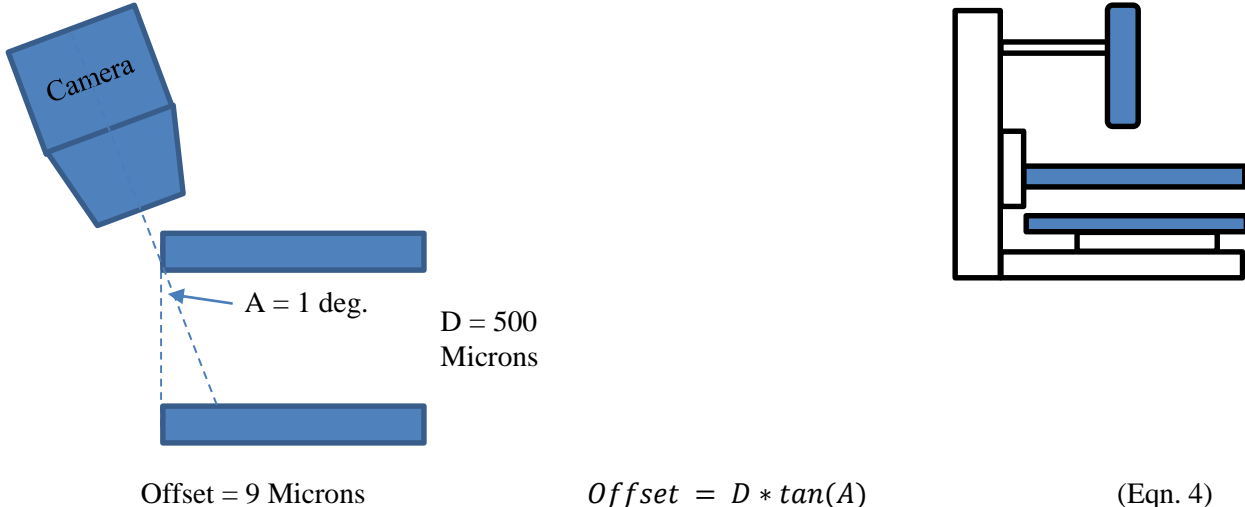
$$\text{Resolution} = \frac{S}{n*M} \quad (\text{Eqn. 3})$$

For example, the Dino-lite premier digital microscope [30] has a 2592 x 1944 resolution (5 megapixels), 20X magnification, and 19.8mm field of view. At this magnification, each discrete pixel on the screen represents 7.6 microns on the PDMS. For the digital microscopes that offers variable zoom, a higher magnification will allow higher resolutions. For example, a 50X magnification and 7.9mm field of view on the same microscope gives a 3 micron resolution. We used this method to calculate the resolution of the digital microscopes to choose the ideal product.

The resolution of the visualization monitor can limit the resolution of the output image if it is lower than the resolution of the camera. A digital zoom function at the screen can help ensure the full resolution of the camera can be shown on the monitor.

*Camera angle:* in order to accurately view the samples, the angle between the digital microscope and the PDMS layers should be 90 degrees. Any offset from that angle results in alignment inaccuracies. Assuming the distance between the PDMS layers during alignment is around 0.5mm, simple trigonometry shows that an angle of 1 degree offset could cause an alignment error of 9 microns (Fig. 14, p. 28). Therefore, it is crucial that we maintain the perpendicular relationship between the PDMS layers and the digital microscope with an offset less than 0.1 degrees to reduce the alignment error below 1 micron.

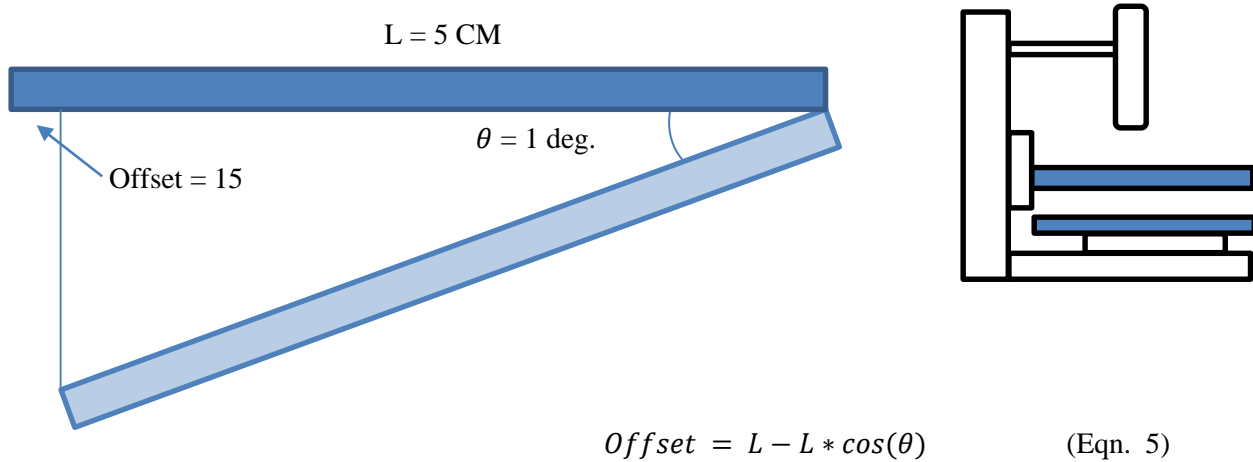
**Fig. 14:** Simple trigonometry showed that the deflection angle needs of the camera to be less than 0.1 degrees.



**Position:** the bottom stage has to move in X, Y and rotate about the z-axis. This is to ensure sufficient degrees of freedom to carry out the alignment process. The accuracy of the stages must be 10 microns or greater. Both of these requirements are identified in the Accuracy section of this report. The top stage must move in the Z-direction to bring the two layers of PDMS in contact to complete the bonding process. Per user requirements, to bond up to 6 layers of PDMS together (each one is 1cm thick, [1]) and hence there should be minimum Z-adjustability of 7cm. In order to achieve the highest alignment accuracy, we have chosen alignment stages that can be adjusted continuously instead of incrementally. This gives the user infinite adjustability and that, with enough time, the alignment can be as accurate as the visualization devices can discern.

Any angular offset between the top and bottom stages will result in significant alignment errors. For example, with a 5 cm wide PDMS substrate, an angle of 1 degree offset can cause a perfectly aligned device appear to be misaligned by 15 microns (Fig. 15). Since the stages will be manufactured and assembled by us, our goal is to minimize the deflection angle between the stages to be below 0.1 degrees, which reduces the alignment error to be below 1.5 microns.

**Fig. 15:** Simple trigonometry showed that the deflection angle,  $\theta$ , needs to be less than 0.1 degrees.



### **Storage: Frame and Holders**

Based on the user requirement of flexibility, we determined parameters that the top and bottom frames and holders needed to meet in order to satisfy the requirement. The top frame has to fit both a 4" diameter silicon wafer [31] and a 2" x 3" rectangular glass slide. These are the two most commonly used dimensions in the lab [1]. Hence the placement area on the bottom stage must be 4" square or higher, and the top stage must have at least a 2" x 3" glass piece to stick the PDMS to. The maximum dimension is limited by the interior dimensions of the plasma etcher available to the graduate students. Based on this the maximum dimensions of the top and bottom frames are 5.25" x 5.25" to be able to fit both stages in the etcher at the same time. Aluminum can be used to manufacture the frames and can be placed in the plasma etcher as well [32]. Both holders are designed to fit the frames.

Since the alignment errors will be evaluated by measuring the magnitudes of the distances between known evaluation marks on the PDMS we accounted for the inaccuracies caused by all of the systems by summing the offsets. For example, the visualization device can be offset by 10 microns radially, the angle of the camera can be offset by 0.1°, and the alignment stages can also be offset by 0.1 deg. After compiling the errors for all the components, the aggregated accuracy came out to be 22.5 microns, which meets the 20 micron accuracy requirement with a safety factor of 1.6.

### **Material Selection**

A brief summary of our material selection is provided in this section. A comprehensive explanation of the process we followed is provided in Appendix C. We used CES EduPack 2013 to quantify the selection of materials for our device. The alignment platform when assembled has several components in cantilever. The material selected for these components had to be stiff to minimize deflections, be lightweight to reduce the weight of the device, and be easily machinable to high precision (Table C1). By approximating the holders to be beams in cantilever that support both their own weight and the weight of the frame, we generated Eqn. 6 (below) to represent the Material Index ( $M$ ) in terms of the Young's modulus ( $E$ ) vs. density ( $\rho$ ) of the beam.

$$M = \frac{E^{1/3}}{\rho} \quad (\text{Eqn. 6})$$

The Young's Modulus vs. Density plot with machinability constraint and line of slope 3, corresponding to the Material Index, was plotted on a material's property chart (Fig. C3, Appendix C) to find that Cellulose polymers, ABS plastic, glass fiber reinforced polymers, aluminum and cast aluminum alloys would fulfil our requirements. We chose aluminum as it is easy to machine to high accuracy with the tools we currently have access to.

We also analyzed the environmental impact of Aluminum (Al) and Glass Fiber Reinforced Plastic (GFRP), since both are candidate materials and are also available in SimaPro. We found that GFRP have a bigger environmental impact in terms of raw, water, and soil emission. However, aluminum's impact in the resources and human health meta-categories (Fig. C7, Appendix C) makes it the material with a larger negative environmental impact, especially considering the entire lifecycle. But in the end, we chose aluminum as it is easy to machine to high accuracy with the tools we currently have access to.

### **Thermal Analysis**

The nature of PDMS makes it susceptible to changes in temperature. Conducting a thermal analysis will allow us to determine how the change of temperature in the room affects the PDMS sample.

Assuming that PDMS expands linearly we can use Eqn. 7 to estimate the change in strain and change in length due to a temperature change, where  $\epsilon$  is the strain on the PDMS,  $\Delta T$  is the change in temperature,  $\Delta L$  change in length, and  $L$  is the original length. The coefficient of thermal expansion,  $\alpha_L$ , of PDMS is 3.010-4C-1[33] from -55 to 150 Celsius. Further assumptions include that the temperature does not change by more than 20 degrees in the laboratory environment.

$$\epsilon = \alpha_L \Delta T = \frac{\Delta L}{L} \quad (\text{Eqn. 7})$$

**Fig. 16:** Plot representing the linear relationship between the strain in PDMS per change in internal temperature

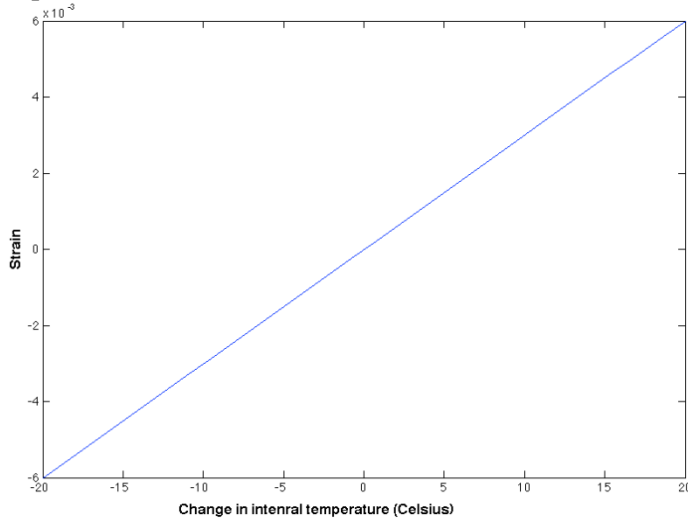


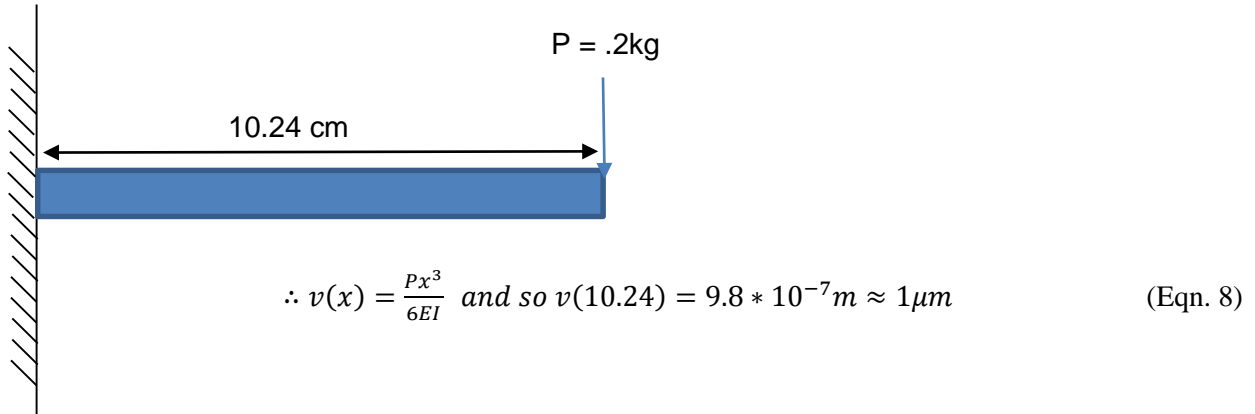
Fig. 16 depicts the expected linear relation between temperature change and strain, the greater the temperature change the greater the strain. A two degree change in temperature results in a strain of  $6 \times 10^{-4}$ . In perspective a one inch long sample will expand by 15.2 microns. At our scale this change is significant and deteriorates the accuracy of the alignment. Bigger samples will expand more and hence have a larger negative impact in the alignment.

In addition to room temperature change, the plasma oxidation process will also heat the PDMS sample. In this case there is a direct transfer of heat into the PDMS which will rapidly increase its internal temperature. The effect of the plasma oxidation will mostly affect a thin layer on the exposed surface [34]. Hence, it will have a minimum effect on the overall sample and can be neglected.

### Structural Deflections

Our device comprises several parts that are in cantilever bending. We approximated these as beams and carried out bending analysis for each part. A detailed explanation of our results is provided in Appendix E. It was crucial that we checked to make sure that our digital microscopes would not cause any deflection in their holders.

**Fig. 17:** Free body diagram of the cameras in cantilever



Using the above methods we found that the deflection in the digital microscope holders was approximately 0.10 micron. This amount of deflection in the digital microscope is within the range specified in the Accuracy Analysis and will not cause significance loss of resolution. We determined this by creating a simple beam bending model with the weight of the component distributed on top of the device. The weight of the cameras was considered as a point force. Based on these forces we calculated the maximum bending moment and the maximum deflection.

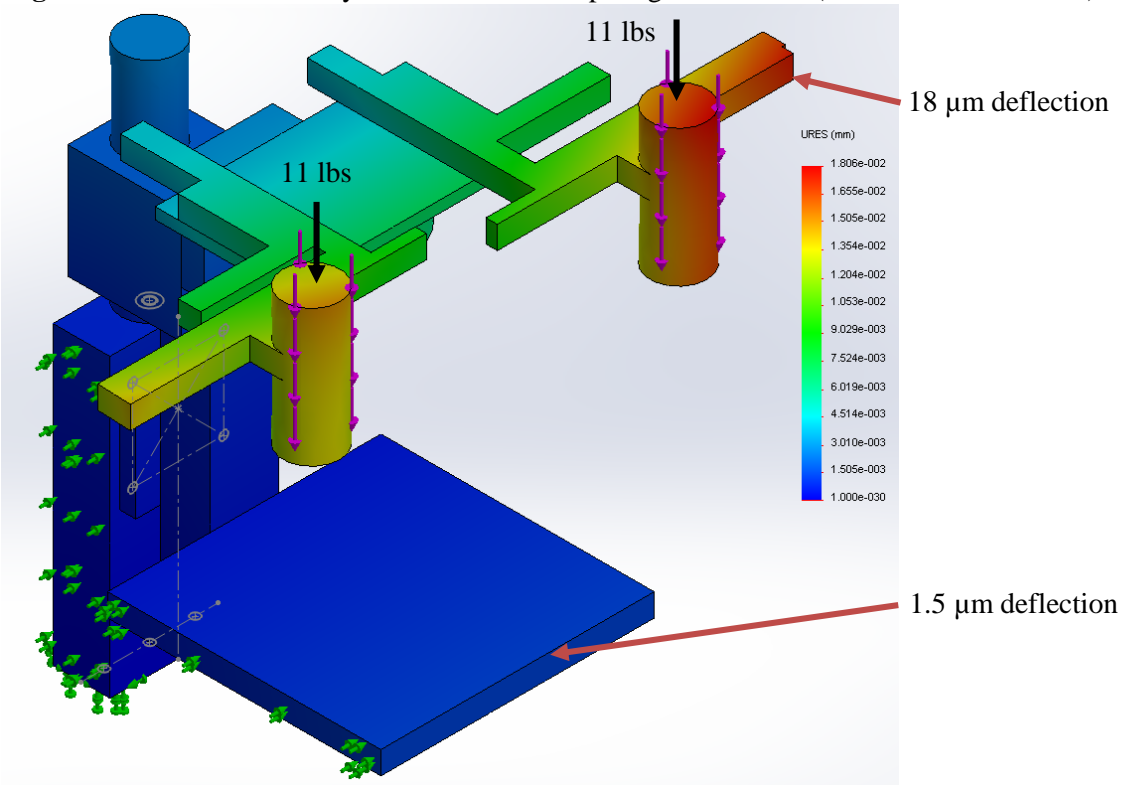
We also similarly analyzed the deflection in the holders. We saw negligible bending due to the fact that the part of the holder is behind the vertical support so there is almost no moment felt by the holder. We found the deflection to be 1 micron. Thus the accuracy within 1.5 microns and it does not affect the alignment process.

### Full Structure Analysis

In order to calculate the total deflection we have in our pillar, we ran a Finite Element analysis on a simplified model of the full structure. This analysis took into consideration the weight of the cameras (2lbs each) and the glass in the top frame as well as the structures holding these two. In addition, a load of 30N (9lbs) was applied to the camera mounting structure to simulate the loading when the user is moving the cameras. The main purpose of this simplified model was to roughly estimate how much the top frame deflects by (and therefore the top layer of PDMS) to see if this was within the range required for the device accuracy.

We found that the maximum deflection was at the cameras (18 micron deflection). The deflection at the end of the top stage was approximately 1.5 microns which is within our required range.

**Fig. 18:** Full Structural Analysis to Determine Top Stage Deflection (Plot of total deflection)



## FINAL DESIGN DESCRIPTION

This section describes our final, manufactured alignment platform. The final design has the same features as the prototype. Included below is a quick summary of all the components of our device, followed by a detailed description of each one.

1. A top stage and bottom stage on which the PDMS layers to be aligned are placed. A piece of glass is integrated into the top stage to allow the top PDMS layer to stick to the bottom and directly face the bottom PDMS layer.
2. Each stage consists of a holder and a frame. The holder is fixed to the alignment device and the frames can slide into the holders. The frame holds the PDMS. Once the layers have been positioned, the frames can be removed to be put in the plasma etcher to activate the PDMS surfaces. Once the activation process is complete, the frames can slide back into the holders for the user to complete the alignment and bonding process.
3. The bottom stage can move in X and Y and rotate about the Z-axis, and the top stage can move in Z. The bottom layer can be moved with respect to the top slab to align them together. To finally bond the two layers together, the top layer can be moved down in Z until the two layers are in contact with each other.
4. To visualize the alignment process, two digital microscopes are integrated into the design. This allows the user to view two different alignment markers separated by a distance. These microscopes are connected to a supporting pillar using translational stages that enable them to move in X and Y. They can move together in Z to allow for focusing with respect to the stages.

**Fig. 19:** Exploded view of our complete prototype design

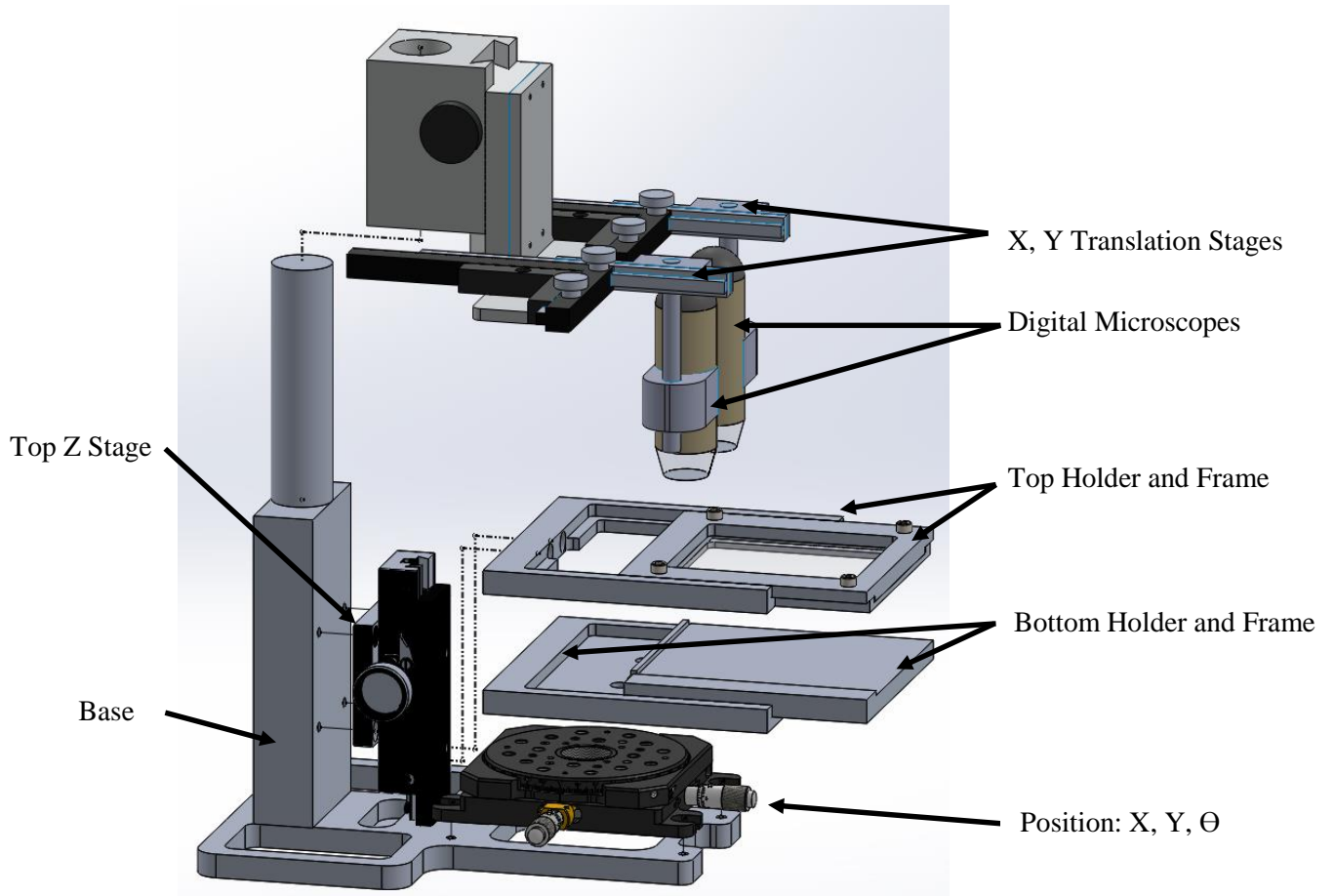
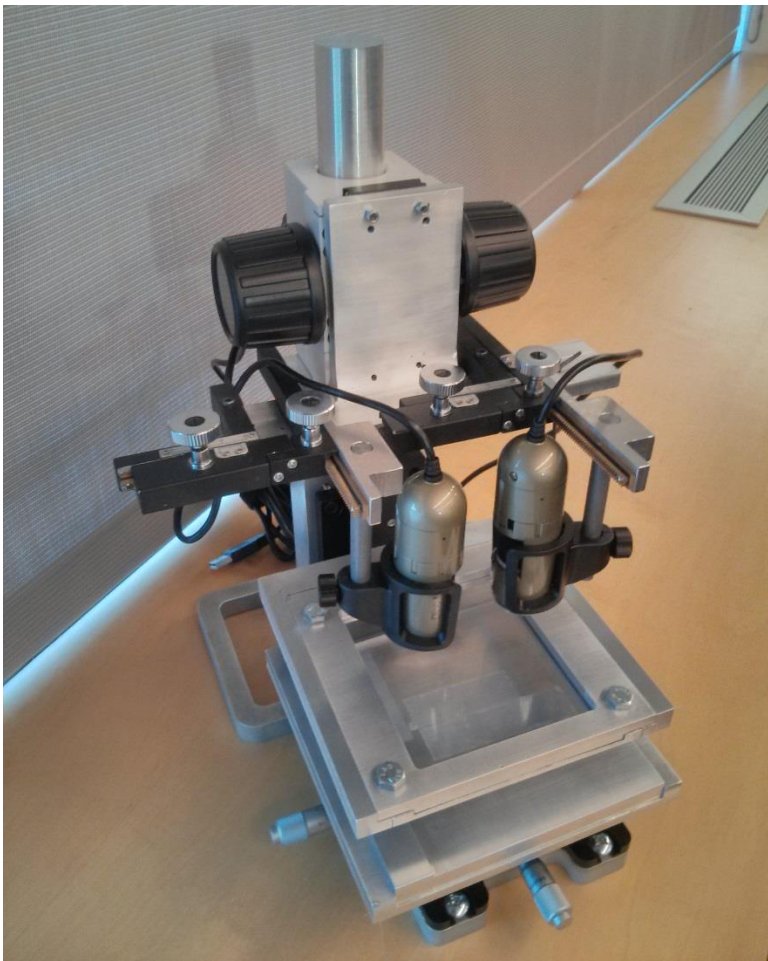


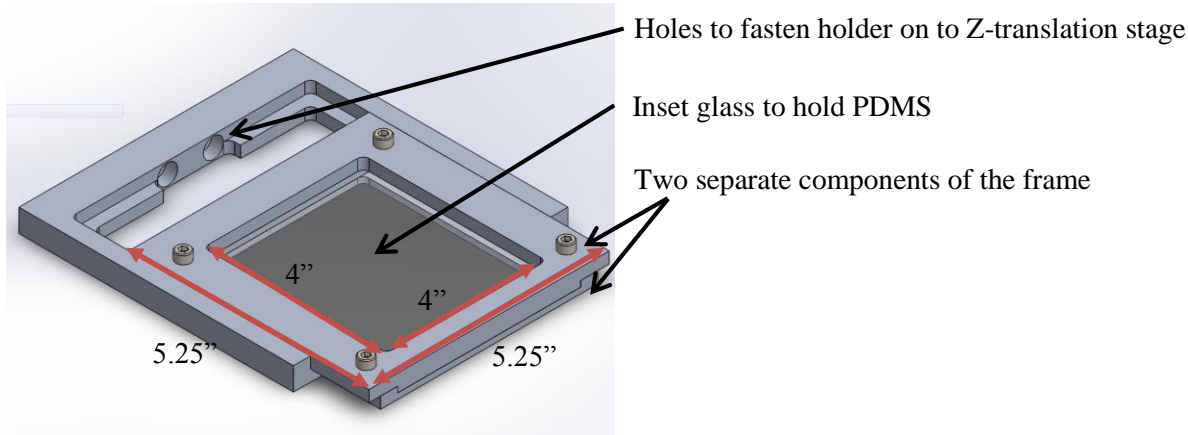
**Fig. 20:** Fabricated Prototype



### Top Stage

The top stage consists of a frame and a holder. The frame holds the PDMS underneath it so it can face the bottom layer. To do this it integrates a piece of glass into the frame that the PDMS can stick to. Per the parameters for the frame, the glass must be greater than 2" x 3" in size (as specified by the user) and the overall size of the frame must be less than 5.25" x 5.25" to fit in the plasma etcher. The final design is a two-piece design that integrates a piece of 4" x 4" glass into the frame. The frame is purchased from McMaster Carr [35]. The two piece design was selected to increase the ease of manufacturability. The two pieces are held together by 4 #10-32 bolts. The design also integrates a slot so that it can slide into the holder. The holder has two holes perpendicular to its back that are used to fix it to the Z-translation stage.

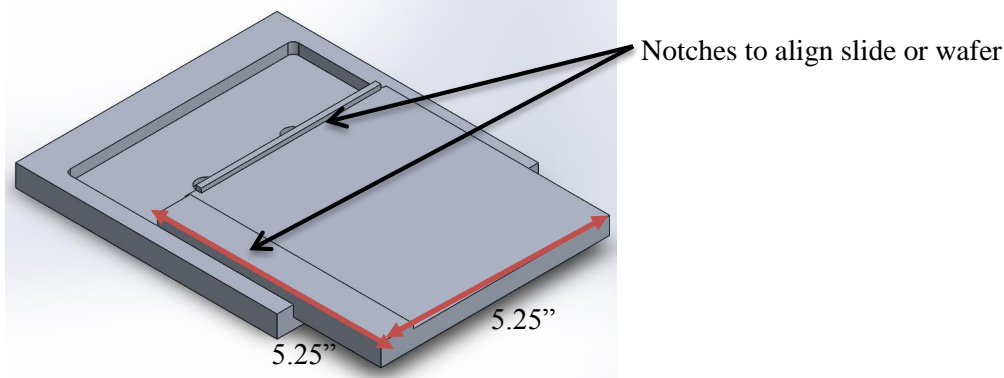
**Fig. 21:** CAD rendering of the top stage showing the frame, with the inset glass piece, sliding into its holder.



### Bottom Stage

The bottom stage consists of a frame and a holder. The frame is designed to either hold a glass slide with PDMS bonded to it or a silicon wafer. Per parameters for the frame, it must be able to hold either a 2" x 3" glass slide or a 4" silicon wafer [1] and must be smaller than 5.25" x 5.25" to fit within the plasma etcher. The current design measures 5.25" x 5.25", and has a notch machined into the top to push the corner of a glass slide or the flats of a silicon wafer against. The notch is located so that the PDMS layer on the bottom roughly aligns with the PDMS layer on the top. The frame has a slot that slides into the holder and also has grooves machined in the bottom to prevent interference with the bolts that fix the holder to the XYR translation stage.

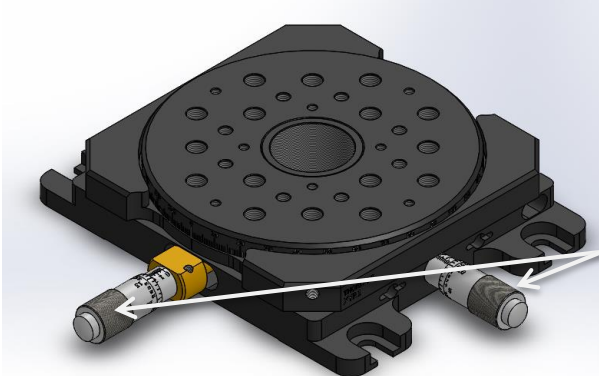
**Fig. 22:** CAD rendering of the bottom stage showing a slide with a notch to align the bottom layer



### XYR Translation Stage

This stage is used to move the bottom stage in X and Y and rotate about Z to align the two PDMS layers with respect to each other. Per the parameters for this device, it must have a translational accuracy of 10 microns or better. We chose the Thorlabs XYR-1 stage [37] to accomplish this. It has a micrometer-style XY translation stage and a rotary stage that rotates about Z. The minimum marking on the micrometer of X and Y is 10 microns, which meets the requirement. However, the micrometers themselves are continuously variable and hence movements of even less than 10 microns are possible. The rotary stage has markings of 1 degree but it is also continuously variable and hence even smaller rotations are possible.

**Fig. 23:** CAD rendering of the base XYR translation stage to carry out a majority of the alignment

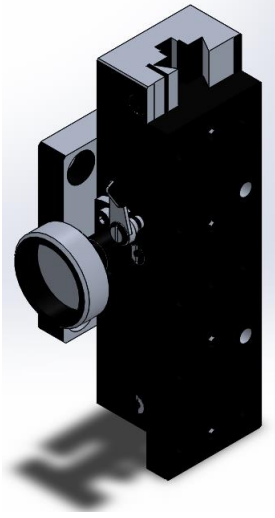


Micrometer-style control knobs for X and Y translation

### Z-Translation Rack and Pinion

This rack and pinion is used to move the top stage in the Z direction to bring the two PDMS layers close together for the alignment process and then into complete contact to complete the bonding. Per the parameters for this device, it must have a range of at least 7cm to accommodate up to 6 layers of PDMS. We chose to use a dovetail-style rack and pinion from OptoSigma [36] with a range of 8cm. We chose this device because it was cheaper and easier to integrate into our device than a micrometer-style stage and was also easy to use.

**Fig. 24:** CAD rendering of the rack pinion that will be used to finally bring the two layers together.



### Digital Microscope System

We chose digital microscopes based on the working depth and required resolution. We needed a minimum magnification of 20x and a working depth of at least .75". For the chosen DinoLite AD4113T digital microscopes, the working distance is 0.95" at 30x magnification and the field of view is 0.6" x

0.25". The resolution at this magnification is 6 microns, which meets our required parameter. The resolution was calculated by dividing the field of view by the number of pixels along that length.

**Fig. 25:** DinoLite AD4113T digital microscope with 6 micron resolution at 30x magnification.



#### Digital Microscope XYZ Stage

The design incorporates a positioning mechanism for the digital microscopes. The stage is an assembly of repurposed microscopes parts that allow for XYZ translations. Z-translation is required to adjust the focus and to accommodate for alignment of several layers. It will be controlled by a focus rack with a 2" range [Fig. 27(a)]. The digital microscopes move independently in the X-Y plane but not in the Z-direction. Each digital microscope will be attached to a compound microscope attachable X-Y mechanical stage [Fig. 27(b)] with a 3" range in both directions. Due to the small field of view there is the need to translate in X-Y to focus on the different alignment markers. The entire assembly will be mounted to a pillar separate from the rest of the device. This isolation ensures that while the user is making adjustment to the PDMS position, the digital microscope doesn't lose focus and the image remains stable.

**Fig. 26:** The images below correspond to (a) focus rack part used in microscopes. (b) X-Y attachable mechanical stage

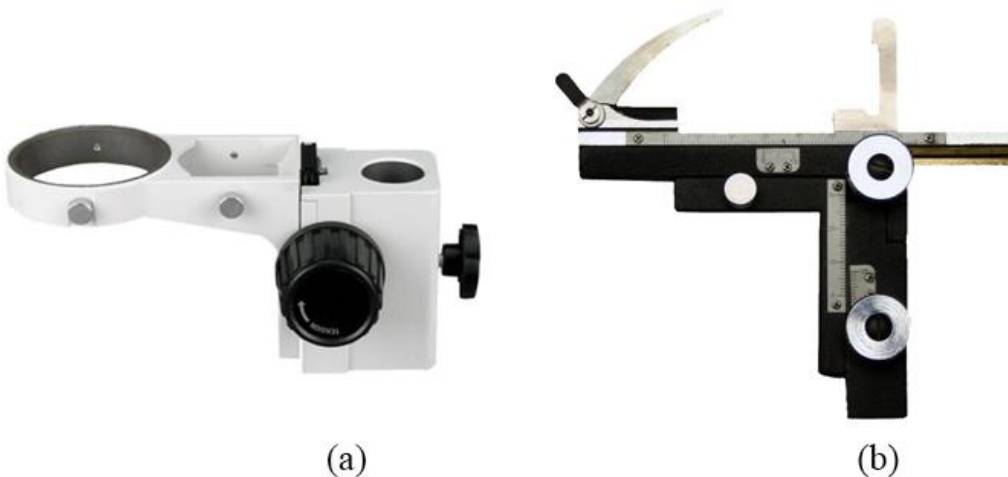
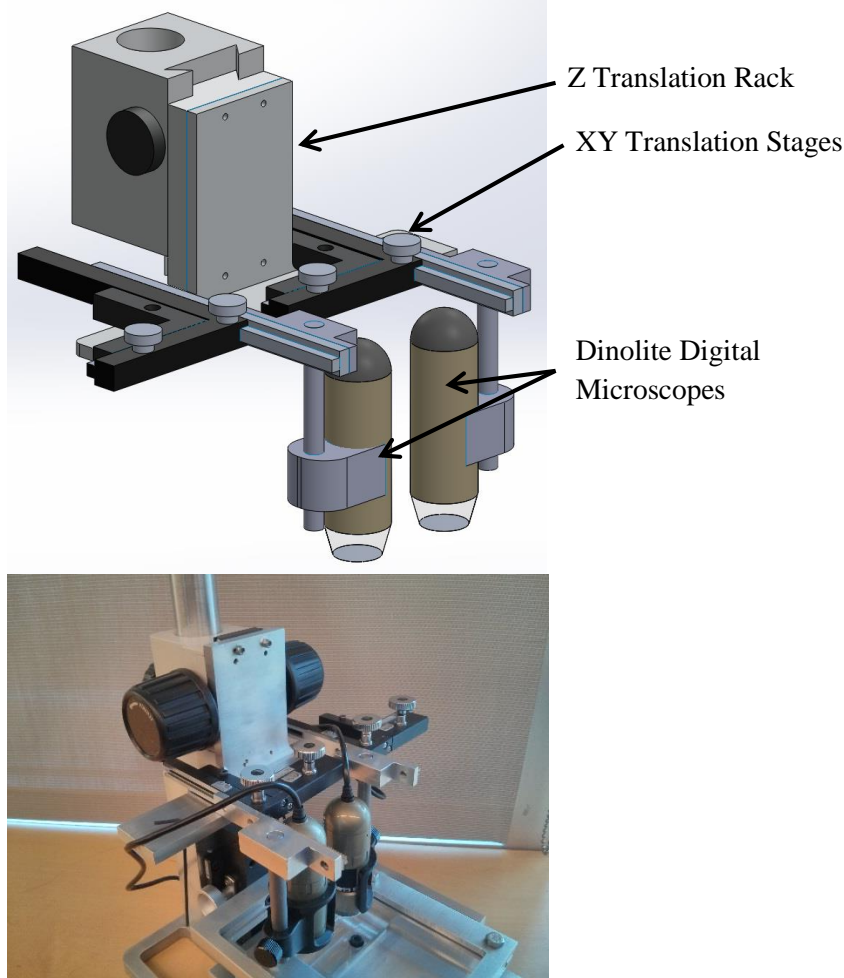


**Fig. 27:** CAD rendering of the complete mount and aligner system for the digital microscopes with final prototype



### Dinolite Transparency Function

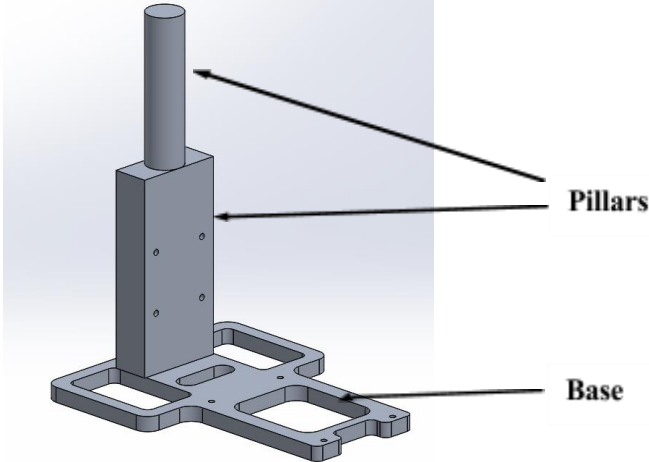
A challenge with the current crude aligners is that the digital microscopes do not have the proper depth of view to focus on two layers of PDMS at the same time. Instead the graduate students typically focus on a spot between the PDMS layers and then align two blurry images of the PDMS layers with each other. In order to view both of the PDMS layers clearly during the alignment, we are planning to use the Dinolite Transparency Function [38] to aid the alignment process. Since only the bottom PDMS layers will be moved during the alignment process, we will capture the focused image of the top PDMS layer and transparently overlay the live feed video of the digital microscope over the image. Then the digital microscope will focus on the alignment marks on the bottom layer, allowing the user to match it to the focused image of the top PDMS layer. This allows the user to see a significantly more accurate visualization of the PDMS alignment marks and therefore improving the alignment accuracy.

### Base and Pillars

The base and pillars hold all the components of the device together. The base holds the X-Y-R translation stage and the main pillar. Per the parameters determined for the base, its footprint must be within 14" x 14". The final design has a foot print of 8" x 10". The main pillar in turn holds the Z-translation stage and the camera pillar. All the components are manufactured out of aluminum due to its high strength, light weight and relatively low cost. The camera pillar is 1.25" in diameter (to fit the camera Z-stage) and this

in turn dictates the 1.25" width of the main pillar. The camera pillar is threaded and threads into the main pillar.

**Fig. 28:** CAD rendering of the base plate with main and camera pillars



### FABRICATION PLAN

In order for our device to be able to generate high accuracy microfluidic devices it needs high tolerance components. The following components were purchased in order to ensure its high quality: X, Y, and rotational aligner for the bottom frame, Z stage for the top frame, two cameras, X and Y aligner for the cameras, and Z stage for the two cameras. There are 7 major components that we are going to be manufacturing. Of these the camera pillar will be made on the lathe. The rest will be manufactured on the mill.

A preliminary Bill of Materials consisting of all our components and a step-by-step manufacturing plan for each manufactured part has been attached in Appendix A. An assembly plan has also been included in Appendix F.

## VALIDATION AND VERIFICATION

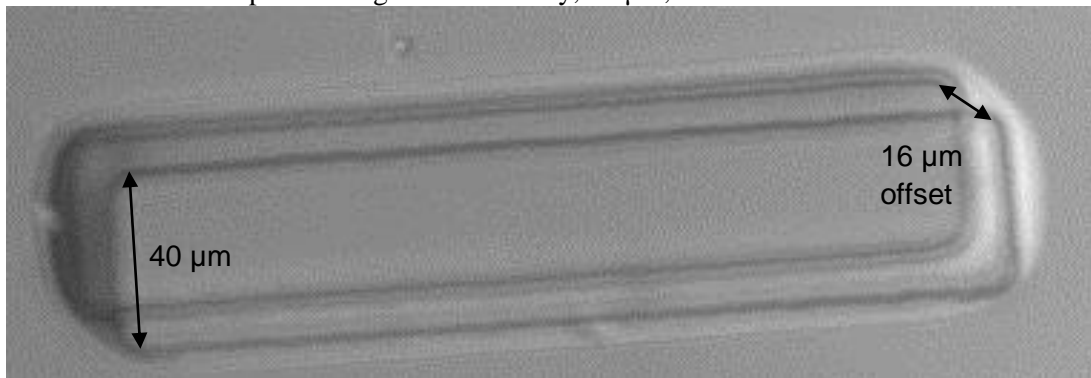
In the previous sections we listed the user requirements for the alignment platform and provided quantified engineering specifications for each one. In this section, we will discuss how we verified that our prototype meets every one of those specifications. We shall go over the experiments we ran, the potential factors and random variables that influenced the tests, and our test results. The alignment procedure we followed is laid out in Appendix G. Please note that our validation techniques are limited by the availability of testing facilities and our project budget. We have summarized our results in Table 6 (p. 43) at the end of this section.

### Accuracy and Less Tedious

Ensuring that our device has an accuracy of 20 microns or better is our primary goal. Our choice of alignment stages and image acquisition tools will ensure that this goal is achieved.

We believe that the best way to validate the alignment accuracy and alignment time is to let new users align typical PDMS slabs that are normally used in the IBBL with our aligner. We have chosen two different sizes of PDMS slabs, one 1 cm by 1 cm slab requiring only one camera, and one 6 cm by 3 cm slab with two alignment marks requiring two cameras. Both types of PDMS slabs have 40- micron alignment marks throughout the slab on both layers as shown in Fig. 31. The absolute distance between features represents the alignment accuracy, as shown below in Fig. 31. Due to the constraint of testing time, only single camera alignment was tested and discussed below.

**Fig. 29:** the micrograph of two bonded layers of PDMS with 40-micron alignment marks captured using Zeiss Axio microscope. The alignment accuracy, 16  $\mu\text{m}$ , is shown here between the features.



We validated the accuracy by aligning and bonding two layers of PDMS and then capturing a micrograph of the alignment markers on PDMS slabs. The Zeiss Axio microscope available at the IBBL allowed us to take high resolution micrographs for this purpose. The micrographs produced by these microscopes were also calibrated for precise distance measurement down to a resolution of 0.623 microns per pixel. Once the micrograph was captured, the magnitude of the distance between the features of the alignment markers were determined using Adobe Photoshop, where the number of pixels between features were measured, and then converted into microns. For each aligned PDMS device, we measured the alignment accuracy at the two opposite corners of the device to get the maximum error in the device. These values were then averaged to give us the overall alignment error.

We considered two methods of quantifying the alignment error. The first method defines X and Y axis on the top layer, and then evaluates the offset of the bottom layer in the X and Y direction individually as well as the rotational offset theta. The advantage of this method is that it illustrates if the major source of error is introduced by the X and Y stage or the rotation stage. However, due to the limited field of view of the micrograph, an accurate measurement of the rotational offset could not be quantified. Instead, we

chose the second method, which measures the maximum offset in the opposite corners of the devices, combining the errors introduced by X, Y, and rotation into one single accuracy value. The downside of this method is that it only quantifies the maximum error in the PDMS structures, giving us a conservative estimate of the accuracy.

The accuracy of finished product is also largely dependent on the user's skill and experience with the device. We aim to develop a product that is easy to use even for a first time user. We conducted 5 trials per new user so we could analyze the pre- and post-activation alignment times and the final accuracy after bonding. The user followed the procedure as described in Appendix G. Each new user aligned five identical PDMS slab pairs for the trials, and the same set of slabs were used for each new user to ensure proper replication of the trials. We chose 5 trials so we could have a more precise mean and a standard deviation of alignment accuracy for a new user [41]. These alignment times and accuracy values were then averaged and are presented below along with standard deviation (Table 4 and Table 5).

**Table 4:** Preliminary testing for single camera alignment show that the alignment accuracy for a new user is 33.6 microns with a standard deviation of 10.5 microns

	New User 1	New User 2	New User 3	New User 4	Total
Average ( $\mu\text{m}$ )	30.4	35.5	37.9	30.5	<b>33.6</b>
Standard Deviation ( $\mu\text{m}$ )	13.7	7.5	6.9	14.0	<b>10.5</b>

**Table 5:** Preliminary testing for single camera alignment show that the average pre-activation alignment time is 4.1 minutes and post-activation alignment time is 4.0 minutes.

	New User 1	New User 2	New User 3	New User 4	Total
Pre-Activation Alignment Average (mins)	3.8	2.8	5.4	4.6	<b>4.1 ± 1.0</b>
Post-Activation Alignment Average(mins)	5.6	3.7	1.6	5.2	<b>4.0 ± 1.9</b>

Due to the constraint of time, this study is limited by the quantity of data. Preliminary results suggests that we met our sponsor's requirement of 20-50 microns as well as 10 minutes post-activation alignment time. Since these tests were performed immediately after the completion of our prototype, we lack data from mid to high level proficiency users, who we expect to turn in significantly better results, especially in the alignment time category.

The experiment procedure included different smaller tasks to ensure that there was a factor of repeatability and replication in the experiment. For replication, the digital microscopes were reset to their starting X and Y positions and were hence needed to be calibrated by the user for each test. We conducted the tests using the same PDMS samples for repetition, which means that we could not oxidize the surfaces before attaching the layers to prevent permanent bonding. The starting positions of the alignment stages were also randomized to simulate different scenarios.

There are several factors that may have altered the results. During testing, the environmental noise factors such as temperature, humidity, and even vibrations from the construction work being conducted nearby all played a role. Since this device is to be used in the open lab (i.e. not in an environment controlled clean room), testing it at our sponsor's lab simulates the effects of these noise factors for the best estimate of the future performance. However, some error factors during testing will not translate into actual usage.

For example, the PDMS structures given to us for testing had noticeable deformations and inconsistent thickness, both of which are significant factors that could contribute to the alignment and bonding errors. Our sponsor has agreed that carefully manufactured PDMS layers for actual experimentation will not have the same flaws. In addition, the fact that we bonded the PDMS structures without oxidizing the surfaces first caused us to increase the contacting force to ensure a solid adhesion between the layers, effectively causing extra deformation in the elastomer during bonding and increasing the alignment error.

### **Adjustability**

We have designed our device to be flexible when it comes to the number of PDMS layers of different sizes and thicknesses that it can accommodate. The thickness requirement was validated by stacking 6 layers of 1cm thick PDMS slabs [1] one on top of the other starting from the bottom stage to check if it fits underneath the upper stage when raised to its upper limit. This only requires one trial to validate the Z stage's range can accommodate 6 PDMS layers while the camera can still focus on the top layer. Our tests have validated that this is possible.

### **Project Cost**

Our project budget was initially fixed at 2000 USD but our sponsor has set this as a soft constraint, where this value can be increased for better performance. Our expenditure totaled to be \$2019.18. A general overview of our expenditures can be found in the Bill of Materials (Appendix A)

### **Repeatability**

The idea behind this specification was to minimize the disturbance to an aligned system after the PDMS samples were put back into the alignment device after activation. To achieve this, the relative position between the two slabs must stay the same even after they have been removed, activated, and then put back again. To test for this specification we measured the misalignment between when the samples are removed for activation and when they are returned. Once pre-alignment has been completed we used our image acquisition tools to capture an image of the alignment markers in focus. We then removed the frames from their holders completely, replace them, and then take an image again. The distance between the alignment features in the images are measured using the DinoCapture software [38]. This entire experiment will be conducted on both our 10 times. Our results have shown that an average offset of 12.7 microns with a standard deviation of 2.7 microns for the bottom stage, and an average offset of 9.0 microns with a standard deviation of 1.7 microns, which satisfies our repeatability requirements, significantly reducing our post alignment time.

### **Stability**

In the currently used device, adjustment of the location, zoom level, or the focus of the imaging device, applies enough force to cause misalignment or oscillation of the cameras. In general, this specification strives to ensure that different components can be adjusted without influencing the other moving parts. The most significant instability and the most quantifiable one is the deflections in the cameras each time that the zooming level is changed. We took an image of the alignment markers of a single slab, and then adjusted the zoom level and adjust it back to the original level. We then captured another image of the slab and compared the two images to compute any possible misalignment. This experiment also had 10 trials and was repeated on both the prototype and the current aligner. Our results have shown an average deflection of 24.9 microns for the prototype with a standard deviation of 12.2 microns. This is outperforms the current aligner, which had an average deflection of 41.9 microns with a standard deviation of 30.8 microns. However, this can still be a cause of concern for the special alignments that require multiple zoom levels, and we advise that, if possible, zoom level to be kept constant for the alignment process.

### **Portability**

Our current device shall be measured to ensure its weight is below the upper limit of 40 lbs. Our design, with all its components, weighs in at 20 lbs. Our footprint of 8" x 10" is also well within the maximum allotment of 14" x 14".

**Table 6:** Summary of the engineering specification alongside the validation results

Requirements	Engineering Specifications	Validation Results
Accuracy	20-50 microns	$33.6 \pm 20.5$ microns
Pre-activation alignment time	< 10 minutes	$4.1 \pm 1.0$ minutes
Post-activation alignment time	< 5 minutes	$4.0 \pm 1.9$ minutes
# of inputs	<14	12
Height adjustability	> 7 cm	8 cm
Alignment stage size	> 2" x 3"	4.5" x 5.1"
Repeatability of top stage	< 500 microns	$12.7 \pm 5.4$ microns
Repeatability of bottom stage	< 500 microns	$9.0 \pm 3.4$ microns
Stability better than benchmark	$< 41.9 \pm 61.6$	$24.9 \pm 24.4$
Portability – Weight	< 40 lbs	20 lbs
Portability – Size	< 14" x 14"	8" x 10"
Cost	<\$2000	\$2019.18

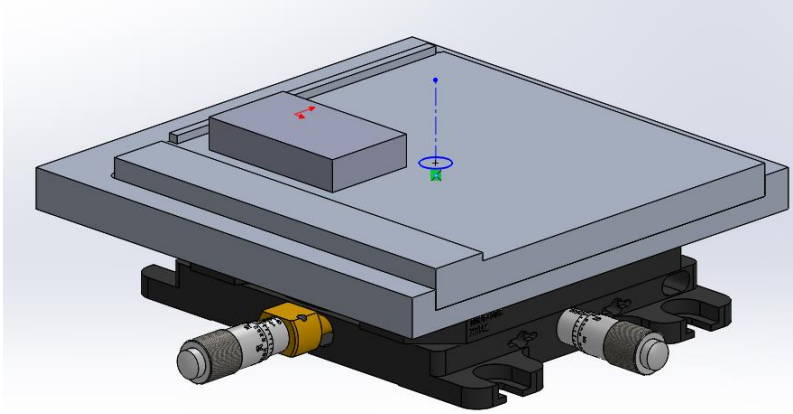
## **DESIGN CRITIQUE AND RECOMMENDATIONS**

The performance of our final prototype meets all of our user's requirements and fulfills all but one of our primary engineering specifications – the budget. That being said, our device is still the first prototype and, hence, there is room for improvement and optimization. This section details the critiques of our design, available solutions, and possible future modifications.

### **Rotation Control of Bottom Stage**

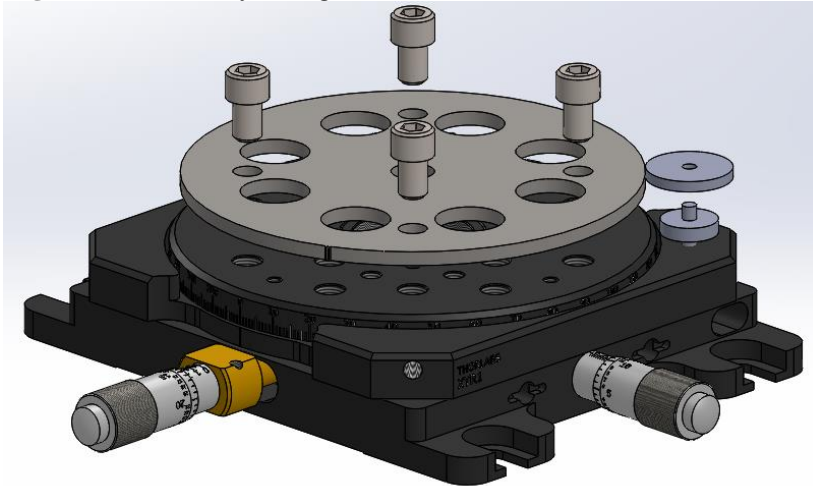
Firstly, our design lacks a knob to control the rotation of our bottom alignment stage. While through our validation we have proven that such a device is not strictly required to achieve the desired accuracy, a knob would improve the ease of use. Another concern relating to the rotational element is that it doesn't rotate about the axis through the center of the PDMS slab. The rotation occurs about the center of the stage. The two axes will not coincide unless the PDMS is centered perfectly on the base during alignment, which it is often not.

**Fig. 30:** CAD rendering of the rotational axes of the stage and the location of the PDMS during alignment.



The decision to purchase a stage without a knob for fine rotational adjustment was made due to budget constraints. In our testing we found that the difficulty in rotational alignment came not from the lack of control but from the field of view offered by our microscopes. Our team is currently working with our sponsor in developing a design to control the rotation using two meshed gears that attach to the top of the stage. This is a separate arrangement with our sponsor and will be completed beyond the scope of this class.

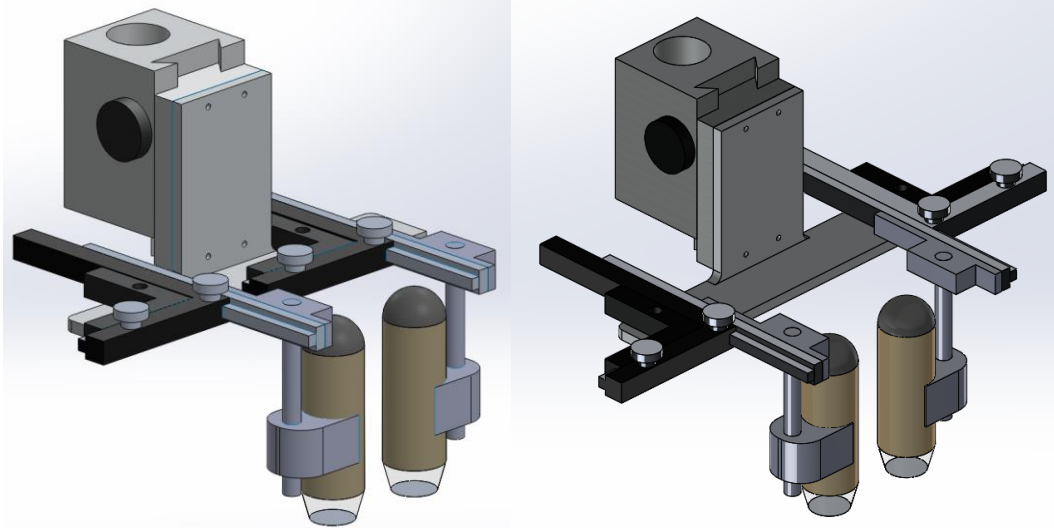
**Fig. 31:** Preliminary Design of Rotational Control



#### Digital Microscope Aligner System and Mounts

The orientation of the mounts for our digital microscope aligner system in our final prototype differs from in our original design. We had designed and ordered two alignment systems that were to be mirror images of each other; in other words the alignment rack for the X direction in the two systems was to point in opposite directions. This allowed for the two digital microscopes to come as close to one another as possible without interference. We instead received two aligners of the same kind – with X axis racks pointed in the same direction. Since we were on a tight schedule we made small changes to our design to be able to work with these aligners instead of ordering new ones. This problem can be easily resolved by purchasing the correct alignment system (refer Appendix A for bill of materials) and fastening it to the holes already in place.

**Fig. 32:** The wrong orientation of the X axis racks for the digital microscope aligner cause an interference. The corrected design has been included on the right.



We also believe that the digital microscope mounting system can be optimized to better individually control the height of the digital microscopes and ensure the two are at the right height. Right now this is done using a set screw that offers little control. The microscopes can also be better supported to eliminate any possible vibrations during adjustment of the microscope position.

### Weight Reduction

While the device meets our portability constraint of 40lbs, there is also a lot of room for weight reduction. The one downside of using aluminum for most of our manufactured components is its weight. We have already removed material from all non-critical regions of the baseplate for this purpose.

### Automated Alignment

With more time and a larger budget there are a few extra features that could be implemented. One such modification includes the introduction of mechatronic components to automate the alignment process. The micrometers for the XY adjustment in the bottom alignment stage can be easily replaced with stepper motors. Additionally, the live feed from the digital microscopes can be analyzed using the MATLAB image acquisition toolbox. The combination of two can help move the PDMS layers with respect to each other until they're aligned.

### LCD Screen

To make our device self-sufficient, two LCD screens, one connected to each digital microscope, can be added to the top of the camera mount. Additionally, an internal computer capable of running the image processing software and displaying it on the LCD can be integrated. The addition of these components will make the device completely standalone and portable. The final prototype is not completely portable as it requires a computer to view the digital microscope images. Though it is not a user requirement for the device to be independent of a computer it is a convenient feature we think will further increase the ease of use.

### Optical Table

Lastly, we can use an optical table as the base of the device. Our vibration analysis showed that day-to-day vibrations will not affect the device performance, however, this is subject to change if used in other

labs. Other labs may be doing research on vibrations, or mechanics. Hence, the optical table will completely isolate the device from any unexpected vibrations.

## **PROJECT DRIVERS AND CHALLENGES**

The following section outlines the foreseeable obstacles and limitation for our project and how they affect our design decisions.

### **Design Drivers**

We have given significant time to analyze the parameters that will influence our decisions in selecting solutions to meet the engineering specifications. We have identified four drivers that will direct our design path, Table 7 provides an overview of the areas of our final design that our design drivers will impact. First is manufacturability of the design. We can generate a design with accuracy of 1 micron, similar to that of mask aligners [8, 9]. However, to accomplish this precision we need manufacturing process, tools and machines that might not available to us within our budget. We need to only consider designs that are feasible to manufacture in the facilities we have access to.

Secondly, we are expected to develop an alignment platform that can withstand daily use for many years, performing reliably and accurately every time. Therefore, we need to design a reliable system, both in terms of endurance and repeatability. Third, as in most projects, cost is a strong factor when selecting a final design. We have a limited budget set by our sponsor that we need to adhere to. However, we need to be cautious and not let the budget be the main design driver.

**Table 7:** List of project design drivers, and what areas of the design they will impact

<b>Driver</b>	<b>What Limits Driver</b>	<b>What Driver Limits</b>
Manufacturability	Cost	Accuracy
	Schedule	Lifetime
	Team members skills	Adjustability Reliability
Reliability	Cost	Accuracy
	Manufacturing	Lifetime
	Off the shelf products	
Scheduling	Class schedule	Manufacturing
Cost	Sponsor decision/requirement	Manufacturing
		Accuracy
		Lifetime
		Adjustability
		Components

### **Specific Challenges**

The project problem and goals were clearly outlined by our sponsor. However, the approach to solving and achieving them was not. Designing an accurate alignment platform is not an easy task. Through our preliminary analysis we identified difficulties that we will face in the future. These are: achieving a high precision alignment of 20 microns or better, measuring the accuracy of our device, manufacturing with high precision, resolving errors in optics, controlling the degrees of freedom, quantifying user experience, and enhancing ease of repeatability by the user. Identifying and addressing these difficulties early on will

prevent delays in the schedule. The project has two sources of difficulties; those imposed by the nature of the MECHENG 450 class, and those imposed by the project problem.

### **Project Challenges**

One major challenge is to design a high-resolution optical device that meets all the following requirements: has a large depth of field, a large field of view to focus on two alignment markers, and that its image is not easily destabilized/unfocused with vibrations. The zoom is inversely proportional to the field of view. To overcome some of this we propose using 2 digital microscopes to increase the field of view, one to focus on each alignment marker. Further, it will be difficult to focus on both PDMS layers because they are at different heights relative to the microscope lens. To solve this an image processing software that can overlay a still picture of the top layer on a real time video of the bottom layer can be used. This will ensure that both layers are focused at all time.

Another challenge is the manufacture of a stage with high resolution and wide range of translation. Manufacturing a stage with resolution of 10 microns will be very hard with the machines available to us. This component will need to be of the shelf. However, from a preliminary research on stages there is a significant trade-off between resolution and range of motion. Stages that have a resolution of 10 microns only have a range of 13mm that is not large enough. Additionally, higher resolution is related to higher price. One option is to have a low-resolution stage with wide range and a higher resolution stage on top of it. We will need to conduct further research to determine what the best solution. This decision will be critical to the success of our platform.

Manufacturing of most of the components in the platform to a high tolerance will be a challenge. Typical tolerances for a mill and lathe are 25.4 and 12.7 microns respectively [26]. Therefore, the lathe would be the machine of preference but this only has limited use for our components. To obtain such tolerances a high level of proficiency with the machines is needed. Developing the skill will require more time than that available. Therefore, it is not realistic that we can obtain these high tolerances. We will need to account for this larger error in our design.

Vibrations introduced by the user input can potentially be a significant challenge. The platform components need to move only when the user wants it to move. For example it is not desirable if when controlling the x-y stage creates significant vibrations on the platform that the microscopes also move. Similarly, components that are designed to be fixed could in reality not be if the joint is poor. Vibrations can also misalign the already aligned PDMS layers. To solve these challenges we can isolate the stand for the microscopes. We can design the platform to have as few joints and manufacture most parts to be one solid piece. Last, we can add a system to lock individual moving parts into position.

### **Special Equipment, Technical Assistance, and Logistics**

The project definition does not ask for any special equipment or logistics to solve the critical problems identified. However, we have determined that technical assistance in the field of optics will be very helpful. Substantial problems exist on the current optical components because of the lack of knowledge in the field. The current prototype designer and manufacturer overlooked the optics of the device because it was outside his scope of knowledge. None of our members have the degree of knowledge required to solve current problems with depth of view, focus and zoom. Further, technical assistance with image processing software such as MATLAB would be helpful but not necessary to be successful.

## **CONCLUSION**

Our project is to design an accurate and easy to use alignment platform for Multilayer Soft Lithography. We interacted extensively with our sponsor and the other stakeholders to determine our design requirements. We carried out literature review, patent searches and benchmarked relevant devices to substantiate these requirements, which then led to development of the engineering specifications for the device. These requirements were ranked in order of importance based on stakeholder feedback and were used to create a QFD chart for the device. We further analyzed the problem to identify the potential challenges we might face due to the nature of the class and the project itself. Our challenges mainly arise from the contrast in having the device be as functional as possible while remaining within our budget.

In the second phase of our design process, we resolved the primary function of our device, which is to align two PDMS layers, into its constituent parts using a Functional Decomposition chart. We next designed several diverse modules to carry out those various sub-functions. We employed a Go/No Go strategy to filter down the ideas and generate five main designs. We used a Pugh chart to select the one that best met our specifications. Using our selected design and the best modules of other concepts we settled on our alpha design.

In the third phase of our project, we conducted a thorough analysis of our alpha design to finalize our parameters and dimensions. The final design was refined and produced in great detail with all relevant components purchased, a complete CAD generated, and a full bill of materials finalized. We also designed the prototype that will be made to demonstrate the device functionality and the features that could be added to it in the future. We outlined all the tests we plan to carry out to ensure that the device meets all the specifications. And finally we have included a manufacturing plan to aid us in the next step of our project plan.

In the final phase of our design, we began manufacturing our device. We bought all of our high tolerance components and machined our customized parts. After assembling our final prototype we began validating all of the design specifications we had set out for ourselves earlier in the term. After conducting multiple test with a variety of users, we found that we met all of our design criteria, but slightly exceeded the budget in the process.

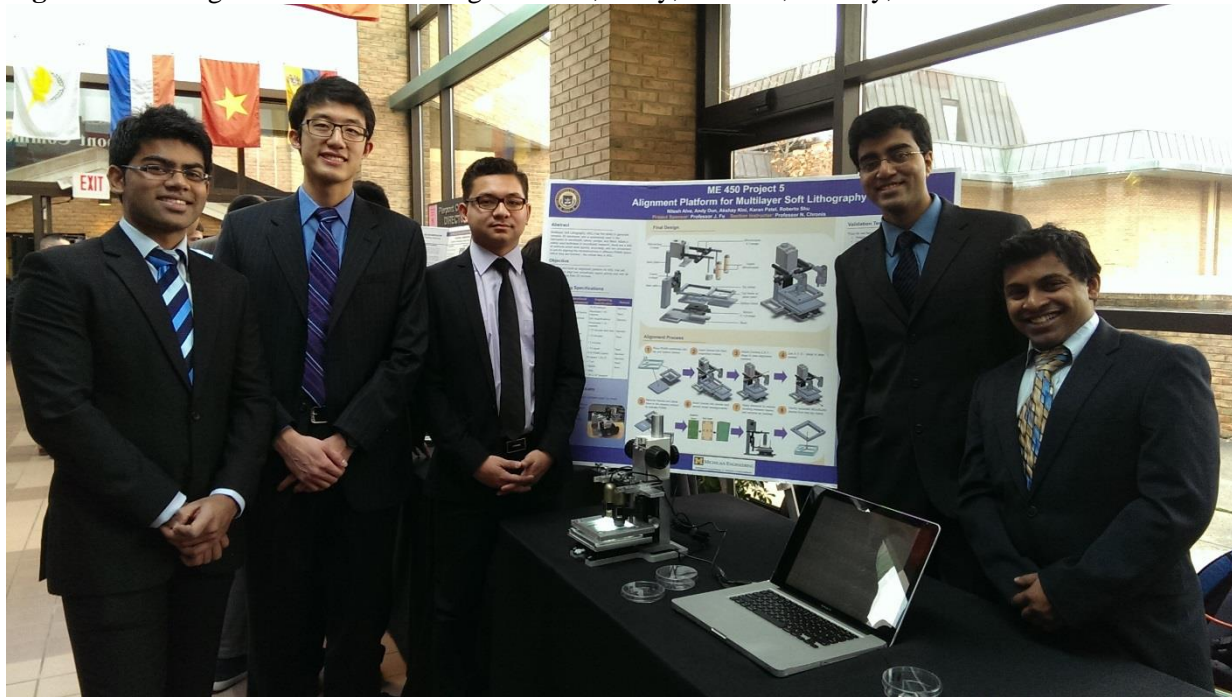
When we presented the prototype to the sponsor and the research staff, they were satisfied with the result. They were eager to work with the device and provide us more feedback in a real setting outside the bounds of our validation. Like all first iterations of a design, there was definitely room for further improvement. Some stakeholders suggested extra design features and that some of our parts could be executed better. We plan to continue working with the sponsor outside the scope of this project to further refine the product.

## **ACKNOWLEDGEMENTS**

This project was a great learning experience for each of us and we owe it all to the people who made it possible. We want to thank our sponsor, Professor Jianping Fu, for the opportunity to take on such a project. We offer our sincere gratitude to our section instructor, Professor Nikolaos Chronis, for his generosity with his time and knowledge. We also offer thanks to Dr. Dan Johnson and the rest of faculty of MECHENG 450 for their support. Additionally, we want to thank and acknowledge the help of Dr. Zeta Yu and PhD candidates Li Xiang, Amrita Chaudhury.

## TEAM PROFILE

**Fig. 33:** The design team from left to right: Karan, Andy, Roberto, Akshay, Nitesh



### Nitesh Alve

Nitesh is from Pune, India. As an interesting fact, he first came to the University of Michigan to pursue a degree in computer science. Michigan being a large institution and having so many wide options to choose from plans changed. Being dissatisfied with just working with computers Nitesh chose to become a mechanical engineer so that his future involved more hands on work. He likes to build things and mechanical engineering gives him the chance to build devices that can have real impacts. He wants to pursue the 5 year bachelors/master's degree.

### Andy Dun

Andy is from Qingdao, China, but he has been studying in the United States since the 8<sup>th</sup> grade. He chose Mechanical Engineering because of the hands-on aspect and the design courses. Andy is currently the engine team lead on the University of Michigan Supermileage team. Andy is hoping to pursue a Masters degree in Mechanical Engineering. Outside of class, Andy loves basketball, soccer, and table tennis.

### Akshay Kini

Akshay was born in India and raised in Dubai, United Arab Emirates. His curiosity for how things work and his love for problem solving led him to apply to the University of Michigan's College of Engineering. He was drawn to a career in Mechanical Engineering because he believes it will allow him to remain in the forefront of change and development across every sector of society. Outside of the classroom, he is a member of Michigan's Hybrid Racing Team and Pi Tau Sigma (the International M.E. Honors Society). After he graduates he plans on applying to Michigan's SGUS program to further his education in manufacturing and controls.

**Karan Patel**

Karan is from Ahmedabad, India. In addition to majoring in Mechanical Engineering, he is minoring in Electrical Engineering with a focus in Controls and Multidisciplinary Design. He is the team captain on the Michigan Hybrid Racing team, through which he gains most of his design and leadership experience. Karan hopes to get a technical Master's degree after completing his Bachelor's, get work experience for a couple years and then start his own business.

**Roberto Shu**

Roberto is from Guayaquil, Ecuador. He is double majoring in Mechanical and Aerospace Engineering, and minoring in Mathematics. He is actively involved in the engineering community. In the past he has served as the President of the Society of Hispanic Professional Engineers and is currently the Aerodynamics lead on the Michigan Hybrid Racing team. His passion from engineering began at a young age while tinkering in the field of robotics. Roberto aims to pursue a PhD after his bachelor and then become the first Ecuadorian astronaut.

## REFERENCES

- [1] "Project Sponsor Meeting." Interview by Jianping Fu and Xiang Li. Print.
- [2] McDonald, J. Cooper, David C. Duffy, Janelle R. Anderson, Daniel T. Chiu, Hongkai Wu, Olivier J. A. Schueller, and George M. Whitesides. "Fabrication of Microfluidic Systems in Poly(dimethylsiloxane)." *Electrophoresis* 21 (2000): 27-40. Print.
- [3] Apaydin, Elif. *Microfabrication Techniques for Printing on PDMS Elastomers For Antenna and Biomedical Applications*. Thesis. The Ohio State University, 2009. Print.
- [4] Chen, Weiqiang, Nien-Tsu Huang, Xian Li, Zeta Tak For Yu, Katsuo Kurabayashi, and Jianping Fu. "Emerging Microfluidic Tools for Functional Cellular Immunophenotyping: A New Potential Paradigm for Immune Status Characterization." *Frontiers in Oncology* 3 (2013):
- [5] Xia, Younan, and George M. Whitesides. "Soft Lithography." *Annual Review of Materials Science* 28.1 (1998): 153-84. Print.
- [6] Voelkel, Reinhard, Uwe Vogler, Andreas Bich, Pascal Pernet, Kenneth J. Weible, Michael Hornung, Ralph Zoberbier, Elmar Cullmann, Lorenz Stuerzebecher, Torsten Harzendorf, and Uwe D. Zeitner. "Advanced Mask Aligner Lithography: New Illumination System." *Optics Express* 18.20 (2010): 20968. Print.
- [7] Piston, David W. "Choosing Objective Lenses: The Importance of Numerical Aperture and Magnification in Digital Optical Microscopy." Web. 20 Sept. 2013
- [8] "Model 200 Mask Aligner." *OAI*. Web. 20 Sept. 2013.
- [9] MicroTec, SUSS. *Manual Mask Aligner*. Print.
- [10] Komeyama, Yoshihiro, Yukio Kembo, Asahiro Kuni, Akira Sun Paiace Inagaki, Minoru Ikeda, and Keiichi Okamoto. A Projection Aligner of a Lithographic System. Hitachi, LTD., assignee. Patent 85113379.3. 27 Sept. 1989. Print.
- [11] Beebe, David J., Jeffrey S. Moore, Qing Yu, Robin H. Liu, Mary L. Kraft, Byung-Ho Jo, and Chelladurai Devadoss. "Microfluidic Tectonics: A Comprehensive Construction Platform for Microfluidic Systems." *PNAS* 97.25 (2000): 13488-3493. Print.
- [12] Burgoyne, Francesca. "A Novel Technique for Aligning Multiple Microfluidic Devices." *RSC Publishing*, 17 Aug. 2011. Web. 13 Sept. 2013
- [13] Wang, Hua, and Seyed Ali Hajimiri. Low Cost Bonding Technique for Integrated Circuit Chips and PDMS Structures. California Institute of Technology, assignee. Patent WO2010099350 A3. 6 Jan. 2011. Print.
- [14] "Ergonomic Guidelines for Manual Material Handling." *Centers for Disease Control and Prevention*. Centers for Disease Control and Prevention, Web. 20 Sept. 2013.
- [15] Langelier, Sean M. *Acoustic Concepts in Micro-Scale Flow Control and Advances in Modular Micro Uidic Construction*. Thesis. The University of Michigan, 2010. Print.
- [16] Unger, Marc A., Hou-Pu Chou, Todd Thorsen, Axel Scherer, and Stephen R. Quake. "Monolithic Microfabricated Valves and Pumps by Multilayer Soft Lithography." *SCIENCE* 288 (2000): 110-16. Print.
- [17] Verschuuren, Marcus A. Silicone Rubber Material for Soft Lithography. Koninklijke Philips Electronics N.V., assignee. Patent EP2288662 A2. 2 Mar. 2009. Print.
- [18] Moraes, Christopher, Yu Sun, and Craig A. Simmons. "Solving the Shrinkage-induced PDMS Alignment Registration Issue in Multilayer Soft Lithography." *Journal of Micromechanics and Microengineering* 19.6 (2009): 065015. Print.
- [19] McDonald, J. Cooper, and George M. Whitesides. "Poly(dimethylsiloxane) as a Material for Fabricating Microfluidic Devices." *Accounts of Chemical Research* 35.7 (2002): 491-99. Print.
- [20] Dixon, Angela R. *Micro- and Nano- Engineering Cellular Patterns with Plasma Technologies*. Thesis. The University of Michigan, 2010. Print.

- [21] Tung, Yi-Chung. *PDMS-On-Silicon Microsystems: Integration Of Polymer Micro/Nanostructures For New MEMS Device Functions*. Thesis. The University of Michigan, 2005. Print.
- [22] NASA. "System Analysis and Modeling Issues". In: *NASA Systems Engineering Handbook*, 2011. Print.
- [23] Wertz, James R., David F. Everett, and Jeffery J. Puschell. *Space Mission Engineering: The New SMAD*. Hawthorne, CA: Microcosm, 2011. Print.
- [24] Cha, Philip D., James J. Rosenberg, and Clive L. Dym. *Fundamentals of Modeling and Analyzing Engineering Systems*. Cambridge [England]: Cambridge UP, 2000. Print.
- [25] Dieter, George Ellwood., and Linda C. Schmidt. *Engineering Design*. Boston: McGraw-Hill Higher Education, 2009. Print.
- [26] Groover, Mikell P. *Fundamentals of Modern Manufacturing: Materials, Processes, and Systems*. Hoboken, NJ: J. Wiley & Sons, 2011. Print.
- [27] Boehler, Wolfgang, and Andreas Marbs. *Investigating Laser Scanner Accuracy*. Tech. Mainz, Germany: University of Applied Sciences, 2003. Print.
- [28] Mathworks. "Alpha Blending Streamed Image Pairs." *Mathworks*. Web. 5 Oct. 2013.
- [29] Parry-Hill, Matthew J., Kimberly M. Vogt, John D. Griffin, and Michael W. Davidson. "Nikon MicroscopyU - The Source for Microscopy Education." *Nikon MicroscopyU*. Web. 29 Oct. 2013.
- [30] "Digital Microscope." *Dino-Lite-- AM7013MT Dino-Lite Premier*. Web. 25 Oct. 2013. <[http://www.dino-lite.com/products\\_list\\_minute.php?product\\_number\\_abridge=AM7013MT](http://www.dino-lite.com/products_list_minute.php?product_number_abridge=AM7013MT)>.
- [31] Semiconductor Wafer, Inc. "Silicon Wafer." *Silicon Wafer*. Web. 25 Oct. 2013. <<http://www.semiwafer.com/products/silicon.htm>>.
- [32] Dunleavy, C.S., I.O. Golosnoy, J.A. Curran, and T.W. Clyne. "Characterisation of Discharge Events during Plasma Electrolytic Oxidation." *Surface and Coatings Technology* 203.22 (2009): 3410-419. Print.
- [33] Bowden, Ned, Wilhelm T. S. Huck, Kateri E. Paul, and George M. Whitesides. "The Controlled Formation of Ordered, Sinusoidal Structures by Plasma Oxidation of an Elastomeric Polymer." *Applied Physics Letters* 75.17 (1999): 2557. Print.
- [34] Tooley, Wes W., Shirin Feghhi, Sangyoong J. Han, Junlan Wang, and Nathan J. Sniadecki. "Thermal Fracture of Oxidized Polydimethylsiloxane during Soft Lithography of Nanopost Arrays." *Journal of Micromechanics and Microengineering* 21 (2011): Printed.
- [35] McMaster-Carr. "Glass Sheets." *McMaster-Carr*. Web. 25 Oct. 2013. <<http://www.mcmaster.com/#glass-sheets/=p5vfjg>>.
- [36] "Rack-Pinion Dovetail." *Opto Sigma*. Web. 29 Oct. 2013. <<http://www.optosigma.com/products/manual-positioners/rack-and-pinion-dovetail-stages/rack-and-pinion-dovetail-stages/123-4760>>.
- [37] "XY Linear Translation Plus Z Axis Rotation Stage." *Thorlabs*. Web. 29 Oct. 2013. <[http://www.thorlabs.com/newgroupage9.cfm?objectgroup\\_id=3693](http://www.thorlabs.com/newgroupage9.cfm?objectgroup_id=3693)>.
- [38] Dino-Lite. *Dino-lite Digital Microscope Brochure*. Print.
- [39] "The Need For Optical Tables." *Thorlabs*. Web. 29 Oct. 2013. <<http://www.thorlabs.com/tutorials/tables.cfm>>.
- [40] Kim, J.Y., J.Y. Baek, K.A. Lee, and S.H. Lee. "Automatic Aligning and Bonding System of PDMS Layer for the Fabrication of 3d Microfluidic Channels." *Sensors and Actuators* (2005): 593-98. Web. 11 Nov. 2013.
- [41] Stamatis, D. H.. *Essential Statistical Concepts for the Quality Professional*. Boca Raton, FL: Taylor & Francis, 2012.

## APPENDIX A – BILL OF MATERIALS AND MANUFACTURING PLAN

**Table A.1 :** Bill of materials listing the vendors and total expenditure

Item	Qty	Source	ID #	Unity Cost	Total Cost
Mechanical X-Y stage	2	Amazon	B009WXAI9Y	\$44.30	\$88.60
Mechanical X-Y-R stage	1	Thorlabs	XYR1/M	\$578.00	\$578.00
Mechanical Z Stage	1	OptoSigma	1-23-4760	\$226.00	\$226.00
Aluminum 8" x 12" x 0.5"	1	McMaster	-	\$31.76	\$31.76
Aluminum 1.25" x 3" x 12"	1	McMaster	-	\$29.06	\$39.06
Aluminum 12" x 12" x 0.5"	2	McMaster	-	\$46.51	\$96.02
Aluminum Dia 1.25" x 12"	1	McMaster	-	\$10.94	\$10.94
Glass 4" x 4" x 0.125"	2	McMaster	8476K14	\$9.90	\$19.80
Dino-lite Digital Microscope	2	Dino-lite	AD4113T	\$420	\$840.00
Microscope Focus Rack	1	Ebay	FR-A1	\$89	\$89.00
Socket Head Cap Screw 1/4-20 0.375"	4	X50 Room	-	\$0	\$0.00
<b>TOTAL</b>					<b>\$2,019.18</b>

**Table A.2:** Camera Pillar Manufacturing Plan

Step	Process Description	Machine	Fixture	Tool(s)	Speed (RPM)
1	Measure out 4" long 1-1/4" diameter aluminum shaft		Table	Scribe, caliper	
2	Cut to length	Band saw			150
3	Insert shaft into lathe chuck, install tool post, place tool holder on tool post	Lathe			
4	Feed the 1-1/2" of shaft towards the tool bit at an appropriate rate to cut threads	Lathe		60° thread tool	600
4	Drill a hole into the base of the pillar for a threaded rod	Lathe		5/16 drill bit	600
5	Tap holes for threaded rod		Vice	Tap handle, 3/8-16 tap	

**Table A.3:** Main Pillar Manufacturing Plan

<b>Step</b>	<b>Process Description</b>	<b>Machine</b>	<b>Fixture</b>	<b>Tool(s)</b>	<b>Speed (RPM)</b>
1	Measure out precise dimensions		Table	Caliper, scribe	
2	Cut to the dimensions	Bandsaw			150
3	Face off surfaces for precise finishing	Mill		Collet, end mill	800
4	Drill holes for fasteners	Mill		Drill chuck, drill bit	1000
5	Tap holes for fasteners		Vice	Tap handle, 1/4-20 tap	
6	Drill hole for threaded rod	Mill		5/16 drill bit	800
7	Tap hole for threaded rod		Vice	Tap handle, 3/8-16 tap	

**Table A.4:** Base Manufacturing Plan

<b>Step</b>	<b>Process Description</b>	<b>Machine</b>	<b>Fixture</b>	<b>Tool(s)</b>	<b>Speed (RPM)</b>
1	Waterjet the plate into dimension	Waterjet			
2	Mark holes centers at correct position		Vice	Spring loaded punch	
3	Drill holes at marked centers for fasteners		Drill Press, vice	Drill chuck, drill bit	1000
4	Tap holes for fasteners		Vice	Tap handle, 1/4-20 tap	

**Table A.5:** Top Frame Manufacturing Plan

<b>Step</b>	<b>Process Description</b>	<b>Machine</b>	<b>Fixture</b>	<b>Tool(s)</b>	<b>Speed (RPM)</b>
1	Mill window for the bottom half of the top frame	Mill		Collet, 3/8 endmill	1000
2	Bring piece to required thickness	Mill		Collet, 3/8 endmill	1000
3	Mill grooves where the top half of the top frame will fit into the bottom half	Mill		Collet, 3/8 endmill	1000
4	Fillet back corners of the top half	Mill		¼ rounding tool	300
5	Mill window for the top half of the bottom frame	Mill		Collet, 3/8 endmill	1000
6	Bring piece to the required thickness	Mill		Collet, 3/8 endmill	1000
7	Mill grooves where the bottom halve of the top frame will fit into the top half	Mill		Collet, 3/8 endmill	1000
8	Fillet back corners of the bottom half	Mill		¼ rounding tool	300

**Table A.6:** Top Holder Manufacturing Plan

<b>Step</b>	<b>Process Description</b>	<b>Machine</b>	<b>Fixture</b>	<b>Tool(s)</b>	<b>Speed (RPM)</b>
1	Cut a U-shaped piece out of a flat slab of aluminum	Mill		Collet, 3/8 endmill	800
2	Drill holes into the base of the U	Mill		3/16 drill bit	800
3	Countersink holes	Mill		3/8 countersink	300
4	Bring piece to correct thickness	Mill		Collet, 3/8 endmill	800
5	Mill bottom lip of top holder	Mill		¼ endmill	800

**Table A.7:** Bottom Frame Manufacturing Plan

<b>Step</b>	<b>Process Description</b>	<b>Machine</b>	<b>Fixture</b>	<b>Tool(s)</b>	<b>Speed (RPM)</b>
1	Bring piece to correct thickness	Mill		Collet, 3/8 endmill	800
2	Carve out hard stops	Mill		1/4 endmill	800
3	Mill channels on the underside for screw heads	Mill		Collet, 3/8 endmill	800
4	Fillet back corners	Mill		1/4 rounding tool	300

**Table A.8:** Bottom Holder Manufacturing Plan

<b>Step</b>	<b>Process Description</b>	<b>Machine</b>	<b>Fixture</b>	<b>Tool(s)</b>	<b>Speed (RPM)</b>
1	Drill holes to fasten to XY stage	Mill		3/16 drill bit	800
2	Bring piece to thickness	Mill		Collet, 3/8 endmill	800
3	Cut out central slot for top frame	Mill		Collet, 3/8 endmill	800

**Table A.9:** Camera Mount Manufacturing Plan

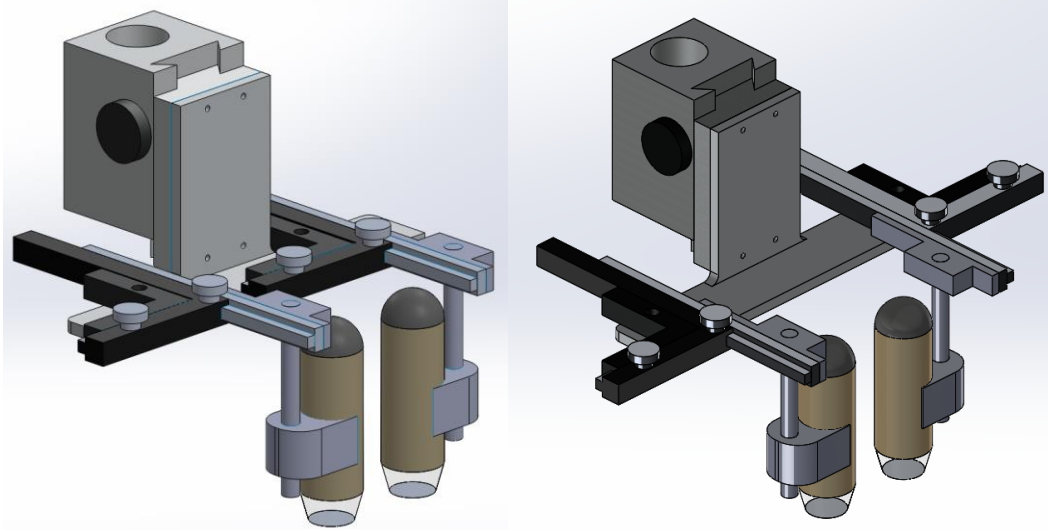
<b>Step</b>	<b>Process Description</b>	<b>Machine</b>	<b>Fixture</b>	<b>Tool(s)</b>	<b>Speed (RPM)</b>
1	Band saw angle stock to correct length and width	Bandsaw			150
2	Cut out side which fits into the camera Z stage	Mill		Collet, 3/8 endmill	800
3	Drill holes for camera holders	Mill		7/32 drill bit	800
4	Drill holes for fastening to Z stage	Mill		5/16 drill bit	800

## APPENDIX B – DESIGN CHANGES

This section includes the major design changes made since the last design review.

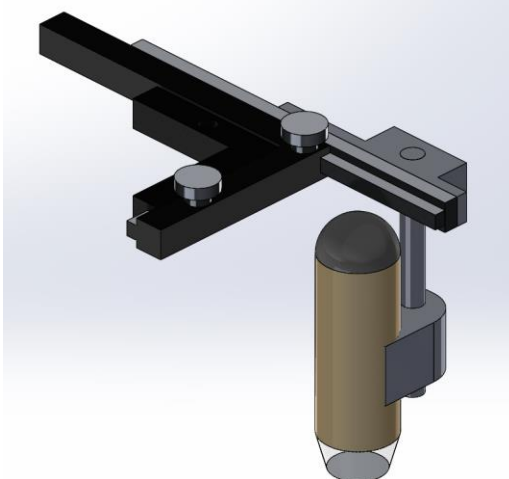
We changed the camera mounts because instead of two mounts which were mirror opposites of each other we received two of the same mounts. Since there was not enough time left in the course to send back for the correct camera mount we decided to re-engineer our design so that we could use what components we had on hand. By shifting the point where they attached to the mounting platform we were able to incorporate the camera mount into our design as can be seen in Fig. B1.

**Fig. B1:** The wrong orientation of the X axis racks for the digital microscope aligner cause an interference. The corrected design has been included on the right.



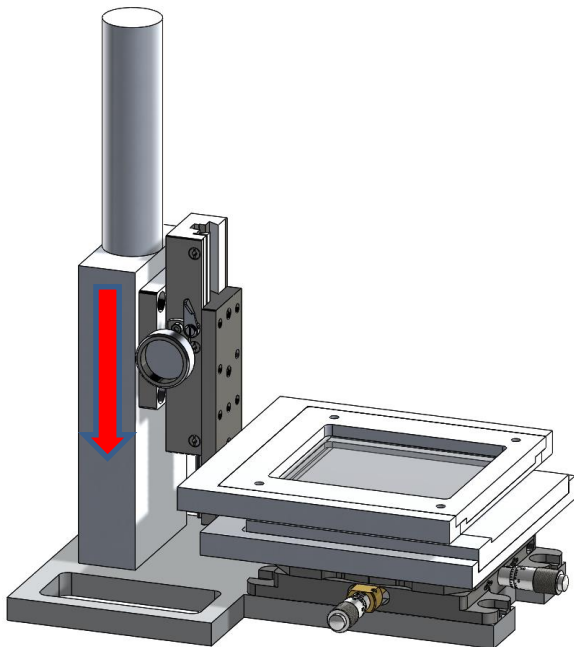
Another design challenge we faced with the camera mount was that the camera did not fit into the grip of the camera mount because the diameter of the camera was too small. To solve this problem we machined a piece which replaced the grips on the holder. Into this piece we press fit a rod and attached to the rod is the digital microscope in a holder maintained in place with the use of a set screw as can be seen in Fig. B2.

**Fig. B2:** Redesigned Camera Mount and Grip



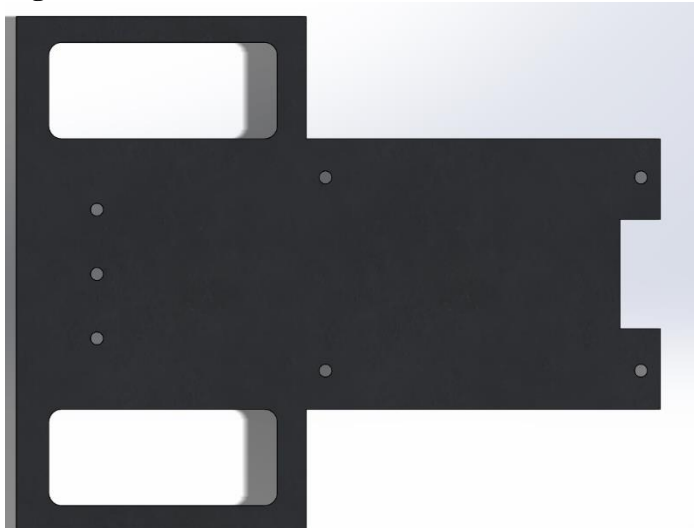
A third design change we made was repositioning the vertical stage associated with the top holder. By moving it lower we were able to avoid interfering with the vertical motion of the cameras and bring them closer to the alignment platform which was required to focus on the PDMS slabs. To move it lower but maintain its range of motion we milled an insert into the base plate so that it could extend lower without interference. By adjusting where we fastened the top holder to the vertical stage we were able to keep the holder in the same position which was important because the gap between the two holders was one of our design specifications.

**Fig. B3:** Repositioning of the Z Stage of the Top Holder



We changed the design of the base plate to make it lighter. By removing material in locations where it was not required the system became a little lighter and easier to hold.

**Fig. B4:** Material Removed from the Base Plate



## APPENDIX C – MATERIAL SELECTION AND ENVIRONMENTAL IMPACT ASSIGNMENTS

### Material Selection

**The model:** the alignment platforms when assembled has several components that are in cantilever; the top holder is one of them. A “C” shape formed by straight edges with dimension 6 inches by 6 inches (Fig. C1(b)). It must be stiff enough so that it doesn’t deflect under the bending moment at the free end due to its own weight and the mass of the top frame ( $m_{tf} = 1.1\text{lb}$ ) (Fig. C2). The mass of the top holder was calculated assuming it was made of Aluminum 6061. Additionally the top holder has to be light weight so that the entire weight of the alignment platform is minimized and it has to be easily machinable to high precision. Table C1 summarizes the design requirements. The mass of the top holder  $m_{th}$  is:

$$m_{th} = (2L + H - 2b)bt\rho \quad (\text{Eqn. C1})$$

Where  $\rho$  is the material density.

The deflection can be approximated to that of beam in cantilever:

$$\delta = \frac{ML^2}{2EI} \quad (\text{Eqn. C2})$$

Where  $I = \frac{bh^3}{12}$

$$\begin{aligned} \delta &= \frac{(m_{th} + m_{tf})gL^2}{2 \frac{bt^3}{12}E} \\ t &= \left( \frac{3(m_{th} + m_{tf})gL^3}{2b\delta E} \right)^{1/3} \end{aligned} \quad (\text{Eqn. C3})$$

Plugin (3) into (1)

$$m_{th} = (2L + H - 2b)b \left( \frac{3(m_{th} + m_{tf})gL^3}{2b\delta} \right)^{\frac{1}{3}} \left( \frac{\rho}{E^{\frac{1}{3}}} \right) \quad (\text{Eqn. C4})$$

Therefore the desired material index is that for a light, stiff beam:

$$M = \frac{E^{1/3}}{\rho} \quad (\text{Eqn. C5})$$

**Fig. C1:** (a) CAD model of alignment platform highlighting the top holder and frame. (b) CAD model of top holder with numeric and symbolic representation of its dimensions

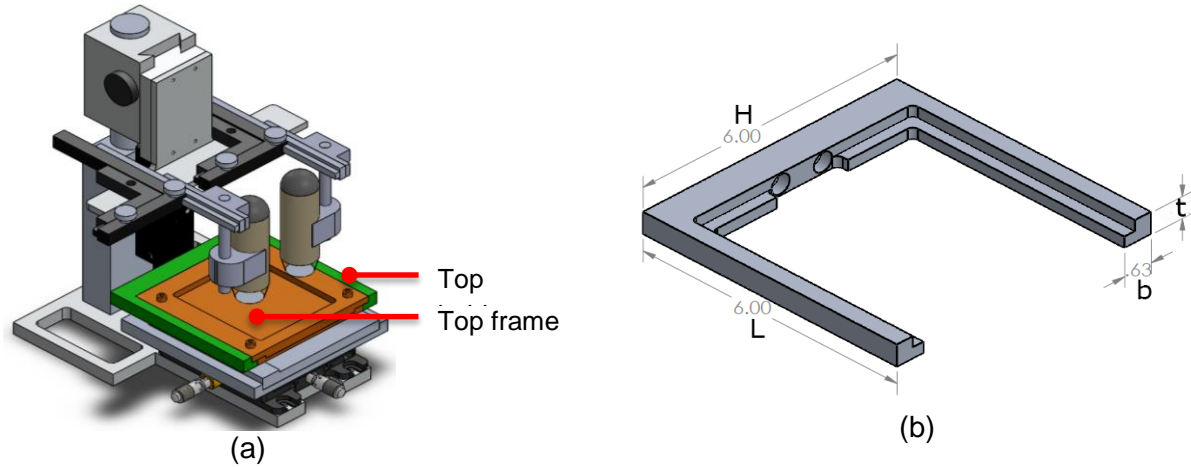


**Fig. C2:** Free-Body-Diagram representation of top holder approximation as a cantilever beam

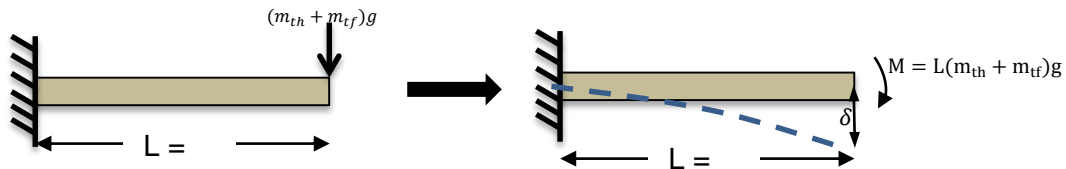


**Table C1: Design Requirements for Top Holder**

Function	Top holder- light weight, stiff beam to hold frame parallel to bottom frame
Constraints	<ul style="list-style-type: none"> <li>• Size 6"x6" (LxH)</li> <li>• Must not deflect under self-weight</li> <li>• Machinability (CES Value of 5)</li> </ul>
Objective	Minimize the mass
Free variable	<ul style="list-style-type: none"> <li>• Thickness, <math>t</math></li> <li>• Choice of material</li> </ul>

**The selection:** the Young's Modulus – Density plot with machinability constraint and line of slope 3, corresponding to the condition  $M = E^{1/3}/\rho$ , (Fig. C3) highlights Polymers, Composites, and Metals as the three group of material that best meet our requirement. From this subset of materials the top 5 materials are Cellulose polymers, ABS Plastic, Glass Fiber Reinforce Polymer, Aluminum and Cast Al-alloys. Table C2 summarizes these materials with its respective attributes. The material with the higher value of  $M$  are better. Clearly from the results Cast Al-alloys would be the best material. However, we do not have the ability to work a material to our desired shape by a casting process. Our second best material is Aluminum. Despite its higher cost and weight this material meets all our requirements. It is easy to machine to high accuracy with the tools we have (mill and lathe). Further with the appropriate thickness it will not deflect. Glass Fiber Reinforces Plastic would also seem to be a good material but again we do

not have access to the tools and budget to work with it. Finally working with ABS Plastic and Cellulose polymers we will not be able to achieve the necessary manufacturing tolerances. If we had a bigger budget and casting was an option then GFRP, ABS and Cellulose polymers would be a more viable option. Since the Top Holder has similar functions and objective than the Bottom Holder we use the same material for both of them.

**Fig. C3:** Material Selection for Top Holder

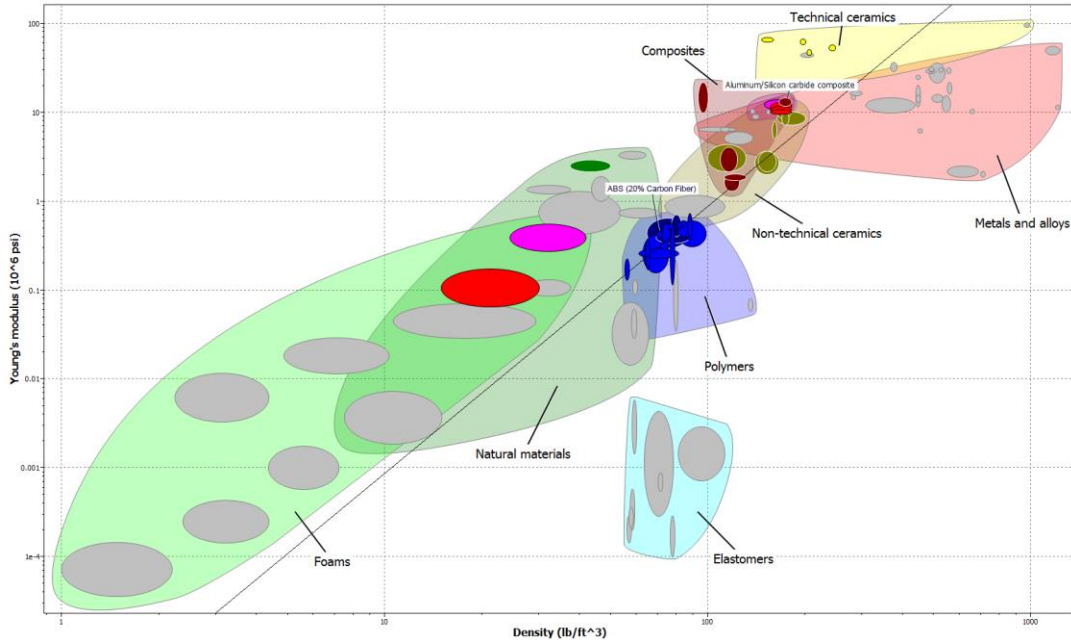


**Table C2:** Material Selection Summary

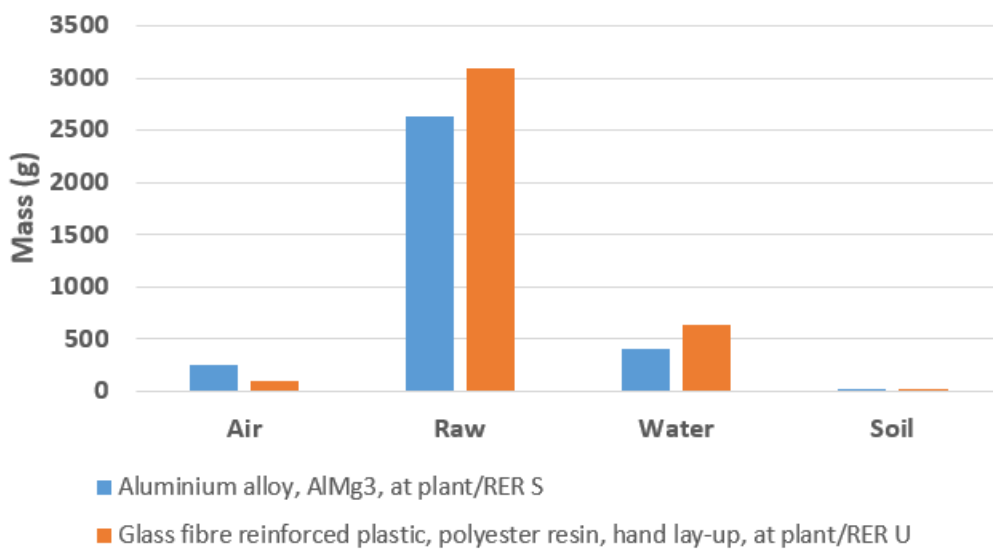
Material	$M = E^{1/3}/\rho$	$M_{th} (\text{lb})$	Comments
Glass Fiber Reinforce Polymer (GFRP)	1.32	0.4191	Heavier material, very expensive.
ABS Plastic	0.956	0.2426	Light and low cost. Susceptible to thermal change, not accurately machinable
Cellulose polymers	0.956	0.2353	Light and low cost. Need molds to cast shape
Aluminum	1.36	0.6383	Heaviest material, considerable less expensive than GFRP, easy to machine with tools available, very stiff
Cast Al-alloys	1.98	0.5998	Heavier material and low cost when mass produced manufacture. Need molds to cast shape, very stiff

Cast Al-alloys are the best material from the analyses; however, we do not have the necessary tools to work with it. Our second best option is aluminum, though it is more expensive and heavier it meets all our requirements.

## Environmental Impact

From material selection using CES the top choice was Cast Al-alloys but we selected aluminum which is similar. The environmental impact of these two materials will be similar. More advantageous is to analyze the environmental impact of two distinct materials i.e. Aluminum (Al) and Glass Fiber Reinforced Plastic (GFRP) which are both available in SimaPro. Different amounts of Al and GFRP would be needed, 0.64lb and 0.42lb respectively to manufacture the part. GFRP produces more total emission mass than aluminum but not by much (Fig. C4). GRRP produce 3100g of raw emission while Al only 2600g. This accounts for the biggest bulk of emission for both materials; air, water and soil are significantly less. Water is the second largest emission (Al – 400g, GRFP – 600g). GFRP will have a bigger environmental impact in terms of air, raw, water and soil emissions. However, since they produce roughly the same amount of each emission type their impact will also be similar.

**Fig. C4:** Total Mass Emission Breakdown



Within the ten different EconIndicator 99 damage classifications Al has a bigger environmental impact in seven of them (Fig. C5). Analyzing the damage meta-categories (“human health”, “ecosystem quality”, and “resources”) (Fig. C6) Al has the biggest impact. The impact of both materials on the ecosystem quality is minimum based on the 0.0002 point value. For Al “resources” is the most important damage meta-category with a point value of 0.022, while for GFRP it is only 0.0005. For the human health category GFRP has the biggest impact with 0.008 compared to the 0.007 of Al. Overall aluminum has a bigger negative impact, due to its impact in resources and human health meta-categories (Fig. C7). Aluminum has a single score of 8.4 while GFRP has almost half the score 4.6. It is important to point out that for both materials the single point score for Human Health is very similar 3.8 and 4.2 respectively. When the life cycle of the whole product is considered it is clear that aluminum will have the biggest impact. For the platform alignment creating and end of life are the most important stages of the life cycle. On its creation stage Al requires substantial more raw material than GFRP hence its higher single point score. The creation process also contributes to the negative impact in human health. Creating aluminum generates more carcinogens and radiation waste than GFRP. However, GFRP also generates a human health impact during the manufacturing process of the alignment platform that Al doesn't. At end of life, both will have a small impact since they can be recycled. Therefore, it is the greater impact of the creation stage of Al that makes it the material with the bigger impact.

**Fig. C5:** EconIndicator 99 damage classifications, Red represents Aluminum and green represents GFRP.

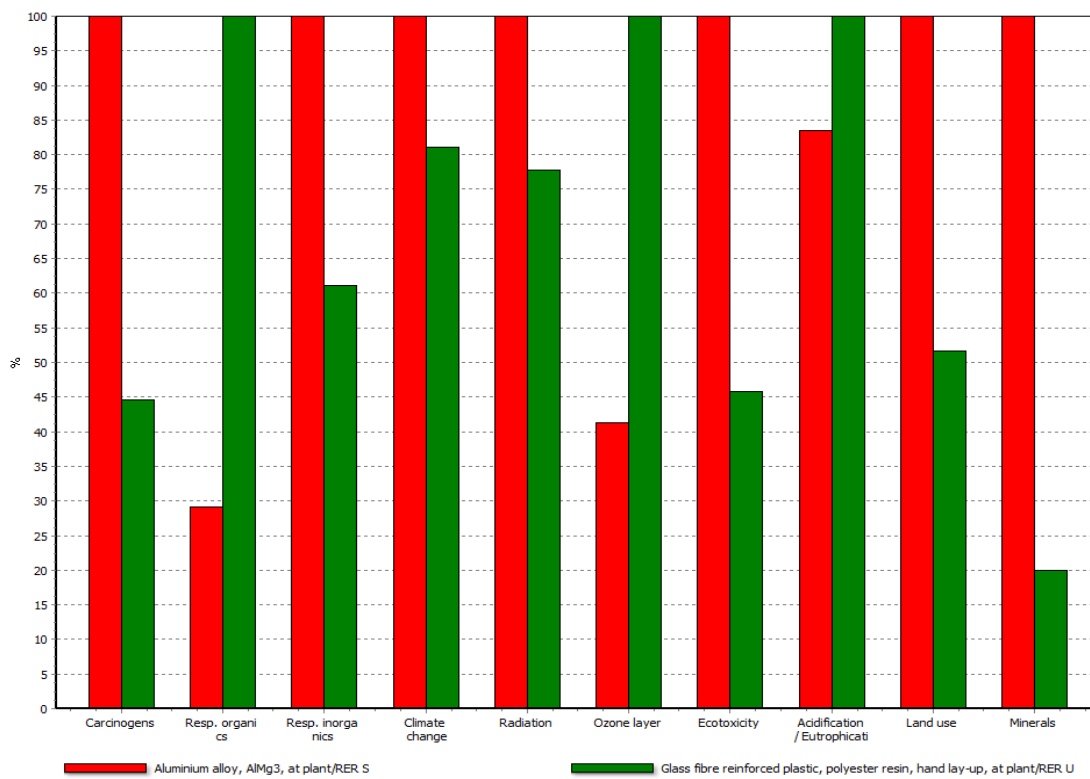


**Fig. C6:** Damage meta-categories point values for each material

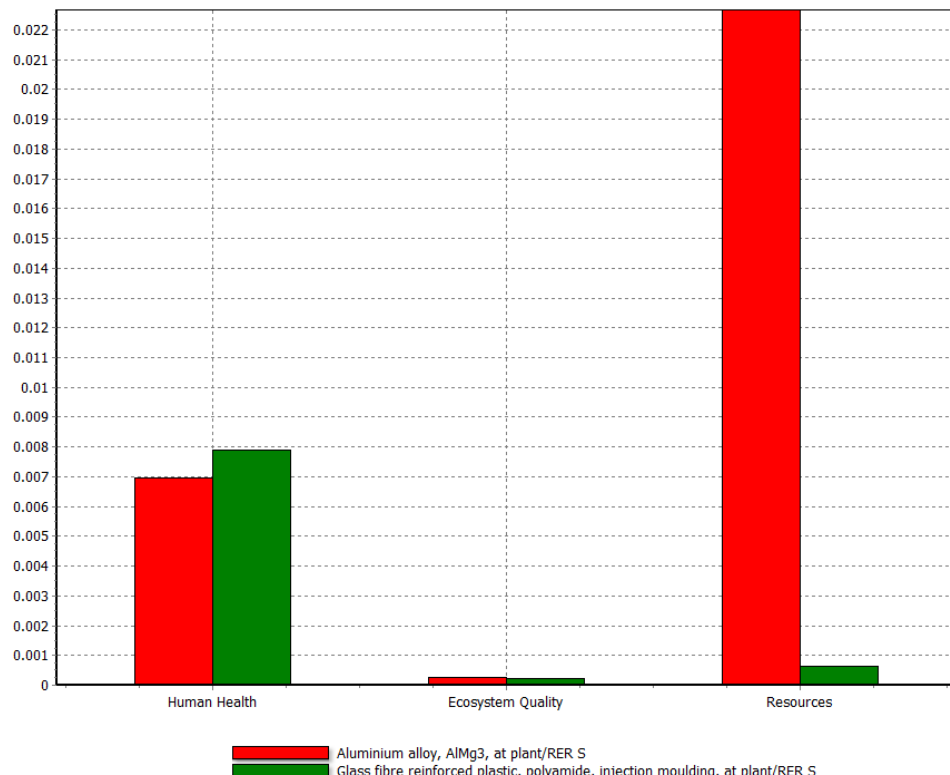
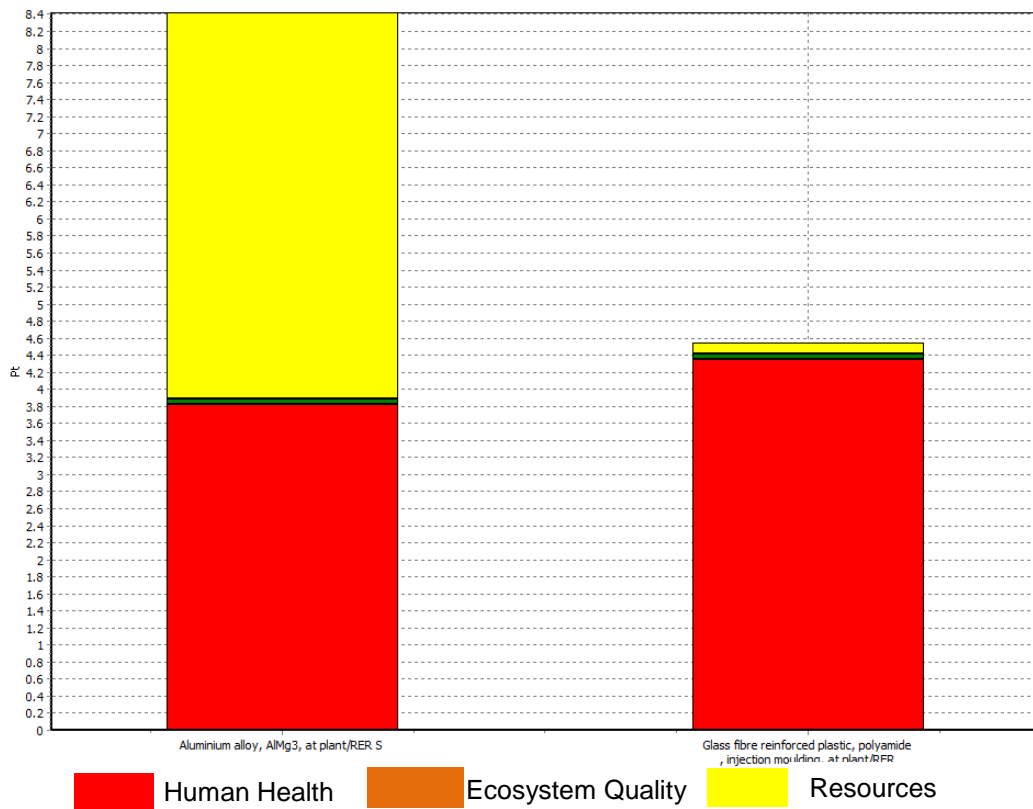


**Fig. C7:** Damage meta-categories Single Score Comparison in “Points”



## APPENDIX D – CONCEPT DESIGNS

### Concept Design Overview

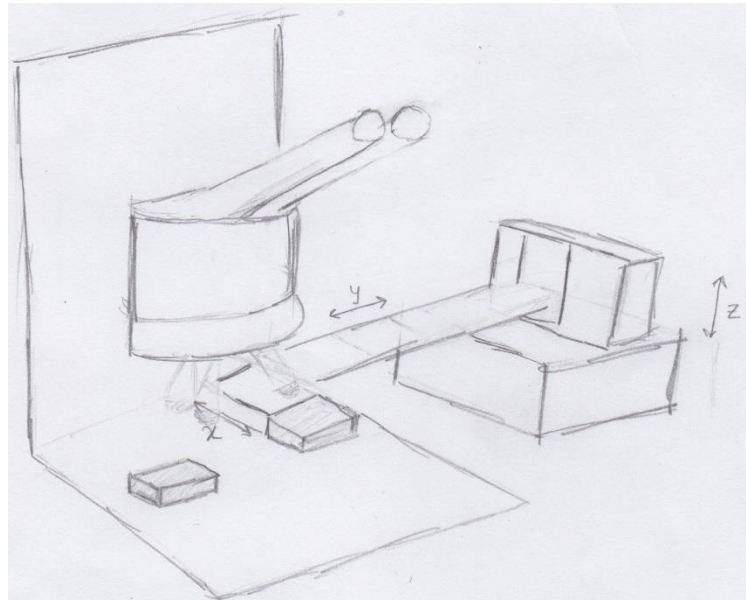
The device was divided into 4 essential components: visualization, position, and storage. For the sake of simplicity in this section we will expand the categories to fit the several ideas that were generated by the team. We have listed all the categories below and have listed our concept design titles under each concerned category.

1. **Position Verification:** it is absolutely crucial that the microfluidic channels and markers in the PDMS slab be easily identified by a user, a digital image processing input, or any tool that will be used to align the two layers. A sensor that gives feedback of the position of the slabs.
  - a. Microscope
  - b. Digital microscope to computer (X and Y)
  - c. Digital microscope to computer (polar)
  - d. Digital microscope to computer (flex joint system)
  - e. Digital microscope with LCD display
  - f. Digital microscope with dual display monitors
  - g. Digital microscope with Raspberry Pi controller
  - h. Lasers and receivers
  - i. Sound sensors
2. **Position:** both the visualization tools and the PDMS slabs have to be moved with high resolution in order for the two slabs to be aligned with high accuracy. This process will be followed by positioning the layers.
  - a. Tactile markers
  - b. Magnetic markers
  - c. Macro markers
  - d. Positioning thread
  - e. Positioning pins
  - f. Surface tension
  - g. Image overlay
  - h. Rough and fine adjustment
  - i. Robotic alignment
  - j. Micrometer alignment
  - k. Hinge alignment
3. **Storage:** this function encompasses how the PDMS layers will interact with the device. Everything from insertion/removal of the slab to constraining it with tight tolerances is included in this block. This function allows for a lot variation in its implementation but has a significant impact on our specifications, especially repeatability.
  - a. Common detachable frame
  - b. Glass slide
  - c. Glass slide with metal frame
  - d. Spring clip
  - e. Set screws
  - f. Cantilevered robotic arm
  - g. Non-cantilevered robotic arm

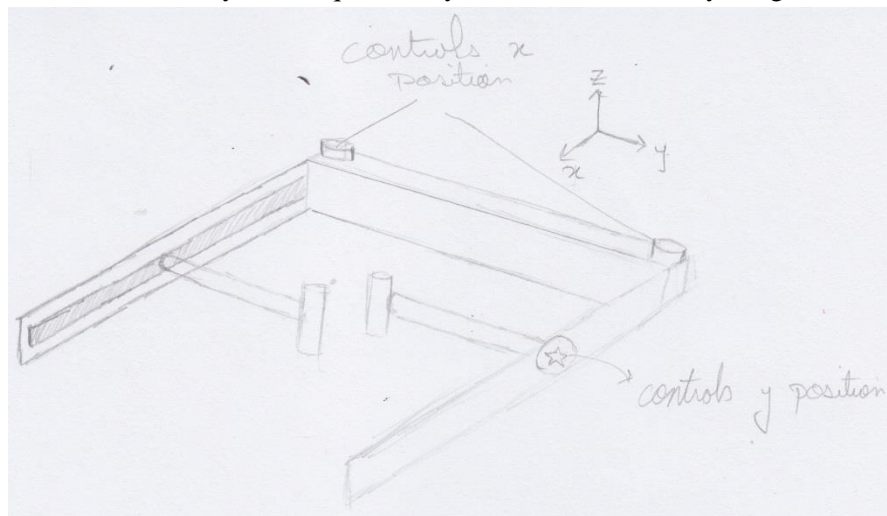
## Individual Concept Sketches and Descriptions

### 1. Position Verification:

- a. Microscope: With a microscope we have the benefit of instant feedback. There is no delay which is present in viewing the images on a computer. Disadvantages include that microscopes are fairly heavy and will take a large chunk out of our ergonomic weight as well as objective lenses have small focal lengths and need to be very close to the object.

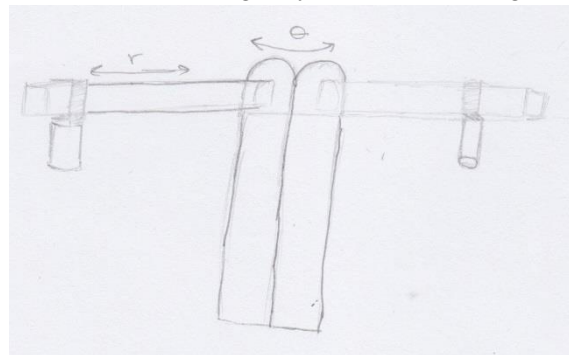


- b. Digital microscope to computer (X and Y): The current benchmark has cameras which allow the user to manipulate them in rectangular directions. The downside is the execution of this system is quite bulky and adds unnecessary weight and materials.

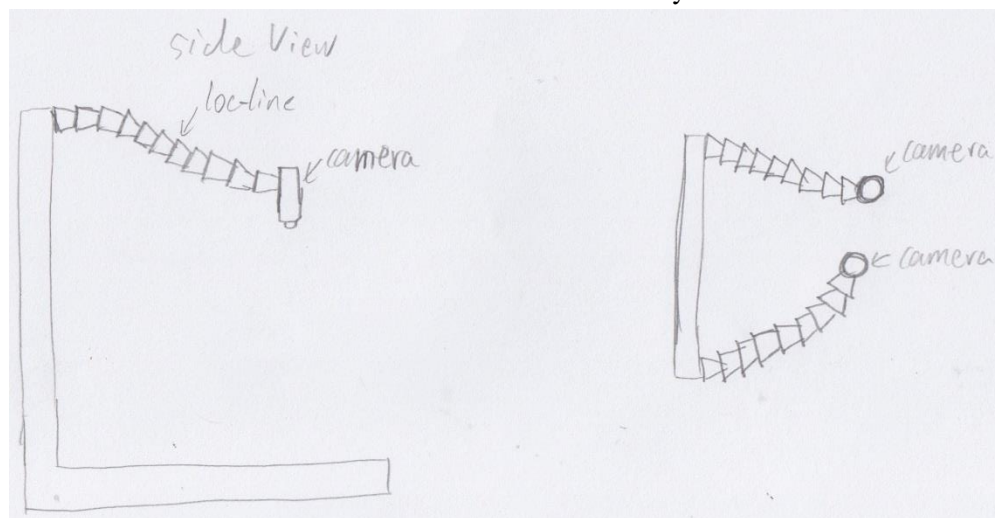


- c. Digital microscope to computer (polar): The polar implementation of the camera system contains fewer parts, but users commented it represents a challenge to control and

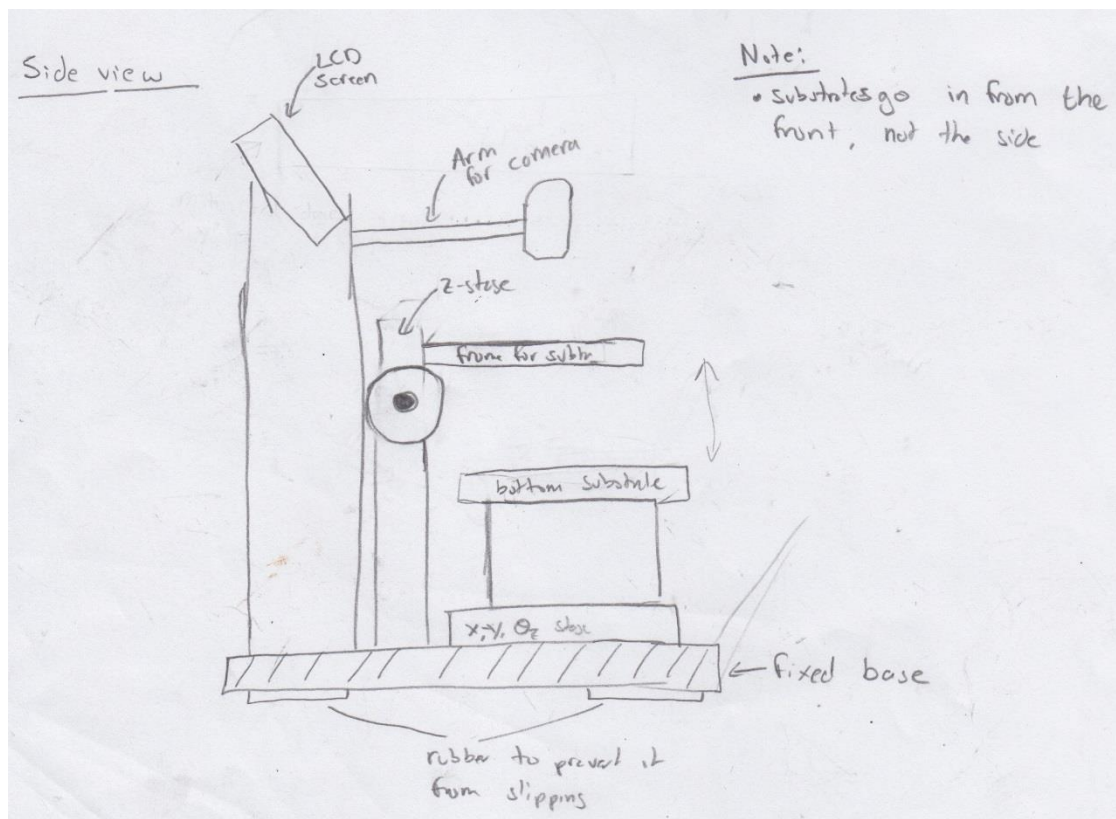
cantilevered bending may wear out the range of motion of the visualization system



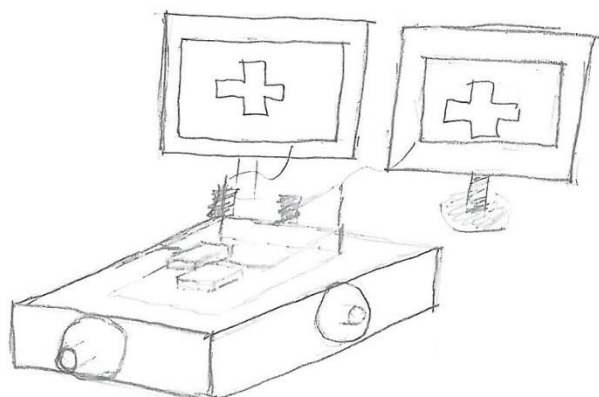
- d. Digital microscope to computer (flex joint system): The loc-line system allows for easy manipulation of the camera to the location the user wants, but due to the number of joints there will be some error associated with accurate positioning of the camera. Depending on the tolerances of the visualization device this idea may not be feasible.



- e. Digital microscope with LCD display: The LCD display will be attached to cameras to make the device more portable, currently the benchmark has usb cables which can plug into a computer to view images. The only things inhibiting this idea is the availability of funds to obtain the screens



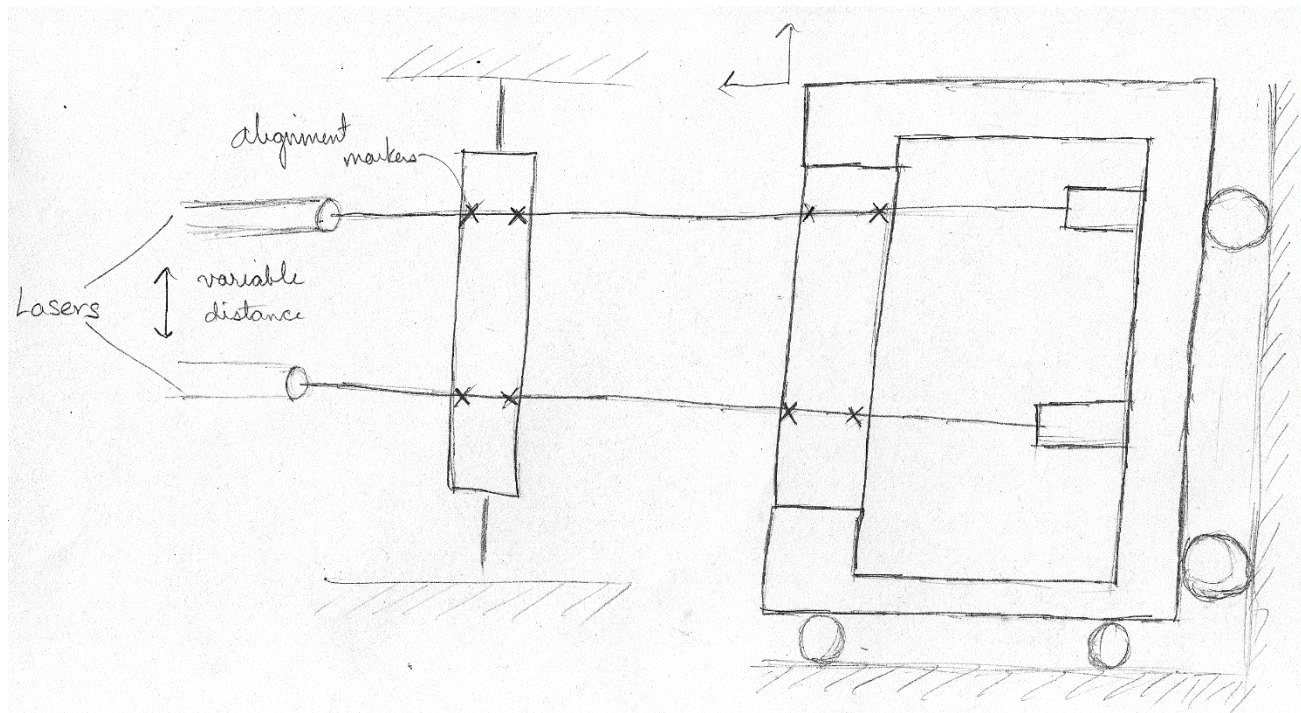
- f. Digital microscope with dual display monitors: Dual display monitors these will let you see both camera outputs clearly but add a lot of space and weight to the device.



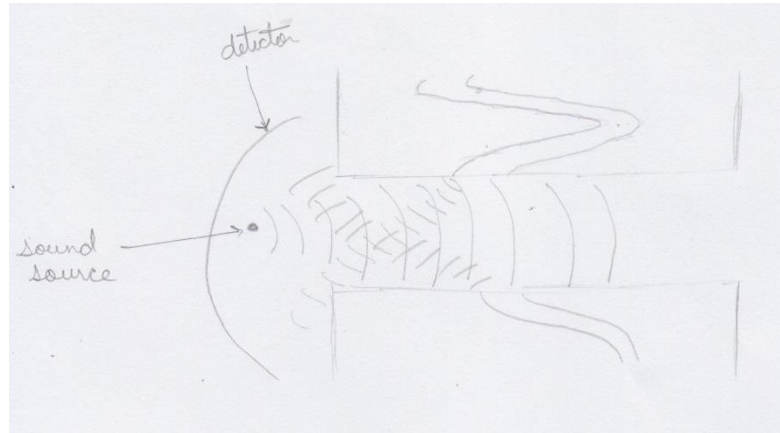
- g. Digital microscope with Raspberry Pi microprocessor: Raspberry pi is a micro-computer with a range of ports to hook up our cameras and screens to and can image process the inputs to produce a clear overlay.



- h. Lasers and receivers: Using lasers to sense alignment of structures seem infeasible because fluidic structures are not always linear and internal reflections could give false positive readings. Furthermore, these devices don't give a measure of inaccuracy.

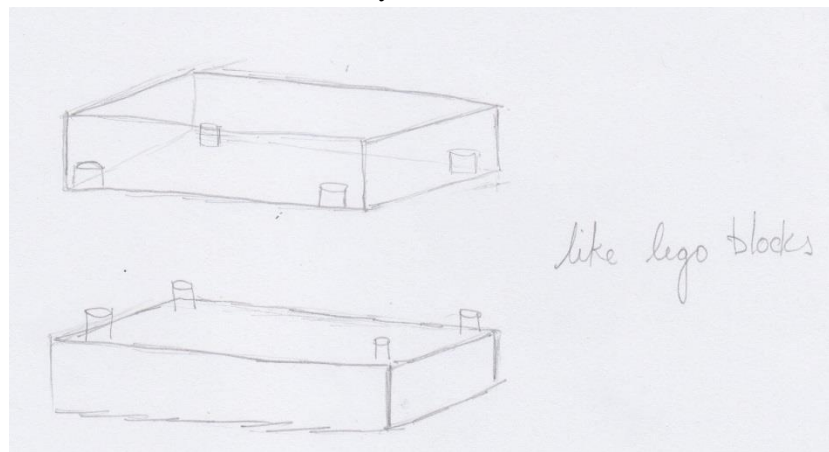


- i. Sound sensors: Using sound is completely unviable because it introduces vibrations into our system which can throw the entire system out of alignment.

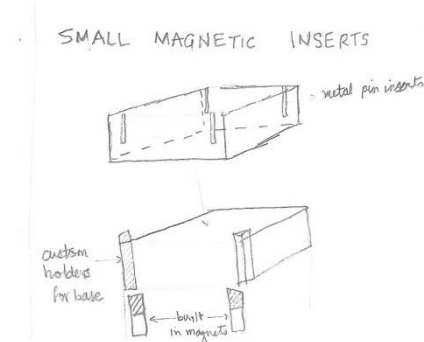


## 2. Position:

- a. Tactile markers: Using tactile markers is also inviable because this requires the users create a new master mold which requires significant time investment input on the part of lab users who wish to use this system.



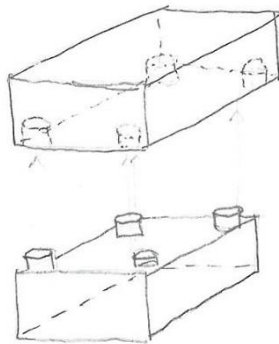
- b. Magnetic markers: Magnetic inserts into the pdms sheet seem economically infeasible. Just as the tactile markers this type of feedback will require a new master mold and each alignment will require multiple disposable ferromagnetic materials and magnet which may quickly get expensive.



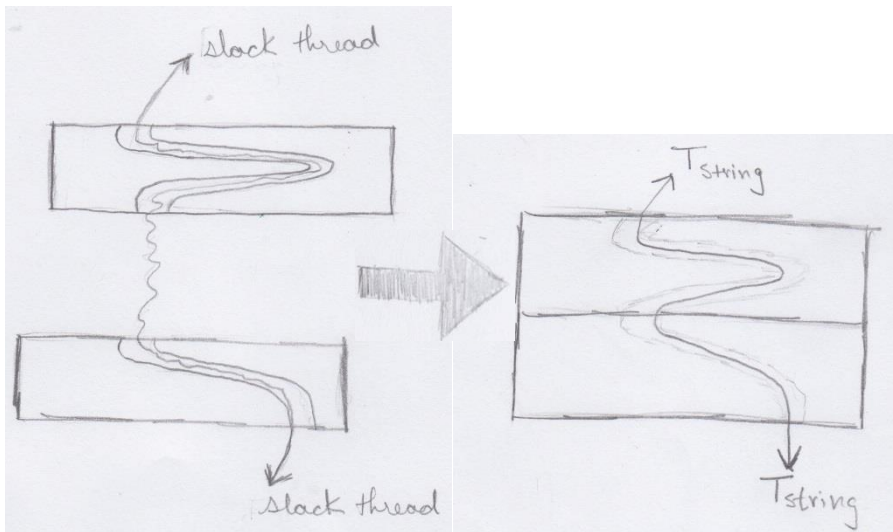
- c. Macro markers: Macro-aligning the module will require PDMS sheets to be cut to an exact specific size. PDMS is an elastic substance and so cutting it down to size seems more tedious than aligning the microstructures

### LEGO BLOCK ALIGNMENT

#### MARKERS

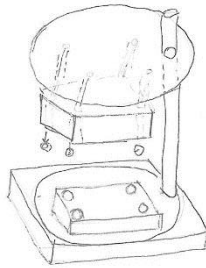


- d. Positioning thread: Alignment using a narrow thread to align specific parts of the PDMS layers by threading it through the microstructures. This design was not feasible because threading the microstructures increases the time taken and tediousness which directly contradict the design and user specifications.

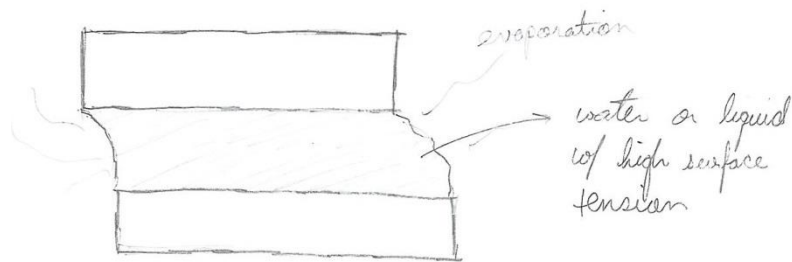


- e. Positioning pins: This process involves creating depressions on the PDMS surface so the pins fall into place on the PDMS surface. This method will require the users to completely re-design their mold masters which is additional effort and time on the part of

the users so this idea was rejected.



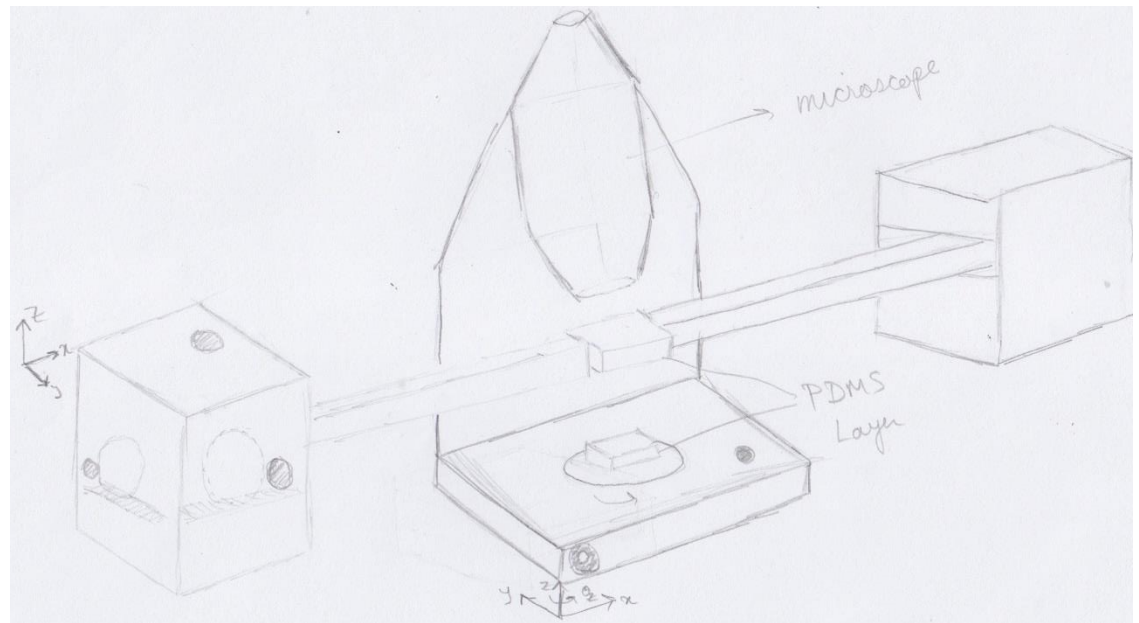
- f. Surface tension: Using the surface tension of water to either macro-align the PDMS layers or aligning the microstructures seemed inviable. The PDMS layers cannot be cut to a precise enough size for this to work nor can the individual channels be wetted to form a good contact. Additionally the water will take time to dry which will increase the time needed to bond and so produce more defects in the bonding process.



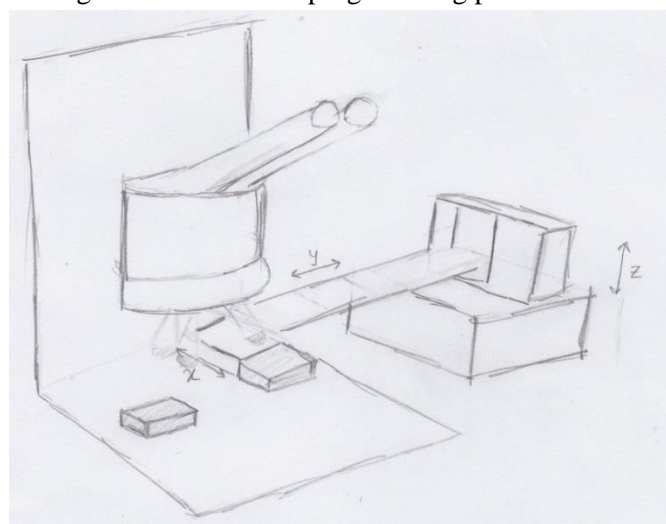
- g. Image overlay: Using an image overlay allows us to obtain sharp images of two different focal planes. This can help us be more accurate when it comes to placing the two layers in contact



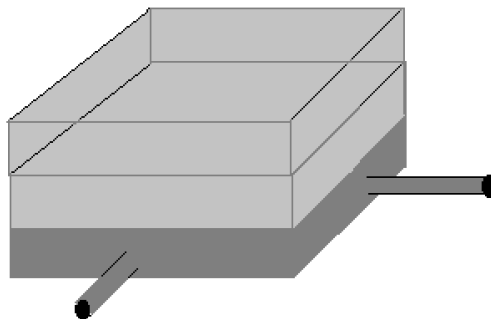
- h. Rough and fine adjustment: Having coarse and fine adjustment knobs of the device would make manufacturability easier but the final product would be less intuitive for the user so this idea was rejected.



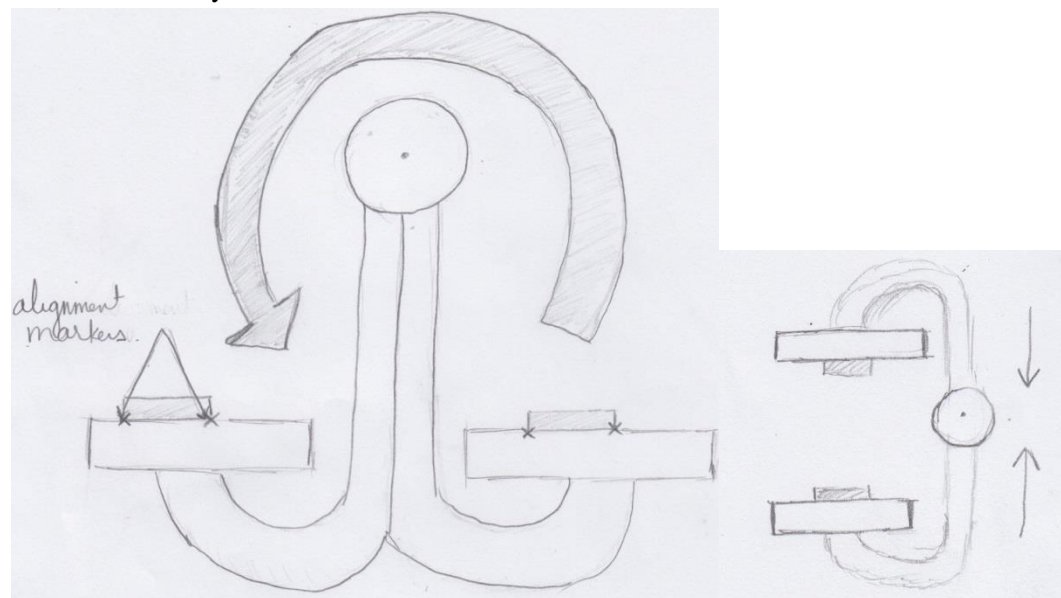
- i. Robotic alignment: Using a computer device for positioning would take a lot of the user effort out of alignment. This idea was rejected because the cost of a robotic device was too high and the controls programming posed an even more difficult challenge



- j. Micrometer alignment: By adjusting the micrometer we could achieve a high level of precision but the trade-off is the limited range of motion.

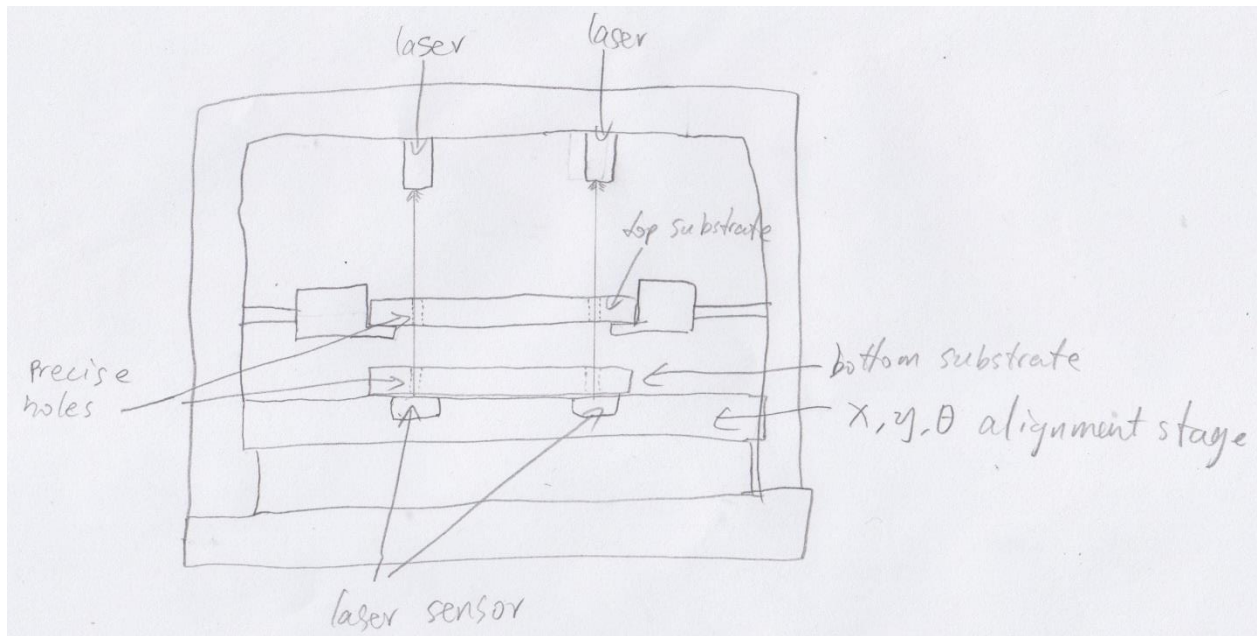


- k. Hinge alignment: A mechanism was considered by which users could pre-align PDMS sheets to a glass surface and after activation post-alignment would be simply folding the glass slides over each other. The problem with this method was that this process did not meet our accuracy tolerances.

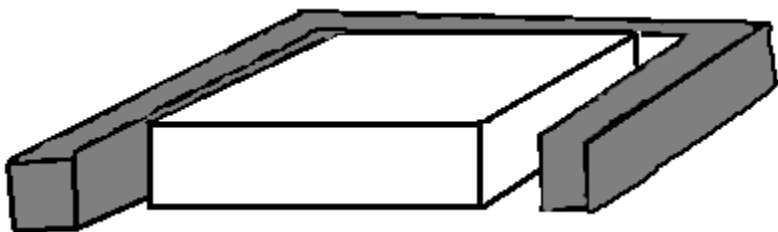


### 3. Storage:

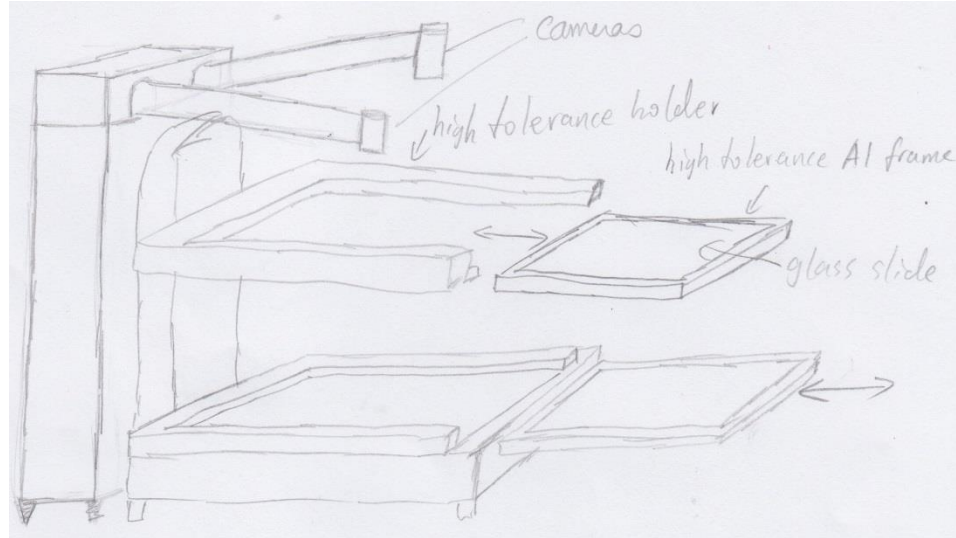
- a. Common detachable frame: A common detachable frame would hold current alignment and allow quick bonding after the plasma oxidation process. Unfortunately, meetings with the sponsor and user showed us design constraints with the plasma oxidizer which made this plan unviable.



- b. Glass slide: Current benchmark uses a glass slide in a holder to provide a surface for the PDMS to attach to. According to our research glass provides the best contact surface, but it has low tolerance and develops play in the holder.

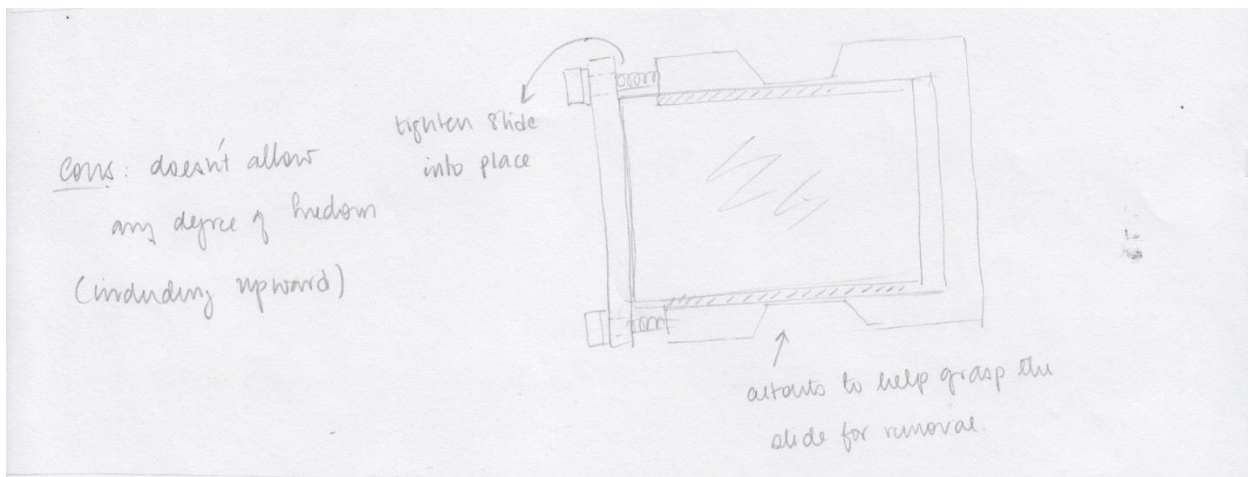


- c. Glass slide frame: The glass slide frame provides for a mechanism to secure the glass slide in place and provides a tight tolerance so that post alignment is made simpler.

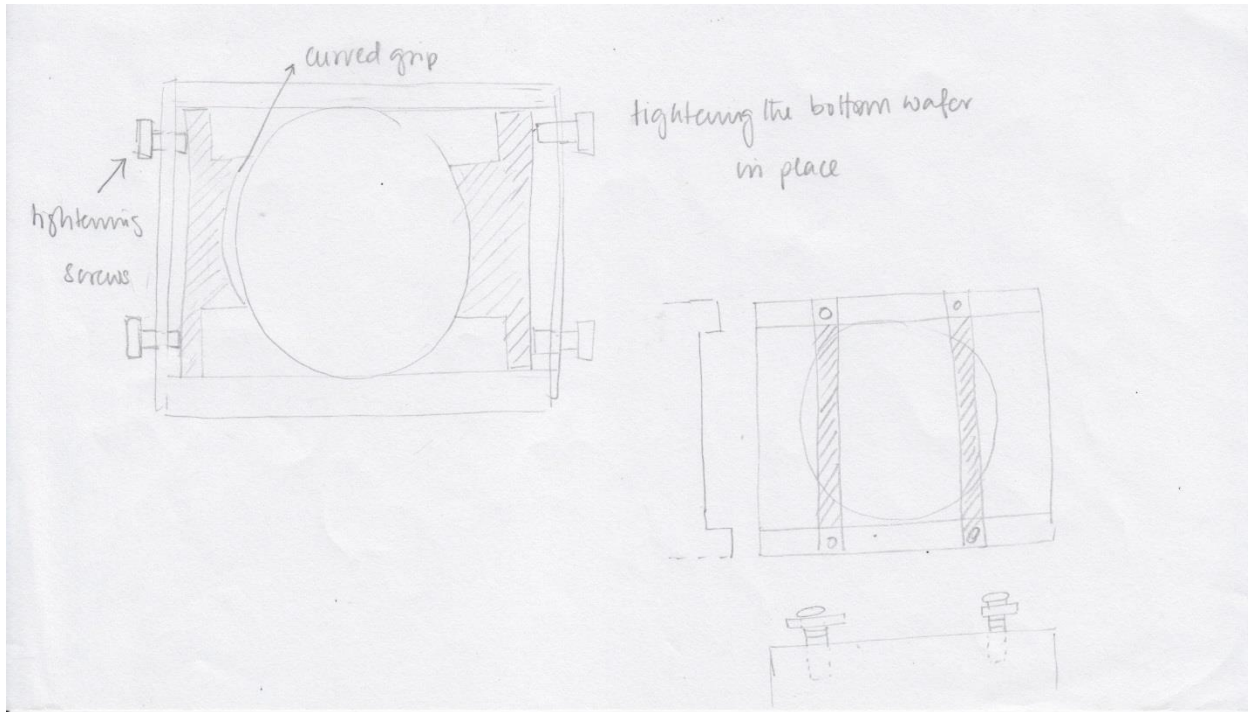


- d. Spring clip:

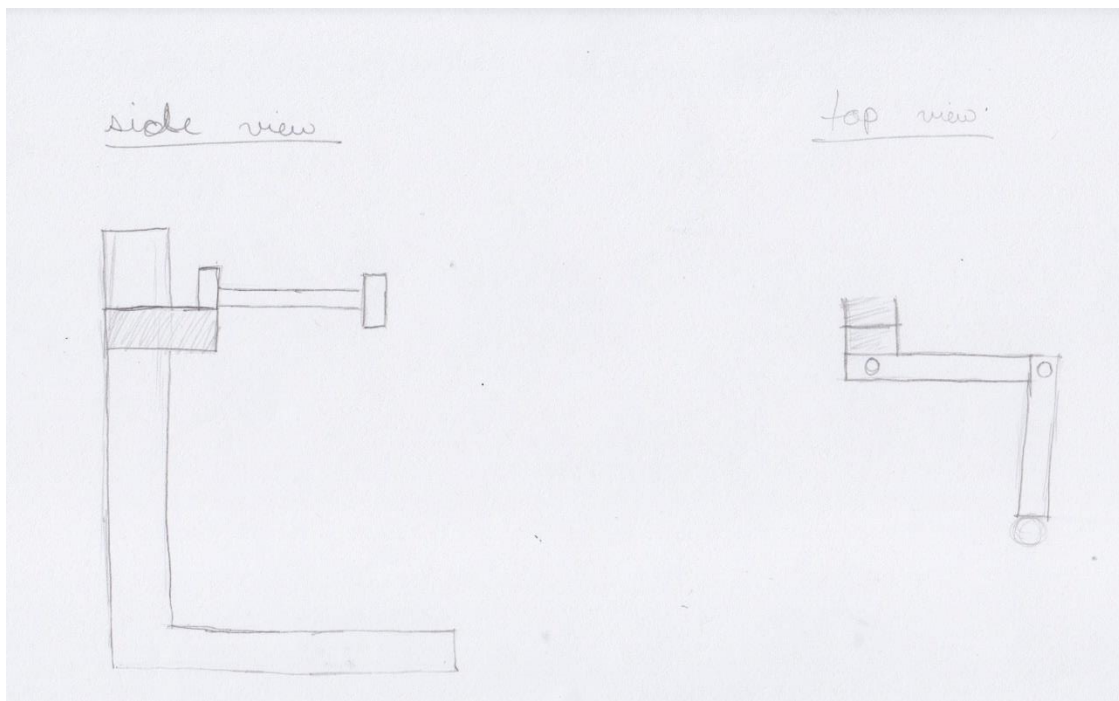
Using just spring clip to hold the glass slide in place would not allow the glass slide to lift up out of the holder. This is crucial to ensure proper contact between the two layers.



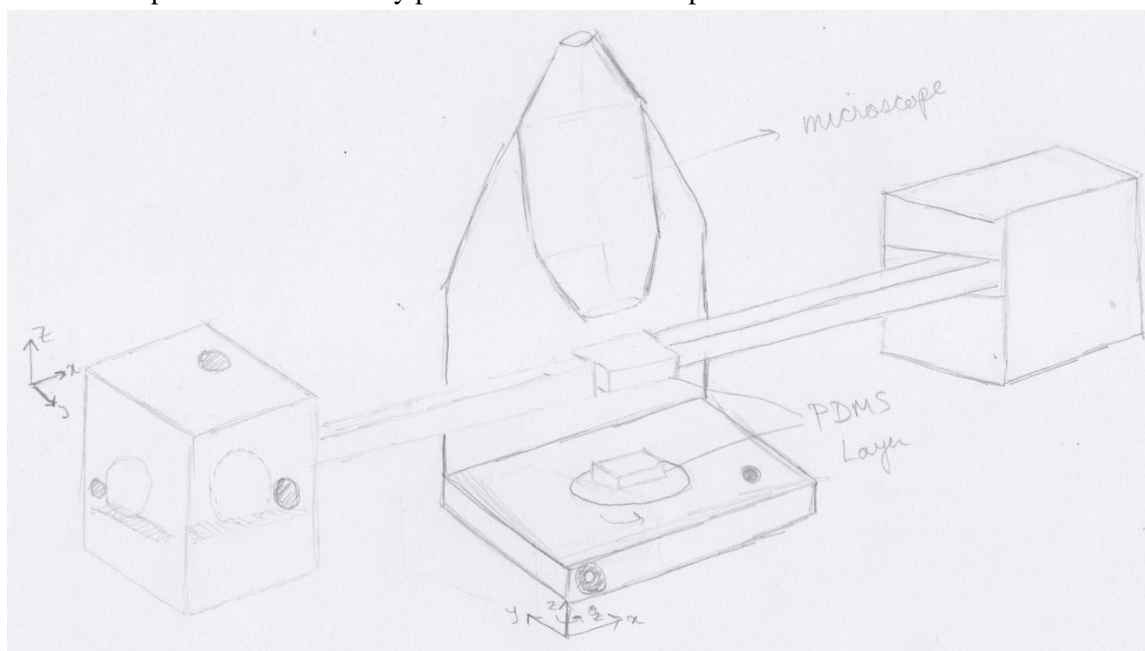
- e. Set screws: Using set screws to lock the slide in the holder would prevent it from lifting out of the holder which is crucial for a good contact between the two PDMS layers.



f. Cantilevered robotic arm: The robotic arm is capable of translating in X, Y and Z. This component adds a lot of complexity without adding much function. In addition the arm is expensive and does not meet our accuracy tolerances



- g. Non-cantilevered robotic arm: A robotic movement system seems bulky and overly complicated. It is not very portable at all and is expensive and difficult to manufacture.

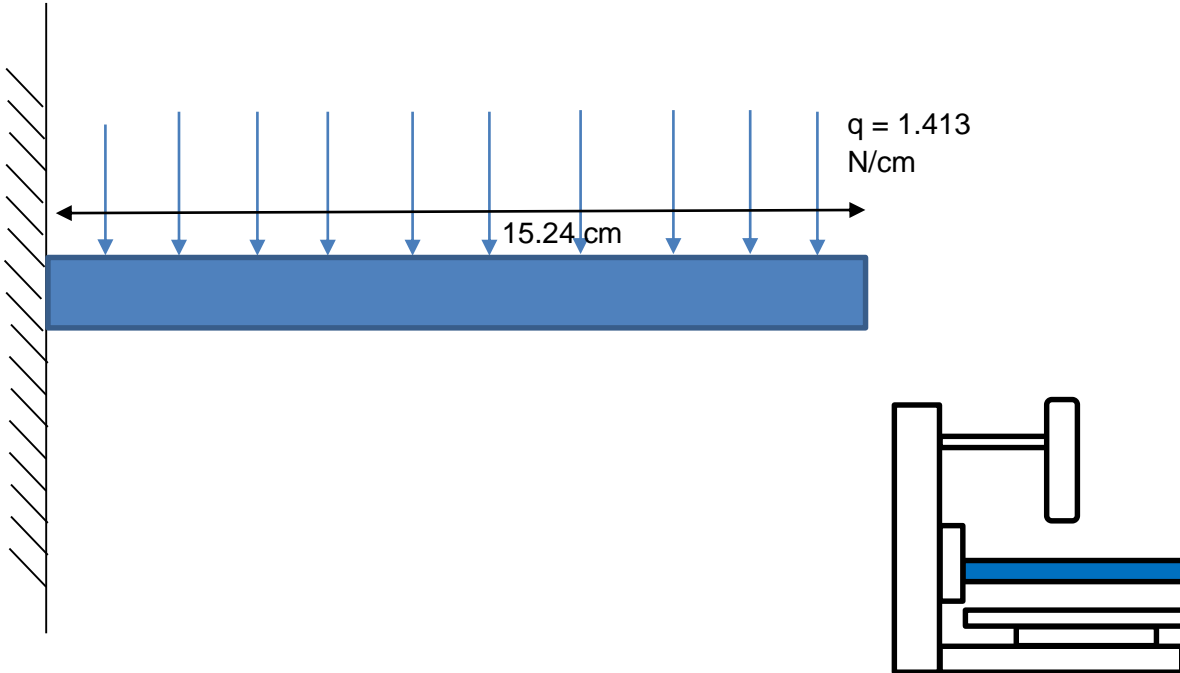


## APPENDIX E – ENGINEERING ANALYSIS CALCULATION

### Structural Deflection Calculation

We made the assumption that the pieces themselves are evenly distributed in weight. All loads applied to components can be modelled as concentrated loads. Components not under consideration are rigid with no deflection.

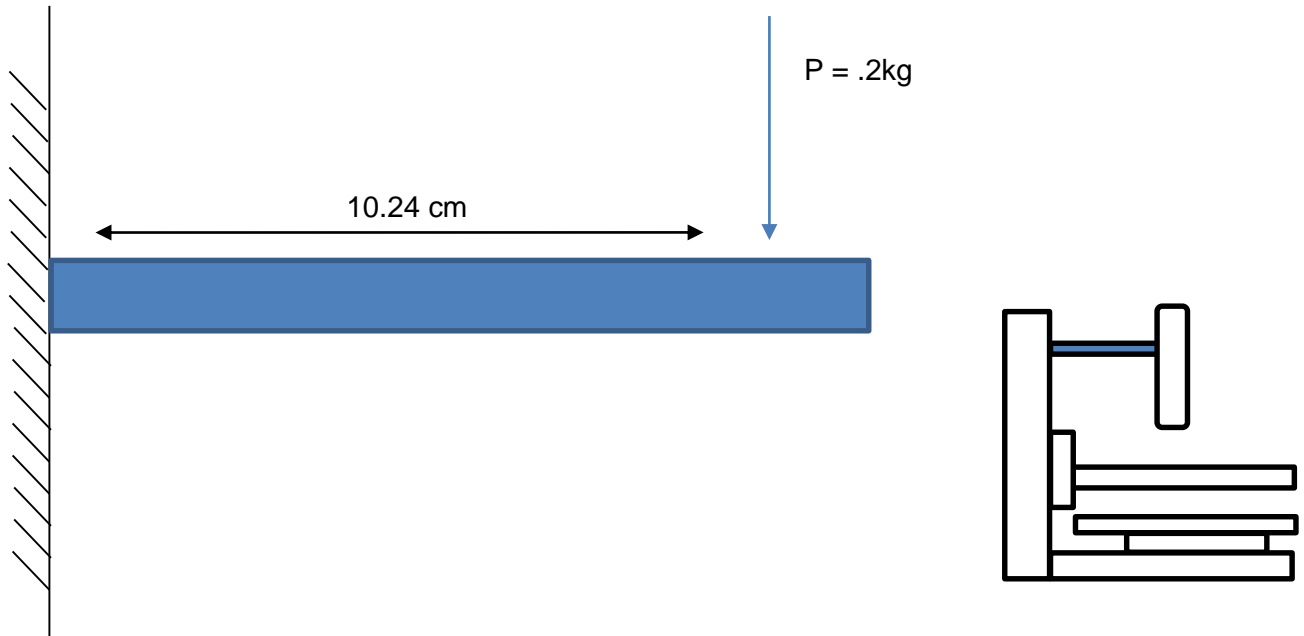
**Fig. E1:** Free body diagram of the top stage in cantilever



$$\begin{aligned}
 M &= \frac{qx^2}{2} \\
 v &= \frac{1}{EI} \left( \frac{qx^4}{24} + C_1x + C_2 \right) \\
 v(0) = 0 \text{ and } \frac{dv}{dx}_{x=0} &= 0 \\
 \therefore v(x) &= \frac{qx^4}{24EI} \text{ and so } v(15.24) = \frac{1.413 * 15.24^4}{69 * 10^7 * (15.24 * 1.27^3)} \\
 &= 3.5 * 10^{-10} m \\
 &\ll 1 \mu m
 \end{aligned}$$

Where x is distance, q is distributed load, M is bending moment, v is displacement, E is Young's Modulus, and I is second moment of area.

**Fig. E2:** Free body diagram of the cameras in cantilever

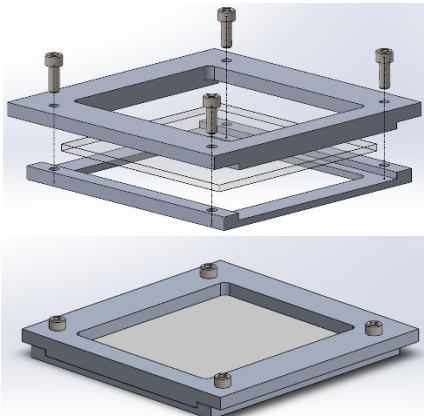


$$\begin{aligned}
 M &= Px \\
 v &= \frac{1}{EI} \left( \frac{Px^3}{6} + C_1x + C_2 \right) \\
 v(0) &= 0 \text{ and } \frac{dv}{dx}_{x=0} = 0 \\
 \therefore v(x) &= \frac{Px^3}{6EI} \text{ and so } v(10.24) = \frac{.2 * 10.24^3}{6 * 69 * 10^7 * (2.54 * 1.27^3)} \\
 &= 9.8 * 10^{-7} m \\
 &\approx 1\mu m
 \end{aligned}$$

Where x is distance, M is bending moment, v is displacement, E is Young's Modulus, P is force, and I is second moment of area.

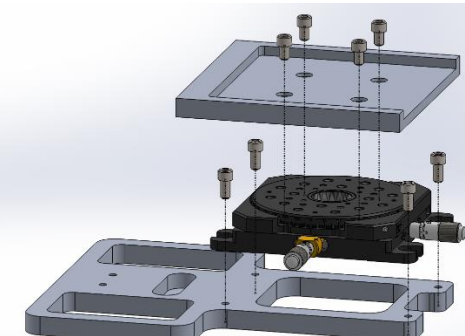
## APPENDIX F – ASSEMBLY PLAN

1



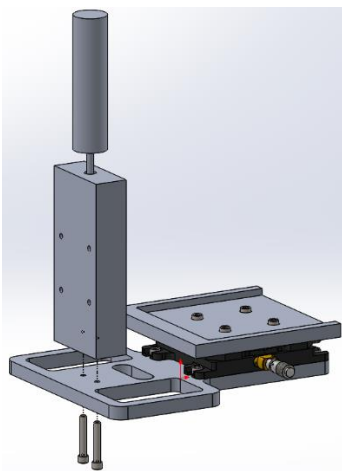
Assemble the top stage by putting together the two halves of the frame with the piece of glass in between and screwing them together with 4 ¼-20 x 0.5” bolts.

2



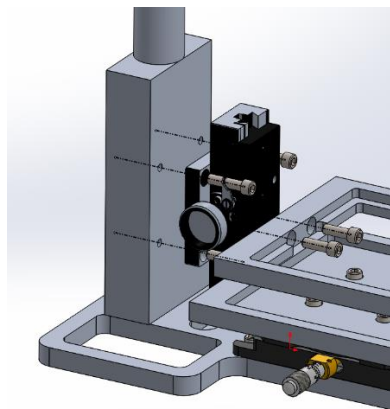
Assemble the bottom stage by bolting the XYR translation stage to the base with 4 ¼-20 x 0.5” bolts. Then bolt the bottom holder to the XYR stage using 4 ¼-20 x 0.5” bolts.

3



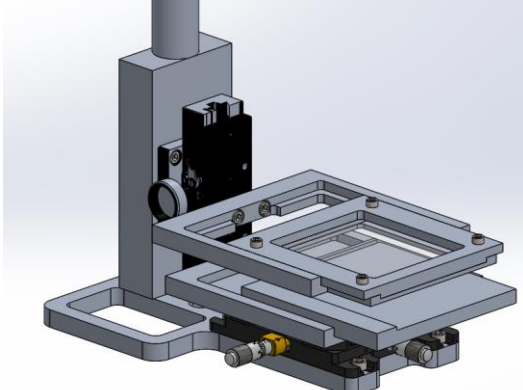
Bolt on the main pillar using 3 ¼-20 x 1.5” bolts by screwing them into the bottom of the pillar through the base.

4



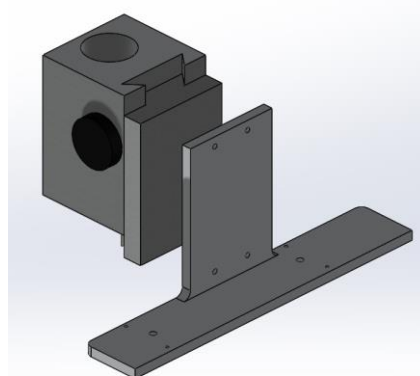
Add the top stage assembly by first bolting on the Z-translation stage to the main pillar using 4 ¼-20 x 0.5” bolts. Then bolt the top holder to the Z-translation stage using 2 ¼-20 x 0.375” bolts.

5

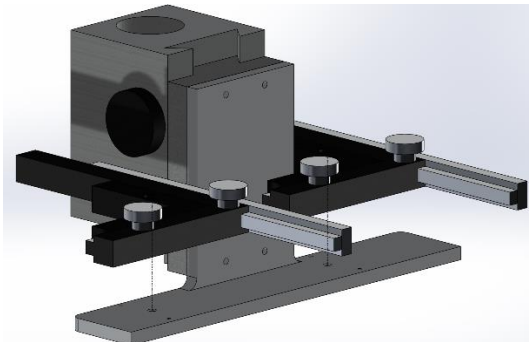


Slide the two frames into the holders.

6

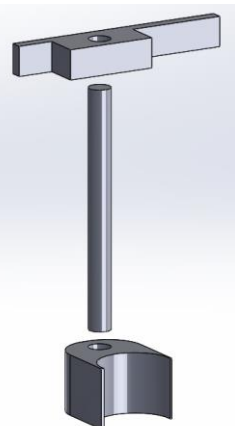


7



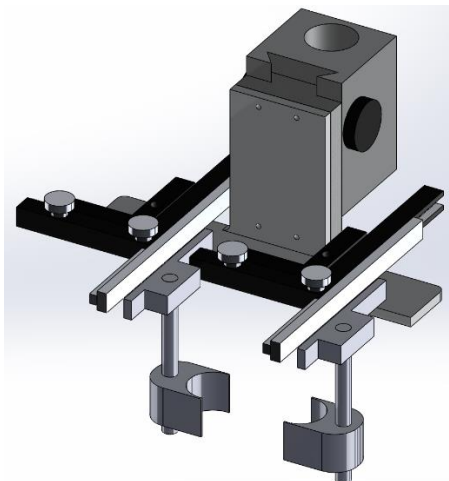
Align the two camera XY stages with the L-support using the two dowel pins built into the stages. Bolt them in using one M3x12 bolt for each stage.

8



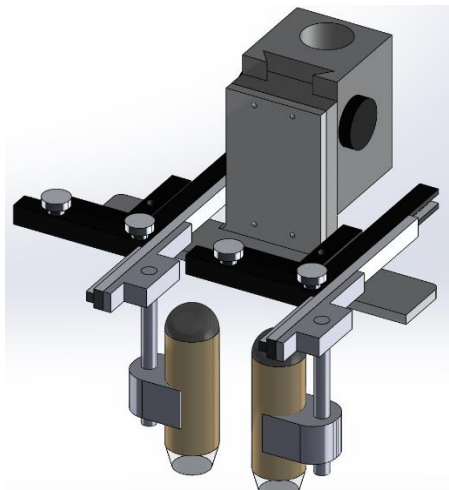
Press the camera rods into the T-brackets and attach the camera holster to the rod.

9



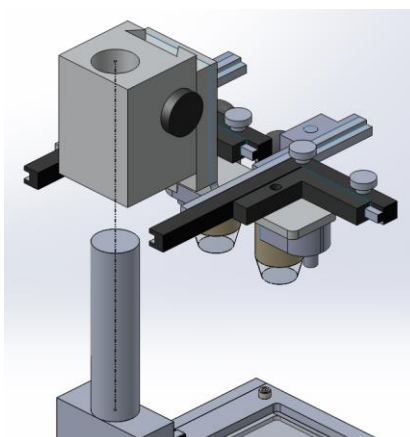
Bolt the T-brackets to the camera XY stages using two M3x4 bolts each.

10

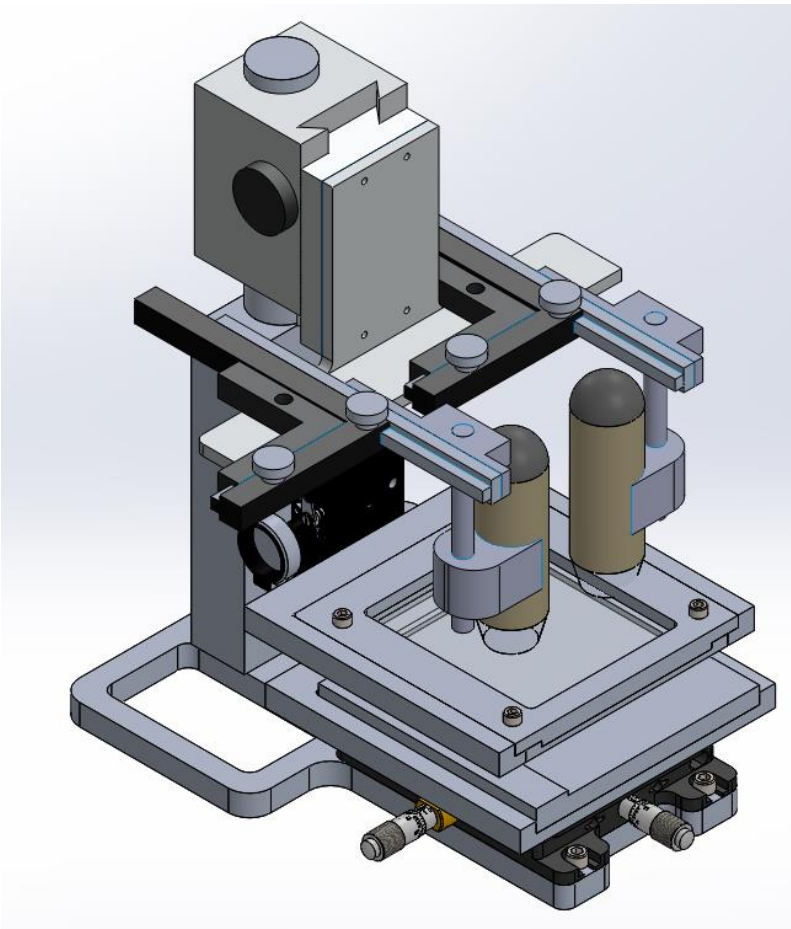


Attach the cameras to the holsters.

11



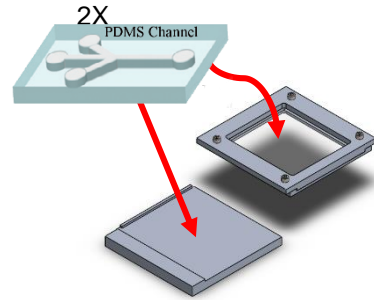
Bolt the focus rack onto the camera pillar.



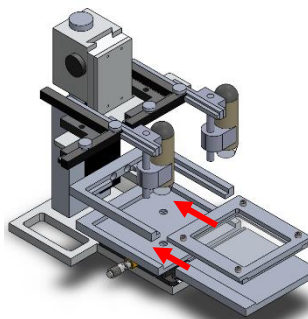
The device is now completely assembled.

## APPENDIX G – ALIGNMENT PROCESS

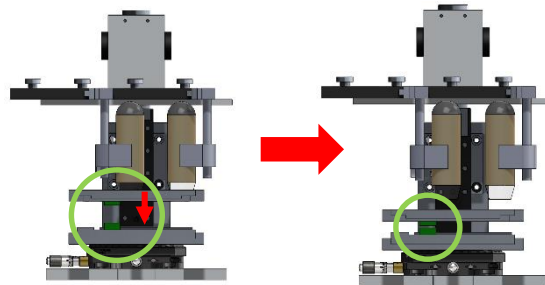
- 1 Remove the top and bottom frames from the aligner. Place the top layer of PDMS on the bottom glass surface of the top frame with the structures facing away from the glass; place the bottom layer of PDMS on the bottom frame with the structures facing up.



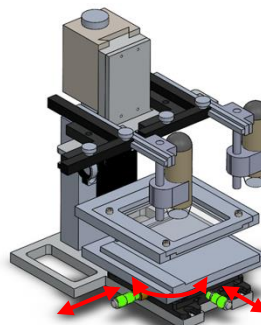
- 2 Slide the top and the bottom frames into their respective stages. Make sure that the top and bottom layers are within 0.5 cm of being aligned.



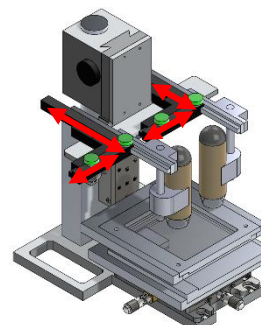
- 3 Lower the top stage using the top stage knob until the PDMS layers are as close as possible without touching. It's recommended to look between the top and bottom stage to make sure that the PDMS layers do not bond accidentally.



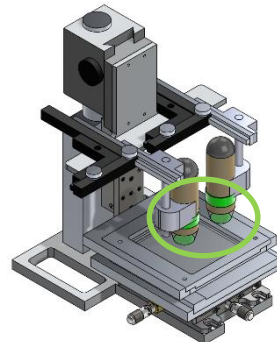
- 4 Adjust the X and Y knobs on the alignment platform and rotate the bottom stage itself until the structures look aligned by naked eye.



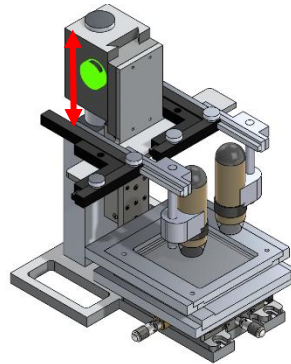
- 5 Rotate the X and Y knobs on the camera mount to put a camera over each alignment marker



- 6 Adjust to the desired zoom level with the knobs on the cameras.



- 7 Rotate the camera Z stage knob to lower the cameras until PDMS patterns appear on the screen.

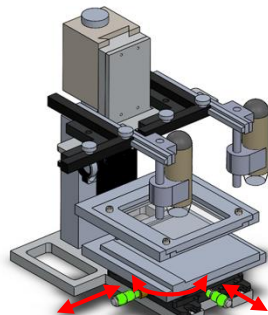


- 8 Capture the image on the screen, right click on the captured image and select "Transparency Mode". Rotate the camera Z stage knob to focus on the bottom layer.



- 9 Scroll down on your mouse to see the live video feed, scroll down to see the captured image. This allows the image of the alignment marker of the top stage to be clear while the camera focuses on the bottom layer.

- 10 Adjust the X and Y knobs on the alignment platform and rotate the bottom stage itself until the structures are aligned. We recommend aligning the rotational first before aligning X and Y.

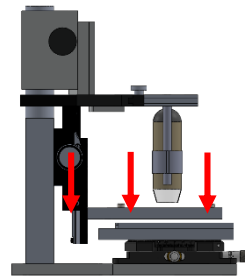


- 11 Once aligned, lock the rotational stage using the hex key provided.

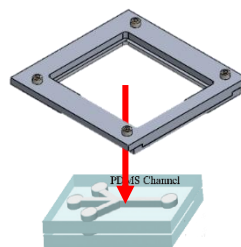
- 12** Remove frames from holders and place them in plasma etcher to activate surfaces



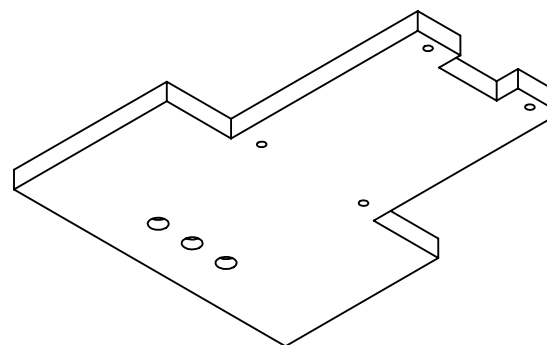
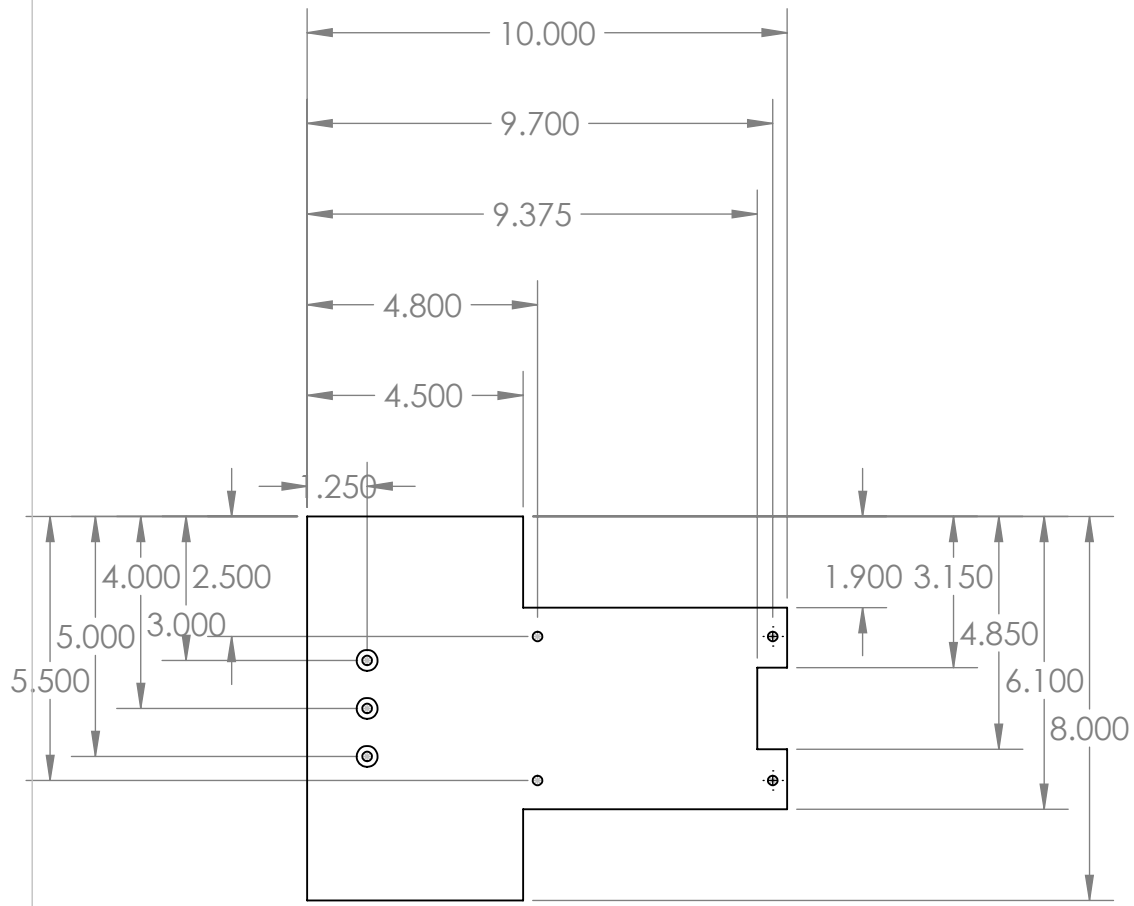
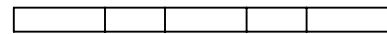
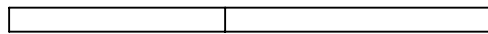
- 13** After activation, replace the frames onto their respective holders
- 14** Repeat step 3, and then steps 6 to 10
- 15** Once aligned, lower the top stage to carefully bond the PDMS layers. Push down so that layers make a firm contact.



- 16** Raise the camera Z stage and the top stage so the bonded PDMS layers can be carefully removed



## **APPENDIX H – ENGINEERING DRAWINGS**



TITLE:

SIZE

**A**

DWG. NO.

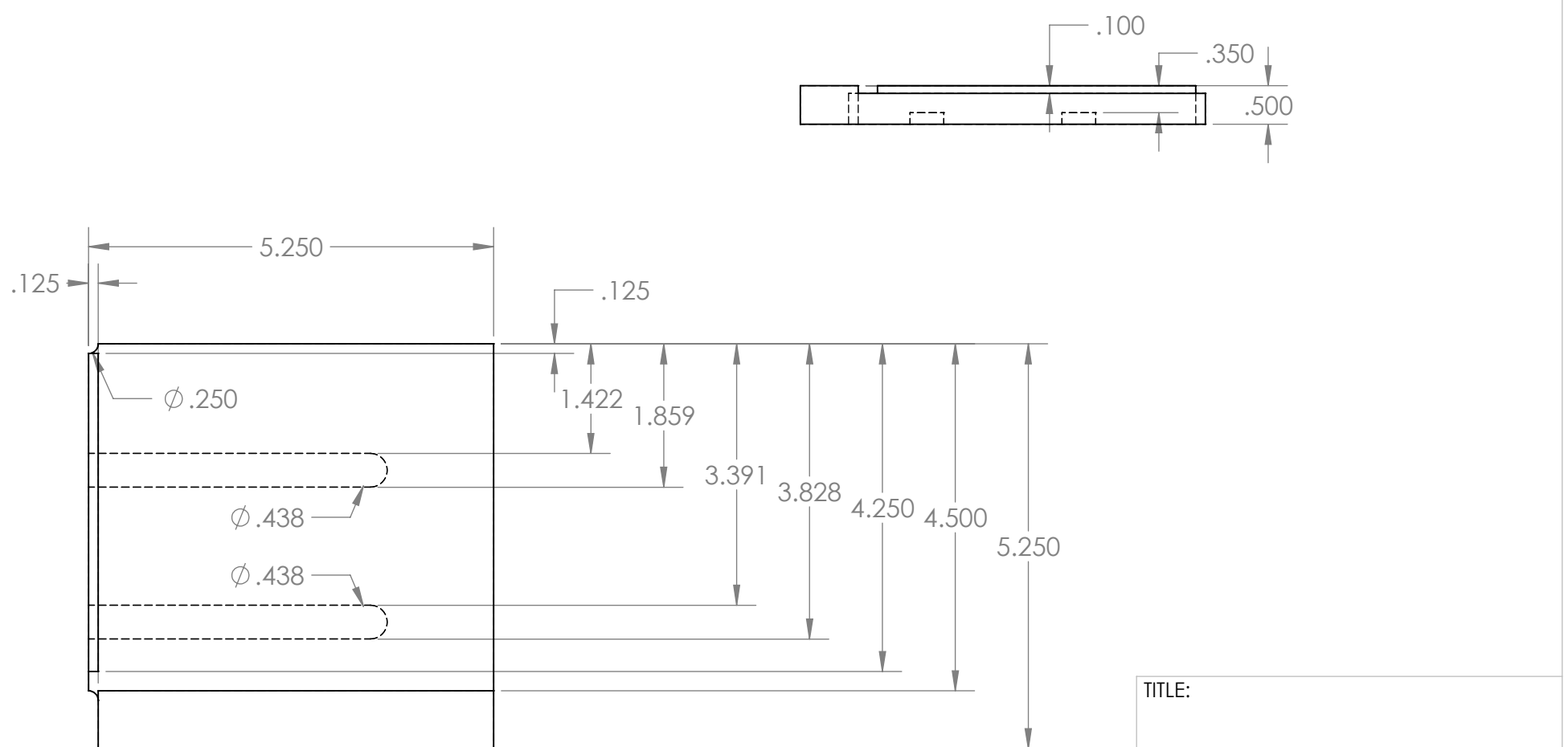
**Base**

REV

SCALE: 1:4

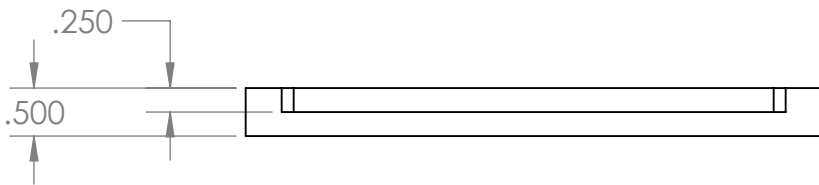
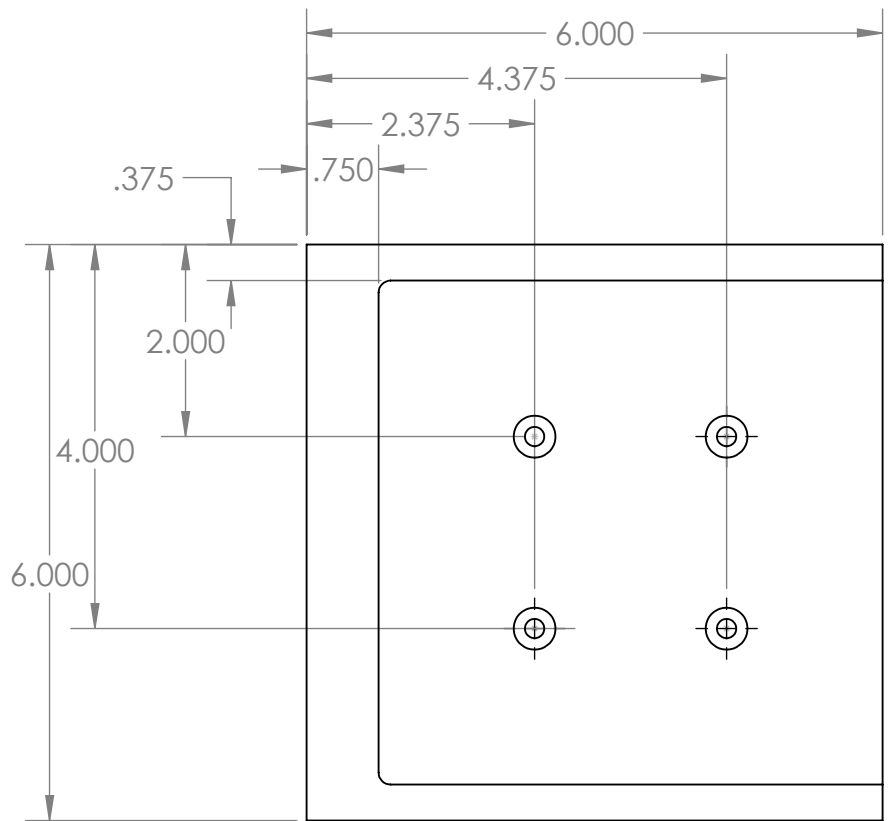
WEIGHT:

SHEET 1 OF 1



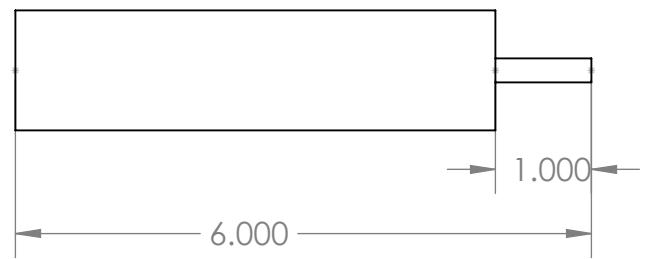
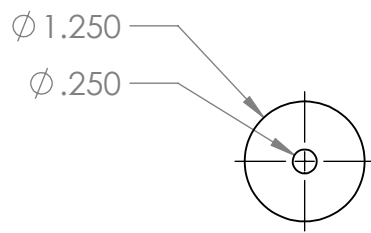
TITLE:

SIZE	DWG. NO.	REV
<b>A Bottom Frame</b>		
SCALE: 1:2	WEIGHT:	SHEET 1 OF 1



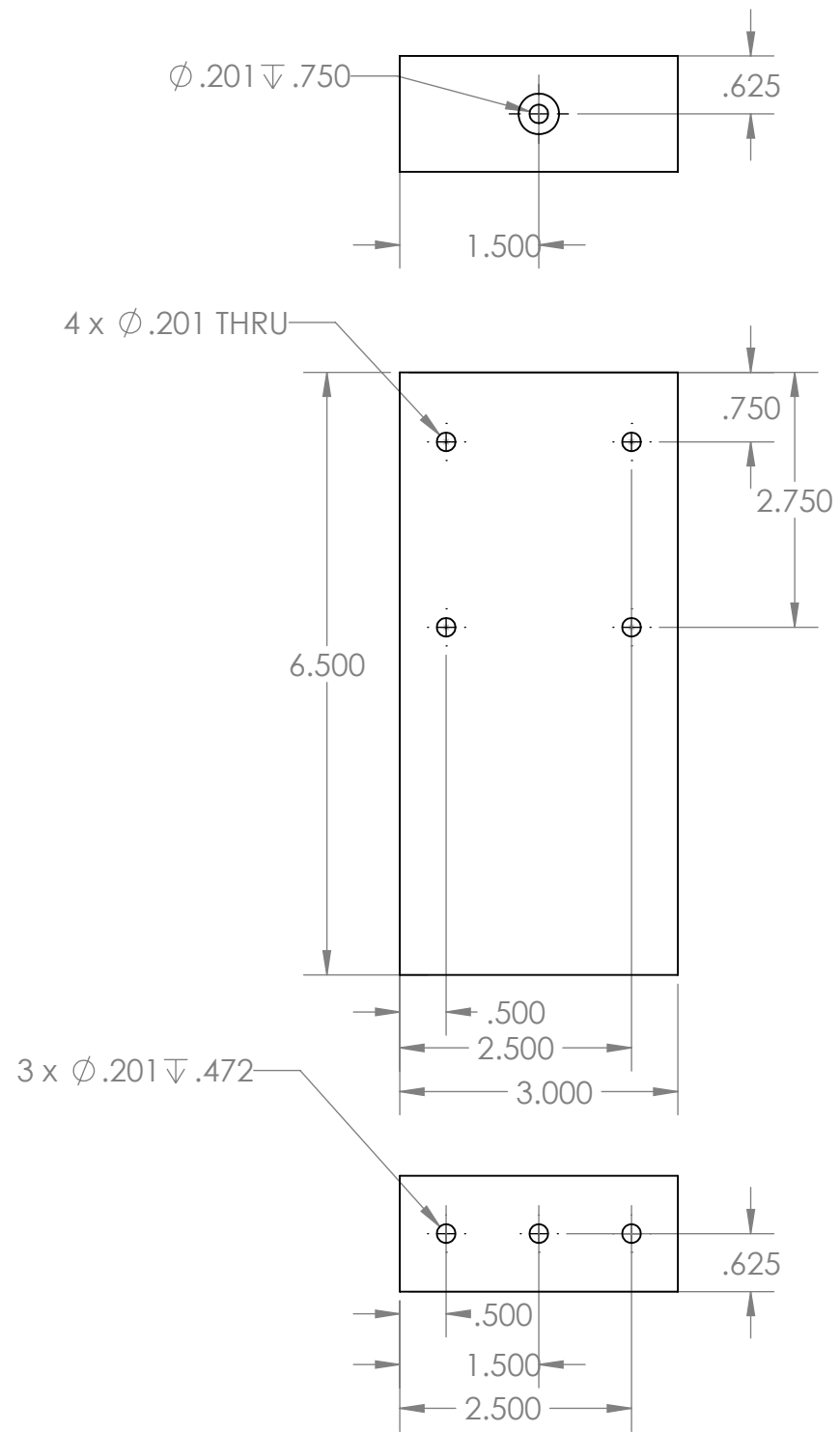
TITLE:

SIZE	DWG. NO.	REV
<b>Bottom Holder</b>		
SCALE: 1:2	WEIGHT:	SHEET 1 OF 1



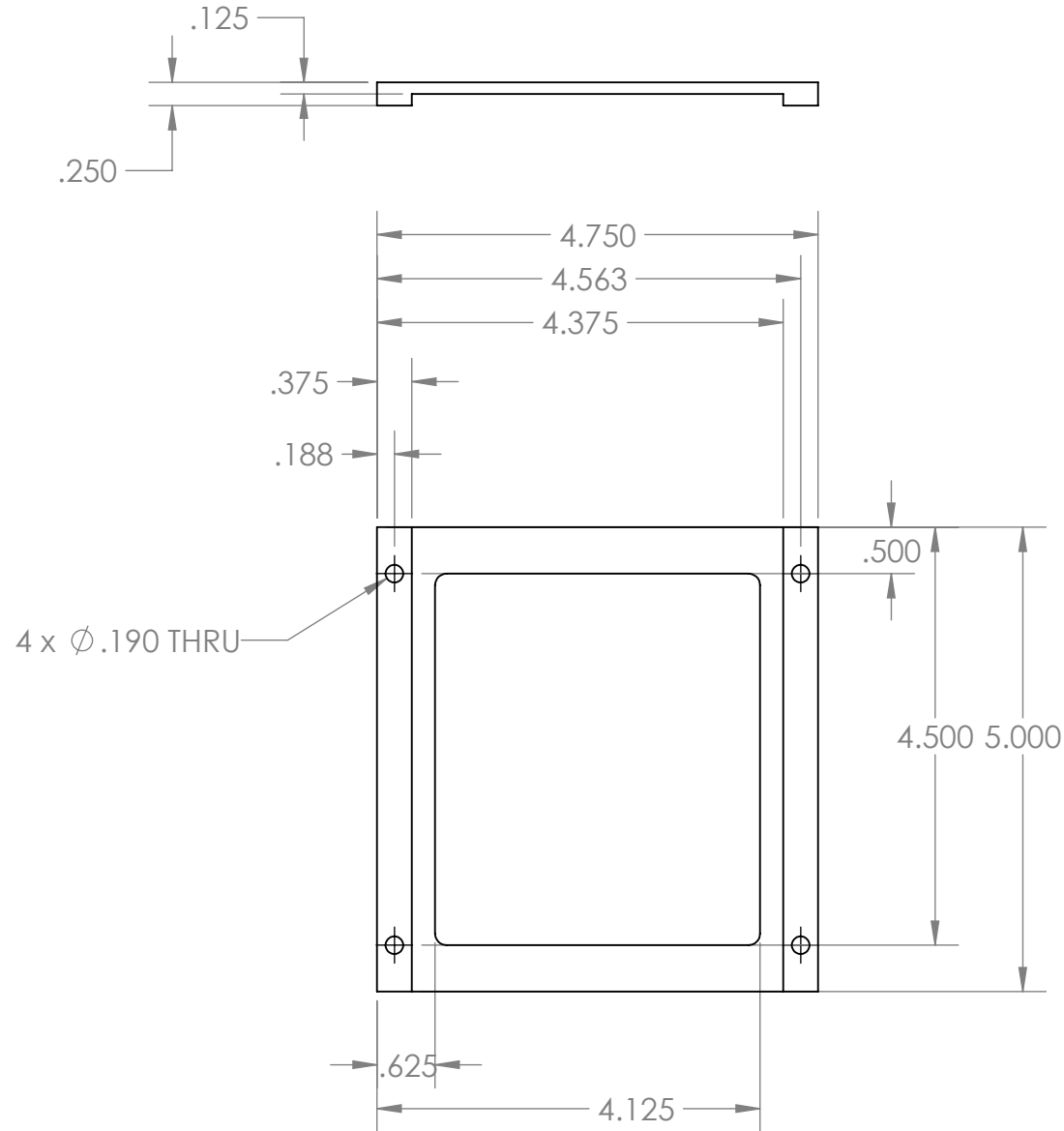
TITLE:

SIZE	DWG. NO.	REV
<b>ACamera Pillar</b>		
SCALE: 1:2	WEIGHT:	SHEET 1 OF 1



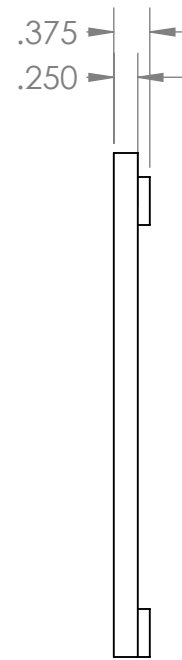
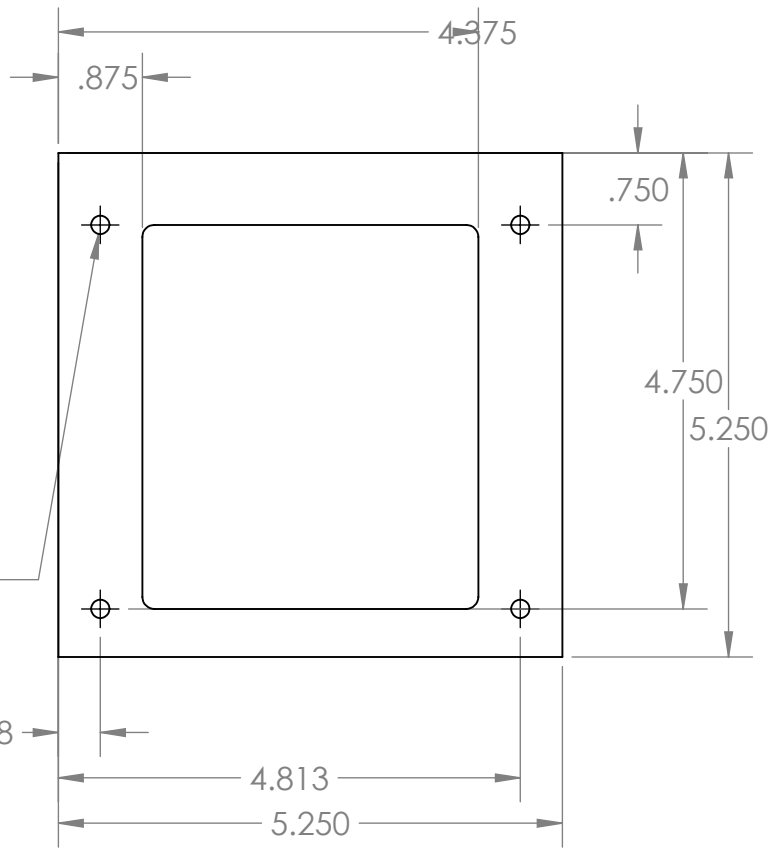
TITLE:

SIZE	DWG. NO.	REV
<b>A</b>	Main Pillar	
SCALE: 1:2	WEIGHT:	SHEET 1 OF 1



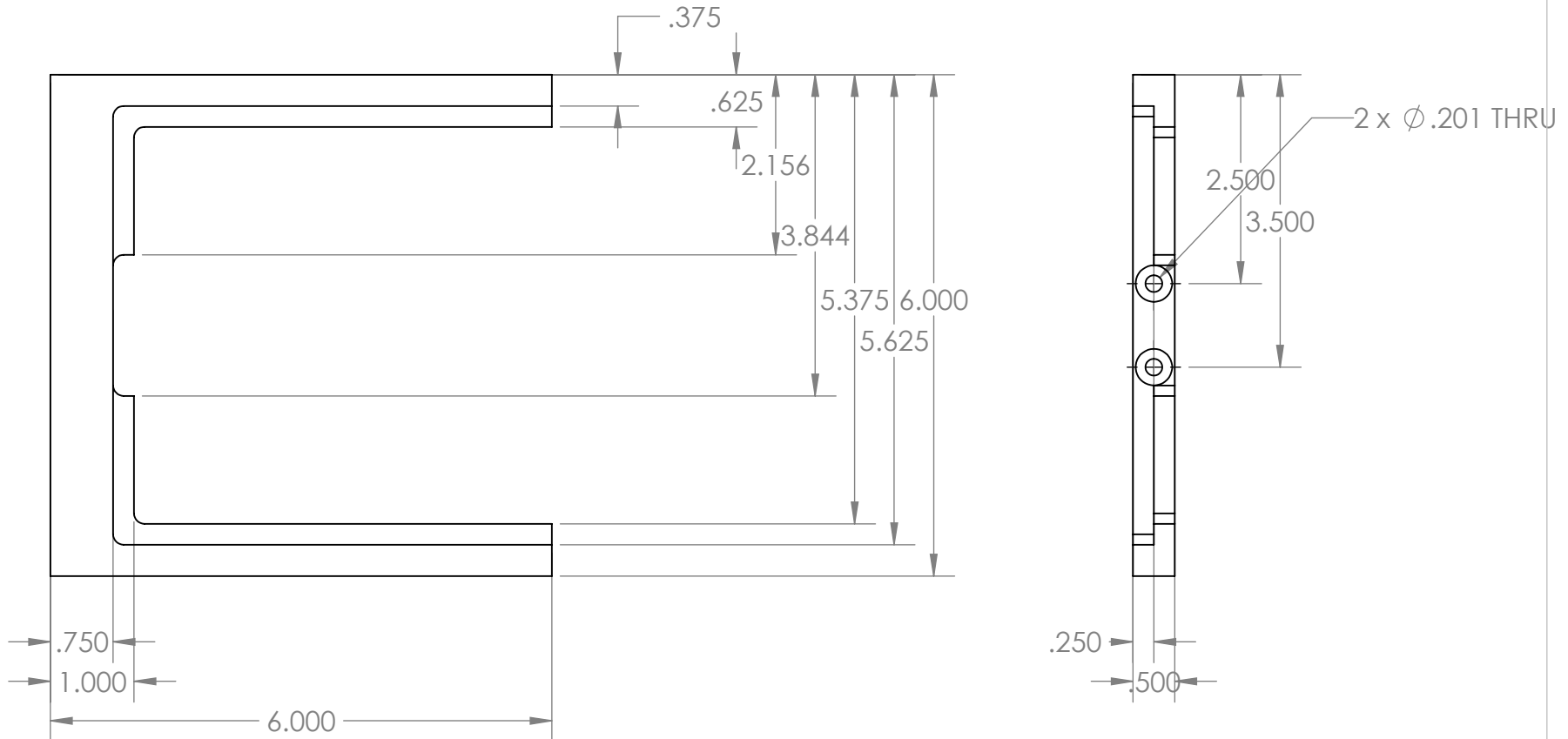
TITLE:

SIZE	DWG. NO.	REV
<b>Atop Frame_1</b>		
SCALE: 1:2	WEIGHT:	SHEET 1 OF 1



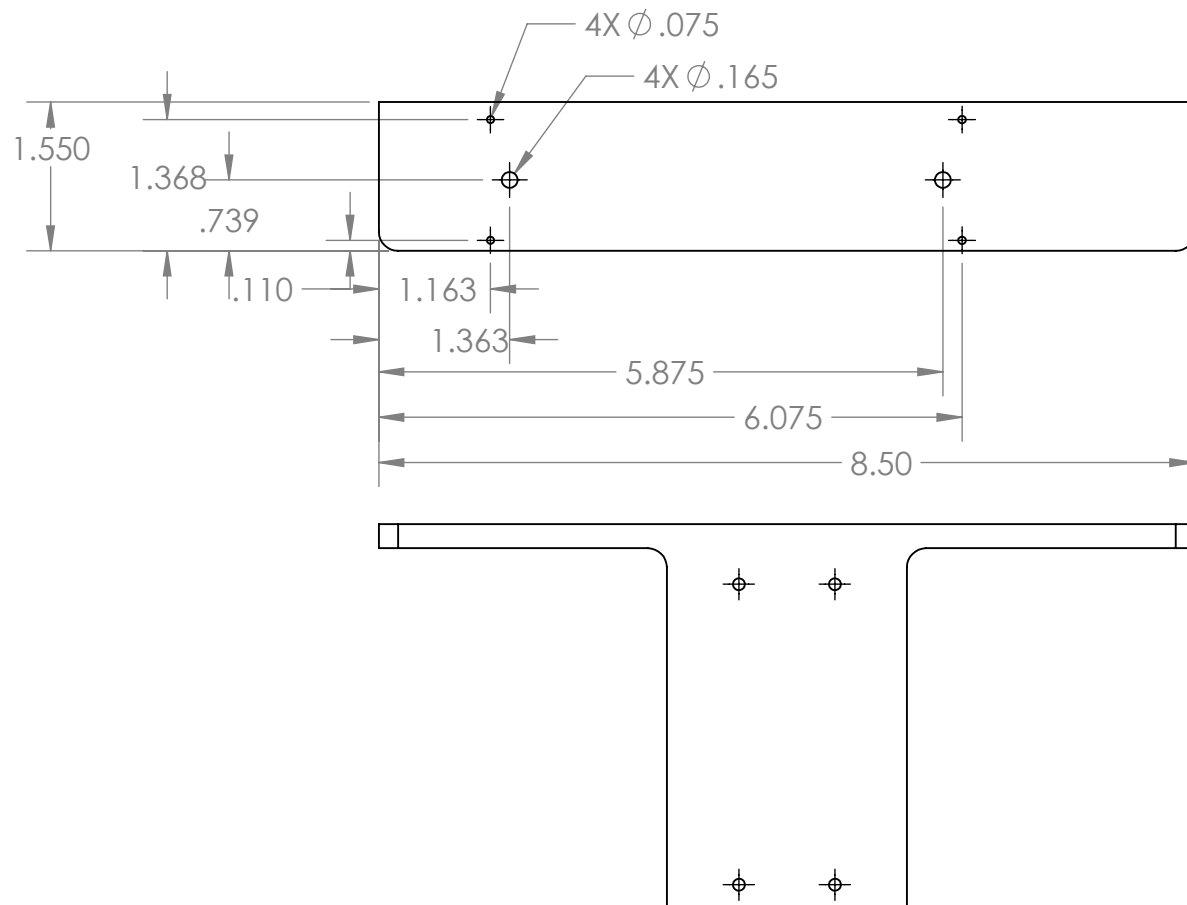
TITLE:

SIZE	DWG. NO.	REV
<b>ATop Frame_2</b>		
SCALE: 1:2	WEIGHT:	SHEET 1 OF 1

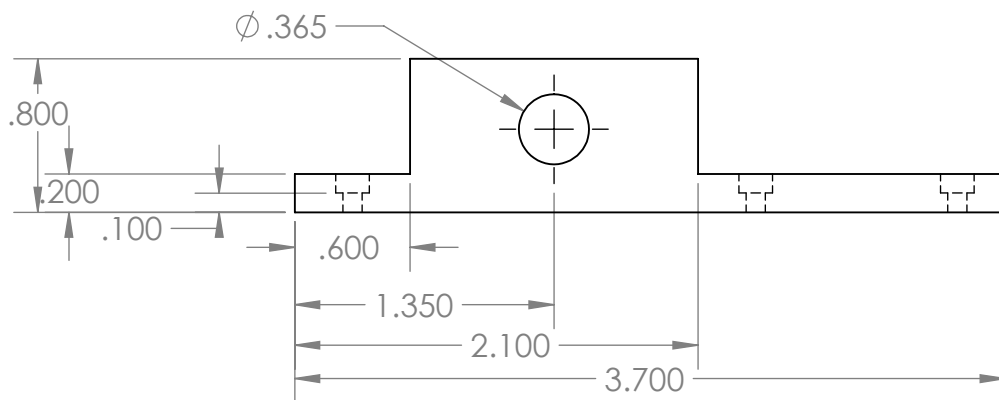
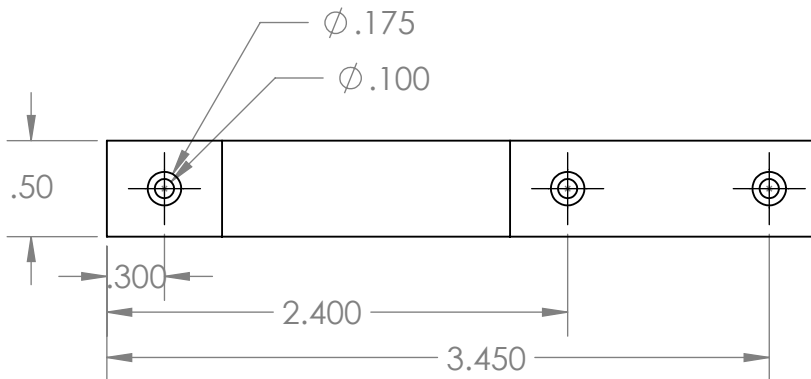
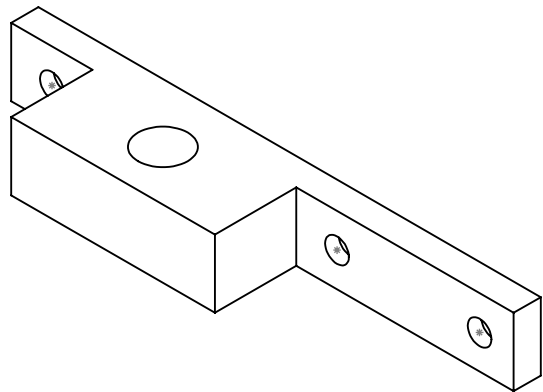


TITLE:

SIZE	DWG. NO.	REV
<b>A</b>	<b>Top Holder</b>	
SCALE: 1:2	WEIGHT:	SHEET 1 OF 1



		UNLESS OTHERWISE SPECIFIED:		NAME	DATE	TITLE:          	
		DIMENSIONS ARE IN INCHES	DRAWN				
		TOLERANCES:	CHECKED				
		FRACTIONAL $\pm$	ENG APPR.				
		ANGULAR: MACH $\pm$ BEND $\pm$	MFG APPR.				
		TWO PLACE DECIMAL $\pm$	Q.A.				
		THREE PLACE DECIMAL $\pm$	COMMENTS:				
		INTERPRET GEOMETRIC TOLERANCING PER:	MATERIAL				
			FINISH				
			DO NOT SCALE DRAWING				
PROPRIETARY AND CONFIDENTIAL				SIZE	DWG. NO.	REV	
THE INFORMATION CONTAINED IN THIS DRAWING IS THE SOLE PROPERTY OF <INSERT COMPANY NAME HERE>. ANY REPRODUCTION IN PART OR AS A WHOLE WITHOUT THE WRITTEN PERMISSION OF <INSERT COMPANY NAME HERE> IS PROHIBITED.							
NEXT ASSY	USED ON						
APPLICATION							
				SCALE: 1:2	WEIGHT:	SHEET 1 OF 1	



		UNLESS OTHERWISE SPECIFIED:		NAME	DATE	
		DIMENSIONS ARE IN INCHES TOLERANCES: FRACTIONAL $\pm$ ANGULAR: MACH $\pm$ BEND $\pm$ TWO PLACE DECIMAL $\pm$ THREE PLACE DECIMAL $\pm$	DRAWN			TITLE:  INTERPRET GEOMETRIC TOLERANCING PER:  MATERIAL  NEXT ASSY      USED ON      FINISH
			CHECKED			
			ENG APPR.			
			MFG APPR.			
			Q.A.			
			COMMENTS:			
				SIZE	DWG. NO.	REV
Camera_T_Attachme						
				SCALE: 1:1	WEIGHT:	SHEET 1 OF 1
APPLICATION		DO NOT SCALE DRAWING				

**PROPRIETARY AND CONFIDENTIAL**  
THE INFORMATION CONTAINED IN THIS  
DRAWING IS THE SOLE PROPERTY OF  
<INSERT COMPANY NAME HERE>. ANY  
REPRODUCTION IN PART OR AS A WHOLE  
WITHOUT THE WRITTEN PERMISSION OF  
<INSERT COMPANY NAME HERE> IS  
PROHIBITED.